QCD EVENT GENERATORS

Conveners: I.G. Knowles and T. Sjöstrand

Working group: A. Blondel, A. Boehrer, C.D. Buchanan, D.G. Charlton, S.-L. Chu, S. Chun, G. Dissertori, D. Duchesneau, J.W. Gary, M. Gibbs, A. Grefrath, G. Gustafson, J. Häkkinen, K. Hamacher, K. Kato, L. Lönnblad, W. Metzger, R. Møller, T. Munehisa, R. Odorico, Y. Pei, G. Rudolph, S. Sarkar, M.H. Seymour, J.C. Thompson, Š. Todorova and B.R. Webber.

Contents

2

1 Introduction

This section is devoted to QCD generators, relevant for LEP 2 processes where hadrons may be found in the final state: $e^+e^- \to \gamma^*/Z^0 \to q\overline{q}$, $e^+e^- \to W^+W^- \to q\overline{q}q'\overline{q}'$, $e^+e^- \to Z^0h^0 \to \nu\overline{\nu}b\overline{b}$, *etc.* In fact, almost all interesting processes at LEP 2 give hadronic final states, ensuring that QCD generators will remain of vital importance.

It is instructive to contrast the EW and QCD generator perspectives for LEP 2. In the EW physics program, the main emphasis is on four-fermion final states. This is different from LEP 1, where the Z^0 line shape was a major focus of attention [1]. Dedicated four-fermion generators are new creations, that have to stand on their own and cannot be tested at LEP 1. Therefore there is little sense of continuity with respect to the LEP 1 workshop [2] and subsequent LEP 1 activities. QCD physics, by contrast, extrapolates logically from LEP 1. New aspects may enter, such as colour reconnection, but these are expected to be relatively small perturbations on the basic picture (though of importance for precision physics). Therefore the QCD generators write-up for the LEP 1 workshop [3] is still partly relevant and subsequent LEP 1 experience very much so. The high Z^0 statistics will make LEP 1 a significant testing ground for many new QCD physics ideas also in the LEP 2 era.

It is thus logical to begin this section with an assessment of experience from LEP 1, with emphasis on areas where generators are known to have shortcomings. Any improvements for LEP 1 will directly benefit LEP 2. This is followed by a comparison of extrapolations to LEP 2 energies, from which the current range of uncertainty can be estimated. Next comes a survey of existing generators, ranging from major programs, with coverage of the full generation chain, to shorter pieces of code for specific purposes. Finally, there is a section on standardization efforts, to help ease life for users who rely on several generators.

This report is not a complete description of the topic. However it should provide a convenient starting point, with ample references to further relevant literature.

2 Experience from LEP 1

2.1 Event shapes and inclusive distributions

A large quantitative improvement in the description of event shape and inclusive distributions has been made at LEP 1 with respect to the era of PETRA and PEP. This is due mainly to the vast amount of high quality data available and the need to achieve good agreement in model/data comparisons so as to obtain small systematic errors for the high precision electroweak measurements. To help facilitate this goal flexible fitting algorithms were developed, based on previous work [4, 5]. In many cases the dependence of the model's response to its parameters is analytically interpolated [6, 7, 8, 9]. This strategy is flexible, allows easy exchange of input distributions but also the simultaneous fitting of very many, 10–15, parameters [9, 10].

Evidently the choice of input distributions used to constrain the model parameters is important. In general a distribution depends on very many parameters, thus the parameters resulting from a fit are in general correlated. A survey has been undertaken to determine which distributions have the highest sensitivity to the individual model parameters [9, 11]. It turns out that semi-inclusive spectra are most important, as has been observed before [8]. The charged particle momentum and transverse momentum spectra strongly constrain the fragmentation function or, alternatively, the cluster parameters. However their dependence on the fragmentation parameters is not exclusive. Inclusive distributions may depend even more strongly on Λ_{QCD} and/or the parton shower cut-off. In fact, the latter parameter strongly influences the high-momentum tail of the momentum spectrum. The 3-jet rate as defined using the Durham or JADE algorithms almost only depends on Λ_{QCD}. This emphasizes the reliability of α_{s} determinations using this quantity. In contrast, and somewhat surprisingly, the AEEC depends strongly on very many model parameters. Measures of the general event topology, e.g. thrust and sphericity, depend mainly on Λ_{QCD} and only in the 2-jet regime on fragmentation parameters. Shape measures sensitive to radiation out of the event plane, like minor or aplanarity, show strong dependence both on fragmentation parameters and on Λ_{QCD}. In summary, model parameters are best determined by fitting the model to inclusive distributions, jet rates and shape distributions simultaneously.

It appears that the "partonic" phase of the models is best tested by studying the properties of jets defined using jet algorithms [12]. At large resolution parameter y_{cut}, when dealing with few jets or the emission of the "first" hard gluons at large angles, fragmentation effects are almost negligible. In contrast at smaller y_{cut}, where higher jet rates are sizable i.e. when the subjet structure described by multiple emission of soft and collinear gluons is important, also fragmentation effects are of increasing importance.

The parton shower models ARIADNE [13], HERWIG [14] and JETSET [15] describe well the general evolution of the individual jet rates with y_{cut}, especially the 3-jet rate [9] (see Fig. 1 [16] and Fig. 2 [9]). A more detailed 3-jet Dalitz plot study using the ordered normalized jet energies x_i ($i = 1, 2, 3$) and $\mathcal{Z} = (x_2 - x_3)/\sqrt{3}$ unveiled slight differences among the models
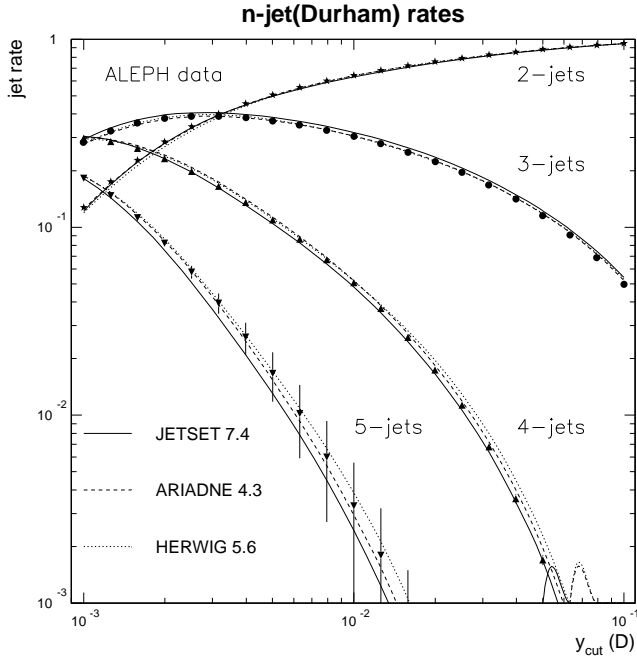
4

n-jet(Durham) rates

Figure 1: Differential n-jet rates compared to ARIADNE, HERWIG and JETSET PS.
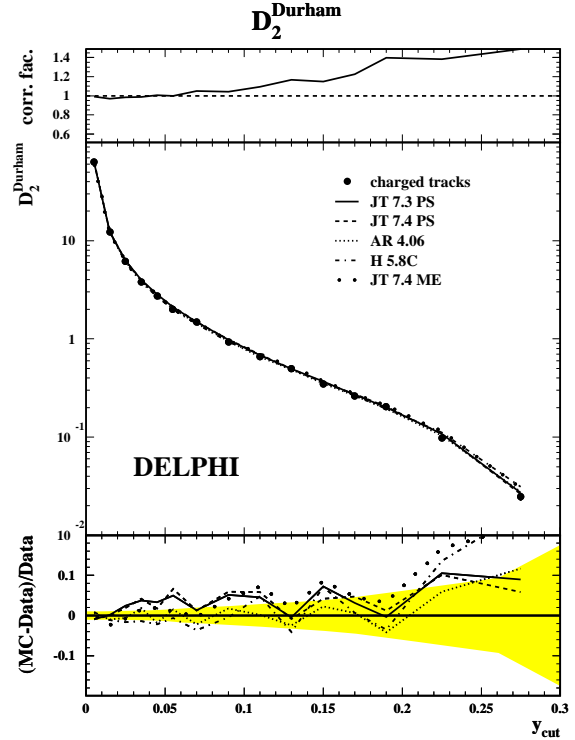

$\mathbf{D_2^{Durham}}$

Figure 2: Differential 2-jet rate compared to ARIADNE, HERWIG and JETSET PS & ME.

[17]. ARIADNE is in perfect agreement with the data, JETSET is slightly below the data in the almost 2-jet like case ($\mathcal{Z} \to 1/\sqrt{3}$) and slightly above when the lower energetic jets have similar energies ($\mathcal{Z} \to 0$). HERWIG shows a somewhat bigger deviation along the diagonal (i.e. the x_3 direction) of the Dalitz plot. Also the $\mathcal{O}(\alpha_s^2)$ ME option of JETSET is in good agreement with the data. It is interesting to observe that the agreement is less good when optimized scales are used to achieve a better agreement for the 4-jet rate.

The discrepancies observed are due either to the different shower evolution strategies used or can be traced back to way in which the PS models perform the matching of the first splitting to the first order matrix element. In ARIADNE this matching is performed naturally, since the splitting function is just the lowest order matrix element expression. If no matching is performed (a possible option in HERWIG and JETSET) the agreement with the data is poor.

The 4- and 5-jet rates predicted by JETSET PS (HERWIG) decrease more (less) rapidly with y_{cut} than the data (see Fig. 1). At large y_{cut} the discrepancy is up to 20% [9]. ARIADNE however is in perfect agreement with the data.

Clear discrepancies have been observed at PEP and PETRA comparing the JETSET ME model to the 4-jet rate. This discrepancy has been resolved by introducing optimized scales [18]. Today using optimized scales the 4-jet rate is perfectly described by the JETSET ME

model [8, 9]. However the 5-jet rate predicted by the ME model, as is to be expected, decreases far too rapidly and is one order of magnitude below the data at large y_{cut}. Recently it has been shown that the 5-jet rate is also correctly described [19] when the $\mathcal{O}(\alpha_s^3)$ tree-level graphs are included in the model [20]. The scale in this case can be chosen similarly to that for the standard $\mathcal{O}(\alpha_s^2)$ case.

The observations made for the jet rates consistently lead to the following picture if the models are compared to event shape distributions: general event shape measures, mainly sensitive to hard gluon radiation, like thrust, sphericity, $M_{high/sum}^2/\sqrt{s}$ or $B_{max/sum}$, are reproduced extremely well by all PS models [9]. The only significant discrepancy is a slight overestimation of very spherical events by HERWIG. Observables sensitive to higher order radiation like minor, aplanarity, $M_{low}^2/\sqrt{s}$ and B_{min} are consistently overestimated (underestimated) by HERWIG (JETSET) for large values of the observables. Due to the normalization of the distributions this must also lead to (in general smaller) deviations at intermediate or small values of these observables. For example the minor distribution in the case of HERWIG is predicted to be too wide. ARIADNE is in perfect agreement for most distributions. As JETSET and ARIADNE both use the JETSET string fragmentation model, it is evident that the discrepancies observed for JETSET are due to the parton shower part of the model.

The general fragmentation part of the models are best tested using inclusive charged particle distributions which depend strongly on the interplay between the partonic and fragmentation phases of the models. The average charged multiplicity $\langle n_{ch} \rangle$ is the integral of the scaled momentum (x) distribution. Both quantities have to be described simultaneously by the models. When fitting only to the scaled momentum spectrum, HERWIG predicts $\langle n_{ch} \rangle \approx 20.8$ close to the the very precisely known LEP 1 average $\langle n_{ch} \rangle = 20.92 \pm 0.24$ [21]. ARIADNE and JETSET PS give values that are too small (≈ 20.3) and JETSET ME gives too high a multiplicity (≈ 22.7) [11].

The HERWIG x distribution oscillates slightly around the data distribution. For small x it is below, for $0.3 \leq x \leq 0.7$ it is above (max. 10%) and for larger x again below the data. If the multiplicity is constrained to the measured value, the x spectrum is well described by the JETSET PS and ARIADNE for $x \leq 0.5$ but drops 20%–30% below the data for large x. This should not to be overinterpreted because experimental smearing is important in this momentum range and systematic errors increase. The data so far available from ALEPH and DELPHI [9, 22] agree here only within the full experimental error. The JETSET ME result also oscillates slightly around the data curve ($\pm 5\%$).

Thus the multiplicity distribution is described well by ARIADNE and JETSET (compare Fig. 4). HERWIG predicts a slightly too wide distribution thus overestimating the dispersion of the number of hadrons; in HERWIG this is strongly coupled to the number of primary partons.

The transverse momentum in the event plane, $p_{\perp in}$, is strongly sensitive to hard gluon radiation and almost correctly described by all models. Only the large $p_{\perp in}$ tail is slightly underestimated. The predicted $p_{\perp out}$ distribution for $p_{\perp out} > 0.8$ GeV falls off more rapidly than the data in all models and at large $p_{\perp out}$ is $\approx 30\%$ below the data! This fact is shown in

6
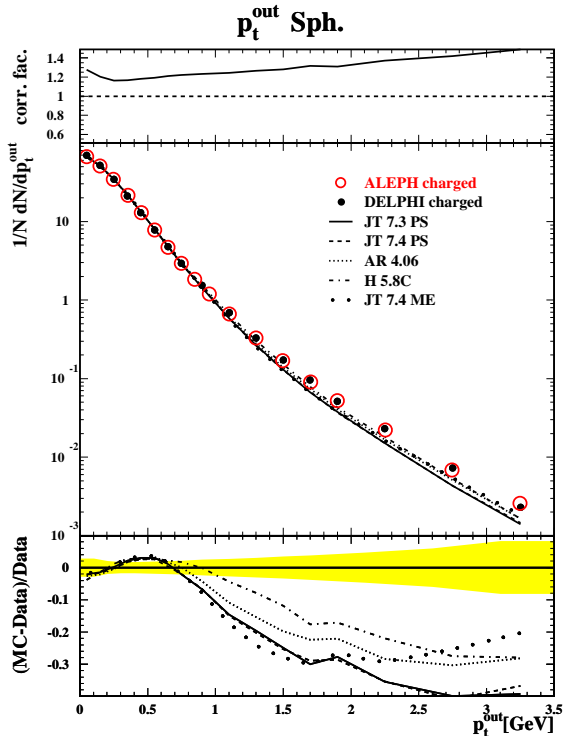
Figure 3: Distribution of $p_{\perp\text{out}}$ with respect to the sphericity axis compared to ARIADNE, HERWIG and JETSET PS & ME [9].
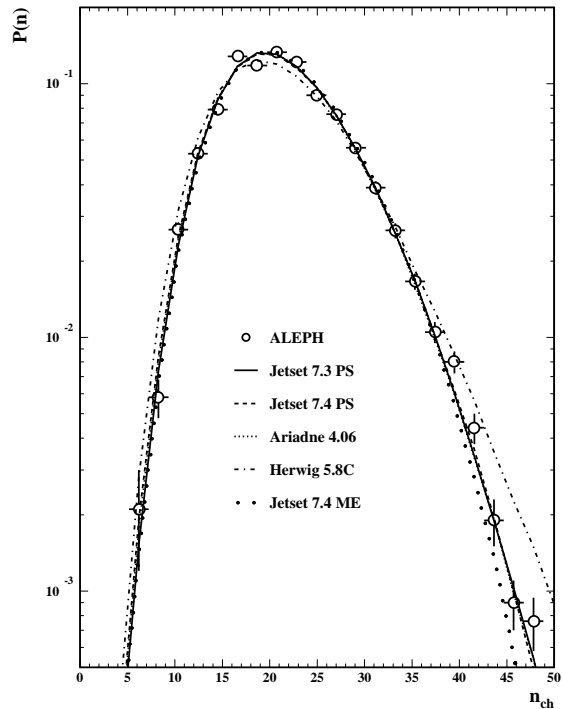
Figure 4: Multiplicity distribution [25] compared to the DELPHI tuning of ARIADNE, HERWIG and JETSET PS & ME [9].

figure 3 which also compares the data of ALEPH [23] and DELPHI [9] to depict the precision of the experimental data. The large $p_{\perp\text{out}}$ tail is mainly due to gluon radiation. This failure of the shower models is presumably due to missing large angle contributions in the basic LLA used by the models. A matching of the second order matrix element and the LLA shower formalism should lead to an improved description similar to that of the matched NLLA and $\mathcal{O}(\alpha_s^2)$ calculations used in α_s determinations [24]. For the ME model the situation can be improved by including higher order terms as has been shown recently by OPAL [19].

2.2 Particle composition and spectra

Experimental studies of the spectra and composition of particles in hadronic jets provide an unique way to understand the fragmentation of quarks and gluons into hadrons. Thanks to the excellent performance of the detectors and high statistics available, very careful work by all four LEP experiments has given us a very complete picture of the production of identified particles from e^+e^- annihilation. All states in the $SU(3)$ pseudoscalar and vector meson nonets, except

7

the ρ^+, and at least one state per isospin multiplet in the baryon octet and decuplet, plus the scalar $f_0(980)$ and the tensors $f_2(1270)$, $K_2^*(1430)$ and $f_2'(1525)$ [26] have been measured. The average production rates per hadronic Z event, together with the predictions from the tuned [9] JETSET 7.4 and HERWIG 5.8, are listed in table 1 [21]. The measurements are in good agreement between experiments for all mesons and octet baryons. However for the decuplet baryons there are still discrepancies between experiments, reflecting difficulties in the measurements. In particular, the Δ^{++} signal is difficult to measure because of its large width and the large combinatorial background in combinations of π^+p. The Ω^- rate seems to be established around the value expected from JETSET, contrary to the old claims of an anomalously high production rate.

Particle rates could depend on many things, such as flavor content, spin, mass, phase space, hadron wave functions, Bose-Einstein interference and other collective effects. The two most frequently used models HERWIG and JETSET use different ways to account for the particle production rates. In the Lund/JETSET approach (similarly to the old Field & Feynman model [27]), the production rate of a specific hadron type depends principally on its flavor content and spin. One can also use essentially pure phase space as in the case of the HERWIG cluster fragmentation approach.

Studies of general features of particle production, such as the strangeness suppression factor s/u or the fraction of mesons produced in spin-1 states, $V/(V+P)$, or in orbitally excited states provide useful information about the main production mechanisms. The (one dimensional) string model suggests the production of orbitally excited states is small $\approx 10\%$ [28] whilst $V/(V+P) = 3/4$ is expected from simple spin counting.

Measurements of the $f_0(980)$, $f_2(1270)$, $K_2^*(1430)^0$ [21] and $f_2'(1525)$ [26] as well as of D^{**} and B^{**} mesons indicate that orbitally excited states, most of which so far were not included in HERWIG, JETSET and other models, are copiously produced ($\approx 30\%$ of the primary hadrons). Thus a quite large fraction of the observed stable particles come from decays of these numerous states. As a result, the $V/(V+P)$ ratio can differ significantly from that when no orbitally excited states are considered. From a global tuning, where the orbitally excited meson states are included, a value of $V/(V+P) \approx 0.4 - -0.6$ is obtained for light mesons [9, 29]. This low value of $V/(V+P)$ could be explained by mass differences between the vector and pseudoscalar mesons, i.e. by the relatively larger binding energy of pseudoscalar mesons[28]. The measured ratio of $V/(V+P) = 0.75 \pm 0.04$ [30] for B mesons agrees well with the expected value of $3/4$. However for D mesons the much lower value 0.46 ± 0.06 [31] is still not understood.

In the string fragmentation model, one expects the strangeness suppression factor s/u to be around 0.3 using the typical values of (constituent) quark masses. This parameter can be measured from the production rates of strange compared with non-strange mesons and from the momentum spectrum of strange mesons. The results, which are summarized in table 2, are very consistent with the expectation[1]. It is interesting to see that s/u determined from

---

[1]However, neutrino experiments at lower energies [32] and recently both ZEUS [33] and H1 [34] require a lower value of about 0.2 for s/u. More careful studies in this area are needed in the future.

Particle	Rate Measured	Experiments	Rate JETSET 7.4	Rate HERWIG 5.8
All charged	20.92 ± 0.24	ADLO	20.81	20.94
π^0	9.19 ± 0.73	DL	9.83	9.81
π^+	8.53 ± 0.22	O	8.55	8.83
K^0	1.006 ± 0.017	ADLO	1.09	1.04
K^+	1.185 ± 0.065	DO	1.12	1.06
η	0.95 ± 0.11	AL	1.10	1.02
η'	0.22 ± 0.07	AL	0.09	0.14
$f_0(980)$	0.140 ± 0.034	DL	0.16	—
ρ^0	1.29 ± 0.13	AD	1.27	1.43
K^{*0}	0.380 ± 0.021	ADO	0.39	0.37
K^{*+}	0.358 ± 0.034	DO	0.39	0.37
ω	1.11 ± 0.14	AL	1.32	0.91
ϕ	0.107 ± 0.009	ADO	0.107	0.099
$f_2(1270)$	0.25 ± 0.08	DL	0.29	0.26
$K_2^*(1430)^0$	0.095 ± 0.035	O	0.075	0.0785
$f_2'(1525)$	0.0224 ± 0.0062	D	0.026	0.03
p	0.49 ± 0.05	DO	0.485	0.39
Λ	0.186 ± 0.008	ADLO	0.175	0.184
Σ^0	0.0355 ± 0.0065	DO	0.036	0.0265
Σ^+	0.044 ± 0.006	DO	0.0343	0.0298
Ξ^-	0.0129 ± 0.0007	ADO	0.015	0.0247*
Δ^{++}	0.064 ± 0.033	DO	0.080	0.077
$\Sigma(1385)^+$	0.011 ± 0.002	ADO	0.009	0.0163
$\Xi(1530)^0$	0.0031 ± 0.0006	ADO	0.00345	0.0125*
Ω^-	0.00080 ± 0.00025	ADO	0.00095	0.00385*
$\Lambda\bar{\Lambda}$	0.089 ± 0.007	ADO	0.085	0.134*
$\Lambda\Lambda + \bar{\Lambda}\bar{\Lambda}$	0.0249 ± 0.0022	ADO	0.023	0.029

Table 1: Average particle production rates in hadronic Z decays (excluding charge conjugates and antiparticles), compared to the predictions of JETSET and HERWIG. A * indicates that the predicted rate differs from measurement by more than three standard deviations.

heavy mesons agrees well with the values obtained from light mesons. This suggests that the strangeness suppression occurs at the quark level.

Technique	Results	References
$\dfrac{K^{*0}}{\rho^0+\omega}$, $\dfrac{K^{*\pm}}{\rho^0+\omega}$, $\dfrac{2\phi}{K^{*0}}$, $\dfrac{2\phi}{K^{*\pm}}$, $\sqrt{\dfrac{2\phi}{\rho^0+\omega}}$	0.29 ± 0.03	table 1 [35]
$\dfrac{K^+}{\pi^+}$ at high momentum	$0.35 \pm 0.07(\text{stat})$	[35, 36]
$\dfrac{K^+}{\pi^+}$ at high momentum	$0.25 \pm 0.03(\text{stat})$	[35, 37]
K^0 momentum spectrum	0.285 ± 0.035	[38]
K^0 momentum spectrum	$0.30 \pm 0.02(\text{stat})$	[39]
Ratio $\dfrac{2f(\text{c} \to \text{D}_\text{s}^+)}{f(\text{c} \to \text{D}^+ + f(\text{c} \to \text{D}^0)}$	0.31 ± 0.07	[40]
Ratio $\dfrac{2\text{B}_\text{s}}{\text{B}_{\text{u,d}}}$	0.32 ± 0.08	[41]
Ratio $\dfrac{2\text{B}_\text{s}^{**}}{\text{B}_{\text{u,d}}^{**}}$	0.28 ± 0.11	[42]
$\text{B}^0\bar{\text{B}}^0$ mixing $(\chi_\text{B}, \chi_{\text{B}_\text{d}})$, f_{Λ_b}	~ 0.3	[43]

Table 2: Measurements of s/u at LEP

The relative rates of the decuplet baryons as well as those of the $\Sigma^{0,+}$ and Ξ^- provide a clean test of models, since they are less affected by resonance decays. From table 1, we obtain the following ratios:

Ratio	Measured	JETSET	HERWIG
Ξ^-/Σ^+	0.29 ± 0.04	0.44	0.84
Ξ^-/Σ^0	0.36 ± 0.07	0.42	0.93
$\Sigma(1385)^+/\Delta^{++}$	0.17 ± 0.09	0.11	0.21
$\Xi(1530)^0/\Sigma(1385)^+$	0.28 ± 0.07	0.38	0.77
$\Omega^-/\Xi(1530)^0$	0.26 ± 0.09	0.28	0.31

One obtains from the above ratios a suppression factor of about 0.28 per s quark for baryons (0.24 if only the decuplet baryons are considered). This is similar to the value obtained for mesons, suggesting that the additional suppression for diquarks might be small.

After being tuned to LEP 1 data, HERWIG and JETSET[2] describe well the measured rates in the meson sector. There is a fairly good agreement in the baryon octet, except that the proton rate is slightly underestimated and the Ξ^- rate is overestimated by about a factor of

---

[2]New parameters have to be introduced, as attempted in [9], to treat the quark type dependent production probabilities for pseudoscalar, vector and orbitally excited mesons.

two by HERWIG. In the baryon decuplet JETSET predictions are consistent with the data while the predictions of HERWIG differ from the data in most of the cases. Differences in the ratios of the baryon rates between HERWIG and data, as shown above, can not be solved simply by tuning the cluster fragmentation parameters, indicating the need for real dynamics beyond phase space and spin counting.

Although in general JETSET describes the measured rates better than HERWIG, it contains a large number of free parameters. As a result, it has little predictive power. The UCLA model [44], a variant of JETSET with less parameters, does a good job in many cases but has problems in the baryon decuplet. Also the copiously produced orbitally excited mesons so far are not included in the UCLA model. In [45] an interesting regularity in production rates is shown for all particles (except pions) belonging to the pseudoscalar and vector meson nonets and the baryon octet and decuplet. The particle multiplicity can be described by a simple exponential fall off in mass squared and $2J + 1$ spin counting factors. This regularity seems to be energy independent and has recently been established similarly also in $\bar{p}p$ interactions [46]. However it is necessary to use generalized isospin multiplets and to not seperate the contributions from resonance decays. Recently a new approach [47] has been proposed which uses only three free parameters but reproduces the measured rates quite well. The basic assumption used is that hadrons reach complete thermal and chemical equilibrium, in contrast to the general belief that $e^+e^- \rightarrow$ hadrons is a rapidly expanding process and during fragmentation the hadronic density is rather low. More tests are needed to check this thermodynamic approach.

Since all fragmentation models contain a number of parameters which can be tuned according to data (more dramatic in the case of JETSET), measurements of production rates do not provide a high discriminating power among different models. A more effective method is to look at baryon correlations. In JETSET the major source of baryon production is the creation of a diquark-antidiquark pair within the fragmentation. The baryon-antibaryon ($\mathcal{B}\bar{\mathcal{B}}$) rate is much higher than the $\mathcal{B}\mathcal{B}$ and $\bar{\mathcal{B}}\bar{\mathcal{B}}$ rate (see table 1) and $\mathcal{B}\bar{\mathcal{B}}$ are more likely to occur close in phase space than $\mathcal{B}\mathcal{B}$ or $\bar{\mathcal{B}}\bar{\mathcal{B}}$. Correlations between $\mathcal{B}\bar{\mathcal{B}}$ can be reduced by the *popcorn* mechanism, allowing a meson to be created in between a $\mathcal{B}\bar{\mathcal{B}}$ pair. As can be seen from table 1, HERWIG overestimates the $\Lambda\bar{\Lambda}$ rate (note that the prediction for the Λ is quite good), while JETSET with popcorn describes the data well. It has been shown in [48] that $\mathcal{B}\bar{\mathcal{B}}$ correlations, for example in rapidity, are overestimated by HERWIG, whilst JETSET with a high probability of the popcorn occurrence ($\sim 80\%$) reproduces the data well. A more impressive test is to study the angle between the baryon and the event axis in the $\mathcal{B}\bar{\mathcal{B}}$ rest frame. The string model predicts that baryon production is preferentially lined up along the event axis, while the cluster model predicts an isotropic distribution. Data [48] clearly favor the string model. Also measurements of baryon and antibaryon production in quark and antiquark jets with polarized beams by SLD [49] and jet charge studies [10] support the string model but disfavor the idea of isotropic cluster decays.

Identified particle spectra have been studied as function of both the scaled momentum $x_p = p/p_{\mathrm{beam}}$ and the variable $\xi_p = \log\frac{1}{x_p}$. In general all models describe the data fairly well, with few discrepancies remaining:

11

- Data show a harder momentum spectrum for the η produced in gluon jets [50].
- K$^{\pm}$ momentum spectra predicted by the models are too soft [36, 37, 51]. This might be caused by wrong branching fractions of b hadrons in the models.
- Momentum spectra of light quark baryons predicted by the models are too hard [36, 37, 48, 51, 52]. This indicates a different production mechanism for baryons than for mesons. Partly it may also be due to missing orbitally excited baryon states in the models. However, so far these states have not been observed in e$^+$e$^-$ annihilation.

The heavy quark fragmentation function has been measured at LEP 1 mainly using D$^{(*)}$ reconstruction in the c-quark case [53] and using high-$p_{\perp}$ lepton spectra [54], D*−lepton combinations [55], and exclusive [56] and inclusive b-reconstruction [57] in the case of b-quark fragmentation. The D-meson distributions are obscured by contributions from b-hadron decays. Today the (experimentally involved) inclusive b-hadron reconstruction yields the best statistical precision. It allows for the first time (besides a precise determination of the average b-hadron energy $\langle x_E \rangle$) a decisive comparison to different fragmentation models. This, so far incomplete comparison, gives best agreement for LLA based parton shower models (ARIADNE, JETSET and HERWIG) combined with Peterson fragmentation [58]. The HERWIG cluster fragmentation as well as the Lund-symmetric and the modified Lund-Bowler ansatz give less satisfactory results. In the case of JETSET ME with Peterson fragmentation a too narrow energy distribution indicates the lack of soft gluon emission.

2.3 Differences between q and g jets

In QCD, the gluon is associated with a color charge $C_A = 3$ and the quark with a charge $C_F = 4/3$. The larger color charge of the gluon means that it is more likely to radiate an additional gluon than a quark, leading to differences in the expected properties of quark- and gluon-induced jets. For quark and gluon jets produced with the same energy and under the same conditions, gluon jets are expected to have a larger mean particle multiplicity than quark jets [59]. The larger multiplicity of the gluon jet implies that its particle energy spectrum, known as the fragmentation function, is softer. A related prediction is that the mean opening angle of particles in a gluon jet is larger than in a quark jet [60]: thus the gluon jets are broader. Much experimental effort has been invested in an attempt to observe these predicted differences (for a recent compilation, see [61] and references therein). Before LEP 1, there were experimental indications that gluon jets were indeed broader than quark jets, based on measurements of the mean transverse momentum of particles in a jet with respect to the jet axis, or similar variables. However, contradictory results were published concerning differences between the quark and gluon jet fragmentation functions, while no evidence was found for a multiplicity difference between the two jet types. In general, it proved difficult to obtain conclusive results on quark-gluon jet differences at facilities before LEP 1 either because biases were introduced by assuming the gluon jets to be the lowest energy jets in e$^+$e$^-$ three-jet events or else because there was no event-by-event identification of gluon jets with a resulting lack of sensitivity.

Due to large event statistics and good detector capabilities, the LEP experiments have been able to settle the experimental question of quark and gluon jet differences [62, 63]. Three aspects of the LEP 1 studies allow this success. (1) Symmetric events were selected in which the quark and gluon jets being compared had the same energy and angles relative to the other jets, allowing a direct, model independent comparison of the jet properties. (2) The quark jets were tagged, leading to identification of the gluon jets with better than 90% purity through anti-tagging. (3) The anti-tagged gluon jet data were combined algebraically with the quark and gluon jet data from the untagged, symmetric events, leading to separated quark and gluon jet measurements with essentially no biases except from the jet definition. In the first LEP 1 studies, the quark jet samples were the natural ones for Z^0 decay, given by the Z^0 coupling strength to the individual flavors, corresponding to roughly 20% d, u, s, c and b quarks. In later studies, b quark jets and uds quark jets were explicitly selected to compare to gluon jets [64].

These studies resulted in a confirmation of the qualitative differences between quark and gluon jets given above. Selecting 24 GeV jets in a so-called "Y" symmetric event topology, it was shown that gluon jets were 60–80% broader than quark jets as measured by the full width at half maximum of the differential energy and multiplicity profiles [65]. The fragmentation function of the gluon jet was observed to be much softer than that of the quark jet. The mean charged particle multiplicity of gluon jets was found to exceed that of quark jets by 20–25%. Besides the Y events, DELPHI [63] studied 30 GeV jets from three-fold symmetric "Mercedes" events and obtained similar results. The comparison of the fragmentation function of quark and gluon jets in Y and Mercedes events shows the expected stronger energy dependence for gluon jets. Extensive comparisons of Monte Carlo predictions to the quark and gluon jet data are presented in [65] and [64]. ARIADNE, HERWIG and JETSET were found to be in good agreement with the measurements. The COJETS agreement was somewhat less good.

ALEPH [66] extended these studies by including a measurement of sub-jet multiplicities [67]. For small values of the sub-jet resolution scale, y_0 (defined using the $k_\perp$ jet finder), the ratio of the gluon to quark jet mean sub-jet multiplicity was found to be similar to the hadron level value of about 1.2 discussed above. After subtracting one from the mean sub-jet multiplicities to account for the contributions of the initiating quarks and gluons, the sub-jet multiplicity ratio of gluon to quark jets was observed to reach a much larger value of about 2.0 as y_0 approached the resolution scale y_1 at which the jets were defined. The explanation for this is that the mean sub-jet multiplicity of the quark jets approaches unity slightly before that of the gluon jets as $y_0 \to y_1$. ARIADNE, HERWIG, JETSET and NLLJET were all found to reproduce the measurement.

Beyond these studies based on symmetric events, ALEPH and DELPHI have examined quark and gluon jet properties in non-symmetric three-jet event configurations. The DELPHI approach [63] is to identify gluon jets in three-jet events using anti-tagging methods as mentioned above. The gluon jet properties were compared to those of quark jets with similar energies found in radiative QED $q\bar{q}\gamma$ events. The qualitative differences discussed above between quark and gluon jets were observed to be present for jet energies between 5 and 40 GeV

and were well reproduced by JETSET. ALEPH [68] introduced a new method to study the multiplicity difference between quark and gluon jets in three-jet events, by examining the mean charged particle multiplicity of the entire event as a function of the energies and opening angles of the jets in the event. Assuming each event to be composed of a gluon jet and two quark jets, and that every particle in an event could be associated with one of these jets, a fit was made to extract a value for the ratio of the mean charged particle multiplicity values of gluon to quark jets, r_{ch}. The result for all jet energies and event topologies was $r_{ch} = 1.48$. The fit results were found to agree well with those from the symmetric Y analyses when they were restricted to that geometric situation.

Thus the basic differences expected between quark and gluon jets — a larger mean multiplicity, a softer fragmentation function and a larger angular width of gluon relative to quark jets — are now all well established by the LEP 1 experiments. The QCD models are in good overall agreement with the measured differences. Future effort in this field at LEP 1 will probably include studies of differences in the identified particle rates in gluon and quark jets, differences in particle correlation phenomena and attempts to reduce the reliance of the analysis method on the jet definition (as the ALEPH study [68] discussed above attempts to do). Already, L3 has presented results which indicate an enhanced η meson production rate in gluon jets compared to the rates predicted by HERWIG and JETSET [50]. This suggests that the models for gluon jets may need to be modified to allow for an enhanced production of isosinglet mesons [69].

2.4   Coherence

Gluon radiation in the parton shower should be coherent. However, gluon interference only becomes apparent when one goes beyond the Leading Log Approximation (LLA). A number of such effects are found in the next simplest approximation, the Modified LLA (MLLA) [70]. Due to the non-abelian nature of QCD, the overall result of this interference is "angular ordering" of the gluon radiation [71], which constrains the angles between the radiator and the radiated gluon to decrease as the evolution proceeds to lower scales.

In parton-shower Monte Carlos gluon interference is either: imposed as an *a posteriori* constraint on gluon opening angles as in JETSET [15]; built into the choice of evolution variable as in HERWIG [14]; or neglected in independent fragmentation models such as COJETS [72]. ARIADNE [13], on the other hand, employs a formulation based on a cascade of $q\bar{q}$, qg and gg dipoles which naturally incorporates interference phenomena. In JETSET the angular-ordering constraint can be turned off. By comparing JETSET with and without angular ordering one can obtain an idea of the importance of the effect.

Some consequences of gluon interference have been calculated directly in perturbative QCD as well as by Monte Carlo. Such calculations apply, strictly speaking, only to partons. Comparison with data relies on the additional assumption of Local Parton Hadron Duality (LPHD) [73, 74], which posits that many distributions of hadrons rather closely follow the corresponding parton distribution, with non-perturbative effects affecting mainly the normalization rather

than the shape of the distributions. However, we shall not emphasize such calculations here, since our main purpose is to evaluate the adequacy of current Monte Carlo programs.

The first effect to be explained [75] as a consequence of gluon interference was the so-called string effect; first predicted using (non-perturbative) string fragmentation phenomenology [76] and later discovered by the JADE experiment [77]. In terms of gluon interference it is explained as a purely perturbative effect at the parton level. The string effect has been extensively studied, most recently by DELPHI [63], L3 [78] and OPAL [79]. These analyses have compared $q\bar{q}g$ and $q\bar{q}\gamma$ events taking care to have samples of comparable kinematic configurations. The string effect appears as a smaller particle flow in the region between the quark jets in $q\bar{q}g$ than in $q\bar{q}\gamma$ events. ALEPH [80] instead compared the particle flow between the quarks with that between quark and gluon. The string effect is found to be rather well reproduced by the coherent Monte Carlo models but not by the incoherent ones. However this success is not entirely due to the coherence at parton level; the non-perturbative modelling in the programs also contributes.

It is also worth mentioning that evidence of gluon interference is also seen in $p\bar{p}$ interactions at the Tevatron. Using events with 3 high-$p_\perp$ jets CDF examined the differences in rapidity and in azimuthal angle between quark and gluon jets [81]. HERWIG, which incorporates co-herence in both space-like and time-like showers, reproduced the data well. PYTHIA/JETSET, with coherence only in time-like showers did less well, although it improved when modified to partially incorporate coherence in space-like showers. ISAJET, with no coherence, performed poorly.

As is well known [70], gluon interference leads to suppression of soft gluons in the shower, which in turn should lead to a suppression of soft hadrons. The distribution of $\xi_p = -\ln x_p = -\ln p/p_{\text{jet}}$ is expected to have a roughly Gaussian shape and its peak position, ξ^*, should increase with $\sqrt{s}$. The dependence of ξ^* on $\sqrt{s}$ is strikingly different in the MLLA from that in the LLA. Assuming LPHD, ξ^* is expected to show similar behaviour. Many comparisons have been made, for many types of particle, using data from PETRA/PEP, TRISTAN, and LEP; they support the form predicted by MLLA and clearly reject the LLA form.

From MLLA+LPHD it is expected [82] that ξ^* decrease with the mass of the hadron. This is indeed found to be the case with ξ^* being approximately proportional to $-\ln M_{\text{hadron}}$. However, the proportionality constant is quite different for mesons and baryons [51]. This difference is due to decays. When the ξ_p distributions are corrected for decays [37, 51, 83], using JETSET, the ξ^* values of mesons and baryons are found to lie on a universal curve [51]. The conclusion is clearly that we must be cautious about the interpretation of LPHD, in particular with the inclusion of decays.

The $\sqrt{s}$ dependence of ξ^* is support for MLLA, but says little about the quality of the Monte Carlo programs, since they are retuned at each value of $\sqrt{s}$. However, accepting the validity of MLLA, the improvement seen in the previous paragraph supports the description of non-perturbative hadronization in the model.

The angular ordering resulting from gluon interference effectively moves the radiated gluons

closer to the jet axis. The size of the effect depends on the colour charge of the radiator and on the initial configuration of the event (i.e. 2 or 3 jets, there being interference effects in the interjet region for 3-jet events as seen in the string effect). The total number of (sub-)jets found in an event has been calculated [67] in the Next-LLA (NLLA) as a function of the jet resolution parameter, $y_{cut} = y_0$, for 2- and 3-jet events classified using $y_{cut} = y_1 > y_0$. Of course, if y_1 becomes too small non-perturbative processes become important and the calculation breaks down. The perturbative and non-perturbative regions are rather clearly separated and the sub-jet multiplicities thus provide a test not only of perturbative QCD calculations and their incorporation into Monte Carlo programs, but also of the non-perturbative models in the programs.

Sub-jet multiplicities have been studied [84, 85] at LEP 1. Quite good qualitative agreement is found between the data and the NLLA calculations in the perturbative region while a simple $\mathcal{O}(\alpha_s)$ calculation clearly disagrees. Of the Monte Carlo programs, ARIADNE does quite well; HERWIG 5.5 and JETSET 6.3 perform somewhat less well; and the incoherent model COJETS gives the worst agreement. Both versions 6.12 and 6.23 of COJETS disagree in the perturbative region while only 6.23 disagrees in the non-perturbative region. JETSET was compared [85] using various combinations of fragmentation and parton shower schemes. Incoherent parton showers resulted in poor agreement in both perturbative and non-perturbative regions independently of the fragmentation scheme. Coherent showers gave much better agreement in the perturbative region. In the non-perturbative region agreement was poor for independent fragmentation whilst good for string fragmentation.

The MLLA predicts [86] a suppression of gluon emission within a cone of angle $\theta < \theta_0 = M_q/E_q$ about the quark direction in a parton shower. This should lead to a lower *primary* multiplicity for heavy quark events. However, the total multiplicity is higher because of the high multiplicity of heavy flavour decays. The difference in multiplicity between heavy and light quark events is predicted to be independent of $\sqrt{s}$, contrary to the naïve expectation that the difference would decrease as the quark mass difference becomes smaller compared to the total energy. Results from PEP/PETRA, TRISTAN, and LEP/SLC agree reasonably well with the MLLA value, both for charm and beauty, particularly when the recent work of Petrov and Kisselev [87] is taken into account. The results [88, 89, 90] at $\sqrt{s} = M_Z$ agree reasonably well with the predictions of JETSET, with the possible exception of light (uds) quarks.

Given the appearance of angular ordering in MLLA, the effects of gluon interference should be apparent in angular correlations. Assuming LPHD, the correlations should persist in the hadrons. Besides the angular ordering in the polar angle, also the azimuthal angular distribution is affected by gluon interference. OPAL [91], has studied two-particle correlations in the azimuthal angle within restricted rapidity intervals. To avoid defining a jet axis they, and more recently ALEPH [92], have also studied such correlations using the Energy-Multiplicity-Multiplicity Correlation (EMMC) [93]. Taking in turn each track's direction as an axis the correlation calculated, the EMMC is the average of these correlations weighted by the axis defining track's energy. The EMMC has been calculated analytically in leading [93] and next-to-leading [94] order; the corrections are large. LPHD must be assumed to apply these calculations to

16

those calculated from hadrons. Nevertheless, qualitative agreement is obtained for $\phi > \pi/2$, where Monte Carlo models show hadronization to be relatively unimportant. Agreement with the data is even better for Monte Carlo models which incorporate gluon interference. Models not incorporating this interference fail to describe the data.

ALEPH [92, 95] and L3 [96, 97] have studied two-particle angular correlations in the full spatial angle using the Asymmetry in the Particle-Particle Correlation (APPC). In addition, L3 has studied the Asymetry in the Energy-Energy Correlation AEEC. The APPC is defined in analogy to the well-known AEEC by simply removing the energy weighting. This results in a correlation which is sensitive to all branchings of the shower, whereas the AEEC is primarily sensitive to the earliest branchings. The APPC is less sensitive to systematics in the correction for detector effects. On the other hand, the energy weighting makes the AEEC less sensitive to the Bose-Einstein effect. The use of the asymmetry serves to cancel some of the correlations arising from other effects as well as some detector effects and Monte Carlo uncertainties.

These correlations have been compared with Monte Carlo models. The conclusion is that the models containing gluon interference agree much better with the data than do the incoherent models. However neither version of NLLJET can be said to agree well.

All of these studies favour the Monte Carlo models ARIADNE, HERWIG and JETSET, which incorporate the gluon interference expected in MLLA. In general the agreement of data with these models is quite good. On the other hand, models that do not incorporate gluon interference, such as COJETS and incoherent JETSET do not in general agree well with the data. Both coherent and incoherent versions of NLLJET have been found also not to agree well with data.

2.5   Prompt photons

The principal source of observable prompt photons in hadronic decays of the Z (i.e. those with energies greater than a few GeV) is final state radiation (FSR) emitted at an early stage in the parton evolution process initiated by the primary quark–antiquark pair. To reduce large backgrounds from non-prompt sources, the first measurements reported by OPAL [98] and followed later by the other LEP experiments selected events with photons well isolated from the hadrons by a geometrical cone followed by a 2-step jet reconstruction process. In this procedure, the candidate photon is first removed from the event and all the hadrons reconstructed into jets. Then, the photon is replaced and its isolation from the jets tested in a second application of the clustering algorithm. It was soon realized that the cross sections are substantially less than those predicted from fractionally charged fermion pairs due to the influence of gluons. Thus, the measurement of prompt photons has become a sensitive test of the predictions of both perturbative QCD matrix element calculations and the Monte Carlo shower models free from the direct effects of fragmentation.

After tuning the parameters of these models in recent versions, namely ARIADNE 4.2, HERWIG 5.4 and JETSET 7.3 to the properties of the hadrons observed in non-FSR events,

17

there is no freedom to adjust the photon emission parameters with the exception of the infra-red cut-off. In the following reported analyses, these cut-off values are chosen to be similar to those employed to terminate the parton evolution, but in any case do not significantly influence the isolated hard photon rates.

All the published high statistics analyses from ALEPH, L3 and OPAL [99] show that both ARIADNE and HERWIG give acceptable descriptions of the total and individual n-jet $+$ γ cross sections as a function of the jet resolution parameter, y_{cut} (JADE E0), as well as the distributions in $p_\perp$ and fractional energy z_γ of the photon. A more critical test to differentiate between these two models is based on their predictions for the rate of low energy photons (< 15 GeV) at large angles ($> 75°$) to the event thrust axis, where the evolution scale ordering used in HERWIG predicts a larger cross section than ARIADNE [100]. Preliminary data from ALEPH indicate that ARIADNE gives the better description but more statistics are needed. However, the above published results show that JETSET is less satisfactory predicting cross sections that are 20-30% low (3σ's). ALEPH showed that this can be improved by either switching off the $\mathcal{O}(\alpha_{\text{s}})$ matching or by keeping α_{s} constant indicating that virtuality as the scale controlling the parton evolution is not the best choice. More recently, DELPHI has also shown [101] that their data are in excess of JETSET by 18±7% in the low energy region of the photon spectrum below 15 GeV. After clustering the hadrons with the Durham ($k_\perp$) algorithm in a similar 2-step procedure, their respective jet rates above $y_{\text{cut}} \geq 0.01$ are in reasonable agreement with JETSET. The excess is largely eliminated since most low energy photons are no longer isolated when the clustering algorithm is applied a second time. This appears to be a different conclusion from the other experiments. However, careful examination shows that the discrepancy between JETSET and data for ALEPH and L3 are largely at low y_{cut} in the total cross section where the use of different algorithms for jet-finding makes comparison difficult with DELPHI. It should be noted also that DELPHI compare with JETSET at *hadron* level before fragmentation corrections are applied.

The 2-step analysis procedure to select isolated photon events does not prevent a significant number of non-isolated hard photons from contaminating the γ + 1-jet event topology. Each of these photons remain within the hadron jet formed from the remnant of the radiating quark and are better separated from the isolated radiation by a "democratic" analysis [102]. Here, the prompt photon candidate is not removed from the event and thus becomes a member of a hadron jet with fractional energy z_γ of its total energy. The true isolated component is now concentrated at $z_\gamma = 1$ broadened downwards in z_γ by hadronization effects to overlap with the high energy tail of the collinear quark fragmentation component. For the γ + 1-jet (ie: 2-jet) cross section, this is well separated from the fragmentation tail when $z_\gamma \geq 0.95$. Fig. 5 shows the comparison as a function of y_{cut} (Durham E0 scheme) between the data measured by ALEPH and the predictions of ARIADNE and JETSET for this isolated component. The continuous curve is a prediction of a leading order calculation dominated by perturbative terms which are derived from a pure QED calculation. HERWIG (not shown) is in close agreement with the data. JETSET falls well below the data in this case showing that its treatment of radiation as independent emission from either quark at the first branching is quite inadequate. This discrepancy diminishes as the jet multiplicity increases. There is more satisfactory agreement
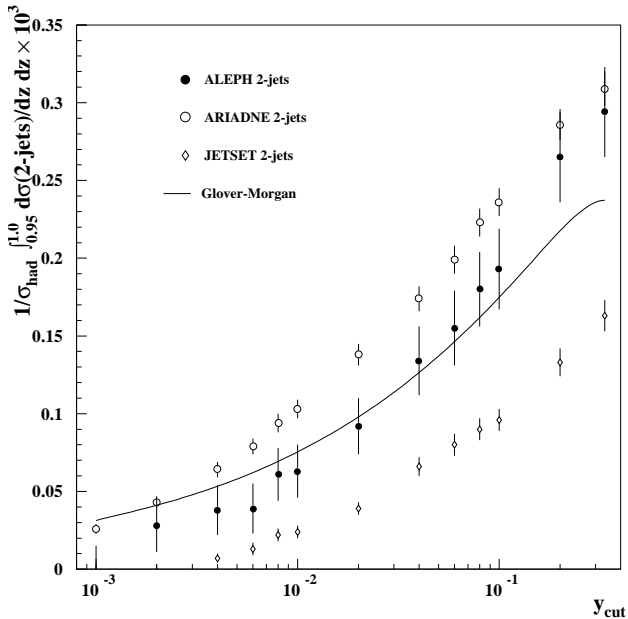
18

Figure 5: Integrated 2-jet rate above $z_\gamma = 0.95$ as a function of y_{cut}, compared with ARIADNE, JETSET and a QCD calculation.

in the fragmentation region below $z_\gamma = 0.95$.

Overall, the conclusion is that HERWIG gives the best description of all prompt photon data at the Z closely followed by ARIADNE.

In this review it is appropriate to mention the difficulties faced in determining the non-prompt photon background coming from hadrons decaying into γ's (mainly π^0). The isolation and energy cuts applied to the prompt photon candidates in the 2-step analyses are insufficient to eliminate this background entirely even when the full granularity of the electromagnetic calorimeters is exploited to recognize single from multiple γ showers. Hence, an irreducible non-prompt component must be subtracted statistically using QCD models or inferred from other data. However, the selection cuts applied choose a region of phase space that is not well understood in these models as they correspond to tails in the fragmentation process which cannot be tuned precisely.

The early analyses made at LEP 1 showed a clear discrepancy in the hadronic background yield predicted by the HERWIG and JETSET models [104]. The magnitude of the differences depends strongly on the isolation and energy cuts. A substantial effort has been made to quantify these discrepancies in detail, most recently by L3 [105]. They are able to reconstruct well resolved π^0s and ηs from two identified photons isolated by a geometric cone in which no other particles are found with energies above 50 MeV. JETSET reproduces the observed rate of π^0s and ηs with energies above 3 GeV for $10°$ isolation, but significantly underestimates the rate for $25°$ isolation. This study was restricted to 8 GeV maximum energy where the direct meson reconstruction procedure is efficient, but has been extended to 45 GeV using a neural network. The observed background rate of non-prompt photons is about a factor 2 larger than the predicted rate over the full energy range and the discrepancy increases with tighter isolation cuts. HERWIG tends to give a slightly better prediction but still underestimates the rate.

In other studies at the Z of the non-prompt photon background both ALEPH [99] and

19

DELPHI [101] have reported that JETSET underestimates the isolated π^0 yields but only in the lower part of the energy spectrum below 20 GeV. In these analyses, the limit allowed for the maximum particle energy accompanying the photon in the cone is set to 500 MeV. They are not inconsistent with the L3 results but instead demonstrate that the comparison with the generators is sensitively dependent on the isolation parameters. In the alternative "democratic" analysis without isolation cones of ALEPH [102] some activity is allowed in the vicinity of the γ which results in a better description by JETSET of the region of phase-space considered for the fragmentation.

2.6   Bose–Einstein effects

Most of the Bose–Einstein interference studies at LEP 1 have concentrated on two-particle correlations between identical charged pions [106] using the quantity

$$R(M) = \frac{\rho_2(M)}{\rho_1 \otimes \rho_1(M)} \tag{1}$$

Here, $\rho_2(M)$ is the two-particle correlation function, usually given as a function of Q, $Q^2 = M^2 - 4m_\pi^2$, and $\rho_1 \otimes \rho_1(M)$ is a reference sample. This sample should resemble $\rho_2(M)$ except for the Bose-Einstein correlations being studied.

Two choices for the reference sample are made, unlike-sign pion pairs or uncorrelated pairs from track mixing. Both alternatives have disadvantages. Unlike-sign pion pairs suffer from correlations due to resonances not present in like-sign pion pairs and the contribution of resonances with poorly known rates, especially η and η' at low Q. Furthermore residual effects of Bose–Einstein interference may also be visible in the unlike-sign pairs (see below). The track mixing has the disadvantage that correlations, other than from Bose-Einstein interference, are missing. In addition cuts to suppress gluon radiation must be applied. For both methods the systematic uncertainties are reduced using the double ratio $R^{\mathrm{data}}(M)/R^{\mathrm{MC}}(M)$. Additional corrections for background, e.g., Coulomb interactions are applied.

Assuming a spherical and Gaussian source the enhancement at low Q is parameterized as $R(M) \sim 1 + \lambda \exp(-r^2 Q^2)$. The chaoticity parameter λ is expected to vary between 0 and 1, and is extracted from data in the range from 0.4 to 1.5; the radius r of the source is measured to be 0.4 fm to 1 fm. In Fig. 6 the background-corrected measurements are displayed for the mesons $\pi^\pm$, π^0, $K^\pm$, and K^0.

Only identical mesons, that are prompt, i.e. do not originate from long-lived resonances, can contribute to the enhancement at low Q. It has been pointed out that the measured value of λ is about the maximum you could expect from direct pairs or even higher [107].

In more recent analyses the fraction $f(Q)$ of direct pions as a function of Q has been parameterized using Monte Carlo and included in the fit. For example DELPHI uses $f(Q) = 0.17 + 0.26Q - 0.12Q^2$, obtained from JETSET, to fit λ and r for charged pions: $R(M) \sim$
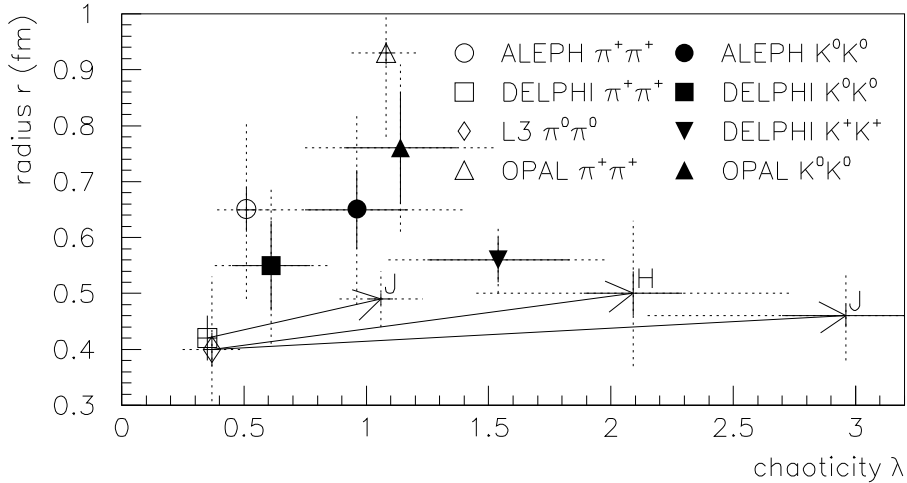
Figure 6: Chaoticity parameter λ versus radius r measured at LEP 1. Measured values are corrected for background with statistical (solid line) and total errors (dots) shown. The arrows indicate the changes, when corrected for non-prompt meson-pairs estimated with HERWIG or JETSET, when it is calculated by the experiment [106, 108, 109].

$1 + \lambda f(Q) \exp(-r^2 Q^2)$ [106]. Whilst the change in the radius is small, λ is changed by a factor 3. A bigger change is reported by L3 for $\pi^0 - \pi^0$ correlations [108]. The corrections are very sensitive to the model used. The corrections for non-prompt mesons are indicated by arrows in Fig. 6. The kaons have higher chaoticity values than pions before correction [109]. Only DELPHI has estimated the corrections for non-prompt kaons. The correction for kaons from c- and b-decay increases λ by ≈ 25 to 30%.

Three-particle correlations have been studied by DELPHI. Whilst JETSET without Bose-Einstein correlations fails to describe the data, JETSET with Bose-Einstein correlations enabled gives a fair description of unlike-sign triplets; the shape is reproduced, but the magnitude is too small [110].

Bose-Einstein correlation affect the unlike-sign spectra as well. In the invariant mass distribution of pions the ρ^0 meson appears shifted towards lower masses [111]. In the framework of the model this can be interpreted as coming from Bose-Einstein correlations between like-sign pion pairs, which induces correlations between unlike-sign combinations, for example seen as a distortion of the ρ^0 line shape. OPAL finds nice agreement between data and JETSET including Bose-Einstein correlations, when the chaoticity parameter is set to 2.5. This value of λ was obtained with a fit to the ratio $R(M)$. ALEPH agrees with this observation and extracts a ρ^0 rate with λ and r as free parameters. The value of $\lambda = 2.1$ is compatible with OPAL in view of the different η' rate and choice of the coherence time parameter χ. (χ gives the minimum width of resonances whose daughters contribute to the Bose-Einstein enhancement). DELPHI,

which observes a shift of the ρ^0, uses its λ value extracted from the Bose-Einstein analysis, after correction, for the ρ^0 analysis. Also with this parameter choice the agreement of data and model mass spectra is satisfactory [112].

Concerns have to be raised about the implementation of Bose-Einstein correlations in JET-SET. The implementation treats them as a classical force, which violates energy-momentum conservation. The rescaling applied to restore the total energy and momentum, however, twists the event shape variables and the model description becomes worse. Multijet rates for larger y_{cut} are reduced by up to 20% and the tails of the thrust and minor distributions are decreased by 5-10%. The amount of particles with low rapidities is depleted by $\approx$5%. A small but significant improvement is observed for small $p_{\perp out}$. The wave structure visible for $p_{\perp out} <$ 0.8 GeV vanishes when well tuned BE parameters are used and the $p_{\perp out}$ distribution here can be perfectly described [11]. Studies on a modified implementation, which also moves unlike-sign pairs to avoid rescaling (additional ϵ parameter) improves the situation but the description of the ρ^0 mass shift is in the wrong direction (positive).

Another new simulation, based on the area spanned by the string, is in preparation. A first result with a toy Monte Carlo predicts that the reconstructed λ should be 2 for π^0, when $\lambda = 1$ is used for event generation [113].

At first glance, the experimental results are different, $\lambda \approx 1$ for corrected direct measurements (DELPHI) and $\lambda \approx 2$ for an extraction tuning the JETSET model. However the following differences must be kept in mind. The use of track mixing for a reference distribution tends always to give lower λ values than the use of the unlike-sign meson sample. The uncorrected values for DELPHI are lower than for the other experiments. For kaons, corrections are estimated for c- and b-decays only, but not for strong decays. ALEPH has used daughters of resonances wider than $\Gamma = 100\,\mathrm{MeV}/c^2$ as prompt pions, excluding the K* which seems not to be affected by Bose-Einstein correlations. Ignoring this and correcting OPAL for the η' rate would bring the values down to $\lambda = 1.7$ in these two analyses.

On the model side more understanding is needed of how to include the correlation without twisting the event shape distribution. The new ϵ parameter is a first step but there is no real success yet. Taking the decay amplitudes, i.e. string area, may be another promising approach.

3 Extrapolation to LEP 2 Energies

A question of interest for LEP 2 is that of how well the characteristics of QCD events are understood at large energies. By QCD events, it is here meant those that are produced through the s-channel decay of a Z^0/γ^* into quark and gluon jets. This question is of interest because W^+W^- events lead to multi-jet states for which one of the principal backgrounds will be QCD events, because QCD events will also form a principal source of background for higgs, chargino and other particle searches, and because QCD events will be interesting in their own right as a means to test perturbation theory in a regime with particularly small hadronization uncertainties. The principal tools to test how well QCD event characteristics are understood are Monte Carlo generators. The main generators, ARIADNE, COJETS, HERWIG and PYTHIA, have been tuned by the LEP experiments or by the Monte Carlo authors to describe global features of hadronic Z^0 data. In many cases, the generators have proven able to describe detailed features of these data as well. It is thus relevant to extrapolate the predictions of the QCD generators to LEP 2 energies and to compare their level of agreement for distributions likely to be of importance at LEP 2. In this section, such an extrapolation and comparison is presented.

For this study, members of each of the LEP experiments generated Monte Carlo event samples at $E_{\rm cm}$= 175 GeV using parameter sets determined within their Collaboration. The Monte Carlo parameter sets used at LEP 1 are continually revised in order to yield as accurate a description of the Z^0 data as possible. Therefore, the parameter sets employed for this study do not necessarily represent official versions which will be published by the Collaborations. The parameter sets used for ARIADNE, HERWIG and PYTHIA are given in tables 3–5. For COJETS, L3 and OPAL results were made available using the parameter values given in table 6. There are numerous parameters and strategies involved in the optimization of the parameters. Comparison of the results obtained using the parameter sets of the different Collaborations therefore provides a systematic check of effects associated with the optimization choice. Samples of 100,000 events were generated without initial-state photon radiation or detector simulation, treating all charged and neutral particles with mean lifetimes greater than $3 \cdot 10^{-10}$ s as stable.

The following distributions were examined using charged particles only:
1. charged particle multiplicity, $n_{\rm ch}$,
2. scaled particle momentum, $x_p = 2p/E_{\rm cm}$,
3. component of particle momentum in the event plane, $p_{\perp\rm in}$, and
4. component of particle momentum out of the event plane, $p_{\perp\rm out}$.

The event plane was defined by the two vectors associated with the two largest eigenvalues of the Sphericity tensor.

The following distributions were examined using both charged and neutral particles:
1. Thrust, T [114],
2. Thrust major, $T_{\rm major}$ [115],
3. Thrust minor, $T_{\rm minor}$ [115],
4. jet rates R_n defined using the $k_\perp$ jet finder [116],

Parameter	Name	Default	ALEPH	DELPHI	L3	OPAL
Λ_{LLA}	PARA(1)	0.220	0.218	0.237	0.220	0.200
$p_\perp$ cutoff	PARA(3)	0.60	0.58	0.64	1.00	1.00
Fragmentation function	MSTJ(11)	4	3	3	3	4
Baryon model option	MSTJ(12)	2	2	3	2	2
$\mathcal{P}(qq)/\mathcal{P}(q)$	PARJ(1)	0.100	0.100	0.096	0.100	0.100
$\mathcal{P}(s)/\mathcal{P}(u)$	PARJ(2)	0.300	0.300	0.302	0.300	0.300
$(\mathcal{P}(us)/\mathcal{P}(ud))/(\mathcal{P}(s)/\mathcal{P}(d))$	PARJ(3)	0.400	0.400	0.650	0.400	0.400
$(1/3)\mathcal{P}(ud_1)/\mathcal{P}(ud_0)$	PARJ(4)	0.050	0.050	0.070	0.050	0.050
$\mathcal{P}(S{=}1)_{d,u}$	PARJ(11)	0.500	0.500	—	0.500	0.500
$\mathcal{P}(S{=}1)_s$	PARJ(12)	0.600	0.600	—	0.600	0.600
$\mathcal{P}(S{=}1)_{c,b}$	PARJ(13)	0.750	0.750	—	0.750	0.750
Axial, $\mathcal{P}(S{=}0,L{=}1;J{=}1)$	PARJ(14)	0.000	0.000	—	0.100	0.000
Scalar, $\mathcal{P}(S{=}1,L{=}1;J{=}0)$	PARJ(15)	0.000	0.000	—	0.100	0.000
Axial, $\mathcal{P}(S{=}1,L{=}1;J{=}1)$	PARJ(16)	0.000	0.000	—	0.100	0.000
Tensor, $\mathcal{P}(S{=}1,L{=}1;J{=}2)$	PARJ(17)	0.000	0.000	—	0.250	0.000
Extra baryon suppression	PARJ(19)	1.000	1.000	0.500	1.000	1.000
σ_q	PARJ(21)	0.360	0.354	0.390	0.500	0.370
extra η suppression	PARJ(25)	1.000	1.000	0.650	0.600	1.000
extra η' suppression	PARJ(26)	0.400	0.400	0.230	0.300	0.400
a	PARJ(41)	0.300	0.500	0.391	0.500	0.180
b	PARJ(42)	0.580	0.810	0.850	0.650	0.340
ϵ_c	PARJ(54)	-0.050	-0.050	-0.0378	-0.030	—
ϵ_b	PARJ(55)	-0.0050	-0.0060	-0.00255	-0.0035	—

Table 3: Optimized parameter sets for ARIADNE, version 4.06 (for ALEPH, version 4.05), from the LEP Collaborations. The parameters listed are those which were changed from their default values by at least one of the groups. The ARIADNE events were generated using PYTHIA version 5.7 to describe the hadronization and hadron decays. The DELPHI Collaboration implements its own procedure to specify the relative rate at which mesons are produced in different multiplets [9], in place of the PYTHIA parameters PARJ(11)-PARJ(17).

Parameter	Name	Default	ALEPH	DELPHI	L3	OPAL
Λ_{MLLA}	QCDLAM	0.180	0.149	0.163	0.170	0.160
Cluster mass parameter 1	CLMAX	3.35	3.90	3.48	3.20	3.40
Cluster mass parameter 2	CLPOW	2.00	2.00	1.49	1.45	1.30
Effective gluon mass	RMASS(13)	0.750	0.726	0.650	0.750	0.750
Photon virtuality cutoff	VPCUT	0.40	1.00	0.40	0.50	0.40
Smearing of cluster direction	CLSMR	0.00	0.56	0.36	0.00	0.35
Weight for decuplet baryons	DECWT	1.00	1.00	0.77	1.00	1.00
s quark weight	PWT(3)	1.00	1.00	0.83	1.00	1.00
diquark weight	PWT(7)	1.00	1.00	0.74	1.00	1.00

Table 4: Optimized parameter sets for HERWIG, version 5.8, from the LEP Collaborations. The parameters listed are those which were changed from their default values by at least one of the groups.

5. normalized heavy jet mass for events divided into hemispheres by the plane perpendicular to the Thrust axis, $M_{\mathrm{heavy}}/E_{\mathrm{cm}}$ [117],

6. normalized difference between the heavy and light jet masses, $M_{\mathrm{diff}}/E_{\mathrm{cm}}$,

7. total jet broadening, B_T [118],

8. wide jet broadening, B_W [118],

9. Sphericity, S [119],

10. Aplanarity, A [120],

11. the modified Nachtmann-Reiter four-jet angular variable, $|\cos\theta^*_{\mathrm{NR}}|$ [121], with four-jet events defined using the $k_\perp$ jet finder with $y_{\mathrm{cut}}{=}0.01$, and

12. the cosine of the angle between the two lowest energy jets in the four-jet events, $\cos\alpha_{34}$.

In addition, the mean values of n_{ch}, T, T_{major} and T_{minor} were examined as a function of E_{cm}.

The results for $\langle n_{\mathrm{ch}}\rangle$, T, T_{major} and T_{minor} as a function of E_{cm} are shown in Fig. 7. For those cases in which the results of at least three Collaborations are similar to each other, the Monte Carlo predictions are shown as shaded or hatched bands. The widths of the bands show the maximum deviations between the results found by the different Collaborations. The widths of the bands are generally much larger than the statistical uncertainties. In a few cases, the Monte Carlo prediction obtained by one of the Collaborations differs significantly from those obtained by the other three groups and is shown as a separate curve. The COJETS predictions are likewise shown as separate curves for purposes of clarity. The results found by the four LEP experiments are labelled A, D, L and O in the figure legends.

Representative measurements from PEP, PETRA, TRISTAN and LEP 1 are included in Fig. 7. For $E_{\mathrm{cm}}{=}$ 175 GeV, an indicative "data point" is also shown, which is taken to be equal to the mean of the PYTHIA predictions from the four groups. The size of the symbol for the LEP 2 point is larger than the statistical uncertainty for 10 000 QCD events. Systematic terms were generally found to dominate the statistical ones for the experimental measurements shown in Fig. 7. The total experimental uncertainties at 175 GeV can therefore be expected to

Parameter	Name	Default	ALEPH	DELPHI	L3	OPAL
Fragmentation function	MSTJ(11)	4	3	3	3	3
Baryon model option	MSTJ(12)	2	2	3	2	2
Azimuthal correlations	MSTJ(46)	3	0	3	3	3
$\mathcal{P}(qq)/\mathcal{P}(q)$	PARJ(1)	0.100	0.095	0.099	0.100	0.085
$\mathcal{P}(s)/\mathcal{P}(u)$	PARJ(2)	0.300	0.285	0.308	0.300	0.310
$(\mathcal{P}(us)/\mathcal{P}(ud))/(\mathcal{P}(s)/\mathcal{P}(d))$	PARJ(3)	0.400	0.580	0.650	0.400	0.450
$(1/3)\mathcal{P}(ud_1)/\mathcal{P}(ud_0)$	PARJ(4)	0.050	0.050	0.070	0.050	0.025
$\mathcal{P}(S{=}1)_{d,u}$	PARJ(11)	0.500	0.550	—	0.500	0.600
$\mathcal{P}(S{=}1)_s$	PARJ(12)	0.600	0.470	—	0.600	0.400
$\mathcal{P}(S{=}1)_{c,b}$	PARJ(13)	0.750	0.600	—	0.750	0.720
Axial, $\mathcal{P}(S{=}0,L{=}1;J{=}1)$	PARJ(14)	0.000	0.096	—	0.100	0.430
Scalar, $\mathcal{P}(S{=}1,L{=}1;J{=}0)$	PARJ(15)	0.000	0.032	—	0.100	0.080
Axial, $\mathcal{P}(S{=}1,L{=}1;J{=}1)$	PARJ(16)	0.000	0.096	—	0.100	0.080
Tensor, $\mathcal{P}(S{=}1,L{=}1;J{=}2)$	PARJ(17)	0.000	0.160	—	0.250	0.170
Extra baryon suppression	PARJ(19)	1.000	1.000	0.500	1.000	1.000
σ_q	PARJ(21)	0.360	0.360	0.408	0.399	0.400
extra η suppression	PARJ(25)	1.000	1.000	0.650	0.600	1.000
extra η' suppression	PARJ(26)	0.400	0.400	0.230	0.300	0.400
a	PARJ(41)	0.300	0.400	0.417	0.500	0.110
b	PARJ(42)	0.580	1.030	0.850	0.848	0.520
ϵ_c	PARJ(54)	-0.050	-0.050	-0.038	-0.030	-0.031
ϵ_b	PARJ(55)	-0.0050	-0.0045	-0.00284	-0.0035	-0.0038
Λ_{LLA}	PARJ(81)	0.290	0.320	0.297	0.306	0.250
Q_0	PARJ(82)	1.000	1.220	1.560	1.000	1.900

Table 5: Optimized parameter sets for PYTHIA, version 5.7, from the LEP Collaborations. The parameters listed are those which were changed from their default values by at least one of the groups. The DELPHI Collaboration implements their own procedure to specify the relative rate at which mesons are produced in different multiplets [9], in place of the PYTHIA parameters PARJ(11)–PARJ(17).

Parameter	Name	Default	L3	OPAL
b_g	FRALOG(2)	46.6	100.0	46.6
d_g	FRALOG(4)	1.52	2.10	1.52
b_q	FRALOQ(2)	30.5	43.0	30.5
d_q	FRALOQ(4)	1.52	2.10	1.52

Table 6: Optimized parameter sets for COJETS, version 6.23, from the L3 and OPAL Collaborations. The parameters listed are those which were changed from their default values by at least one of the groups.
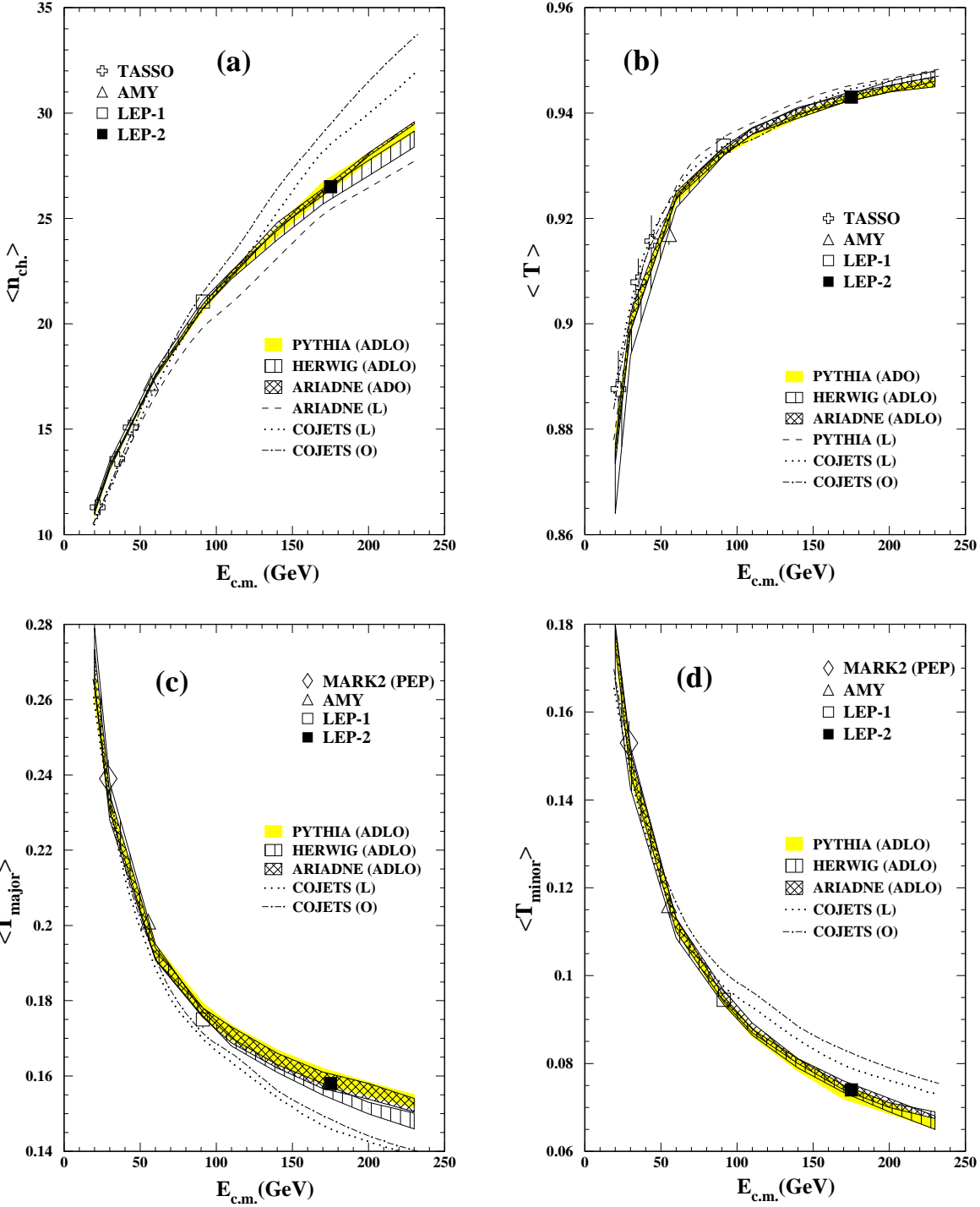
Figure 7: The mean values of n_{ch}, Thrust T, T_{major} and T_{minor} predicted by ARIADNE, COJETS, HERWIG and PYTHIA as a function of E_{cm} in comparison with measurements from PEP, PETRA, TRISTAN and LEP 1. The LEP 2 point is indicative only, based on the PYTHIA prediction. The total uncertainty expected at LEP 2 assuming 10 000 QCD events is smaller than the symbol size.

27

be comparable to those found for the LEP 1 data.

From the distribution of $\langle n_{\rm ch} \rangle$ versus $E_{\rm cm}$ (Fig. 7(a)), it is seen that, with the exception of the L3 ARIADNE curve, the predictions of ARIADNE, HERWIG and PYTHIA are similar. The widths of the ARIADNE, HERWIG and PYTHIA bands are narrow for energies at and below the Z^0 mass, showing that the results from the four Collaborations are in close agreement (with the exception of the L3 curve for ARIADNE). For energies above about 150 GeV, the HERWIG band becomes broader, indicating that there is some divergence in the predictions obtained by the different groups. From Fig. 7(a) it is also seen that COJETS predicts a substantially larger value of $\langle n_{\rm ch} \rangle$ than the other models for energies above the Z^0 mass. This difference is suggestive of coherence effects in the parton shower, which are absent in COJETS but present in the other three models. Coherence reduces the mean soft gluon multiplicity in the parton shower. It is generally expected that coherence will lead to a reduction in the mean hadron multiplicity as well. Thus, a measurement of $\langle n_{\rm ch} \rangle$ at LEP 2 could help to establish the existence of coherence phenomena in the data.

Figs. 7(b)–(d) show the corresponding distributions for the T, $T_{\rm major}$ and $T_{\rm minor}$ variables. Again, ARIADNE, HERWIG and PYTHIA are seen to exhibit similar behavior. COJETS agrees well with the other models for T, but lies below them for $T_{\rm major}$ and above them for $T_{\rm minor}$ in the LEP 2 energy range. Thus the jets from COJETS are less oblate than those from ARIADNE, HERWIG or PYTHIA. (The Oblateness O of an event is given by $O = T_{\rm major} - T_{\rm minor}$.) The differences between COJETS and the other three models become larger as $E_{\rm cm}$ increases.

In Fig. 8, the Monte Carlo predictions for $n_{\rm ch}$, x_p, $p_{\perp \rm in}$ and $p_{\perp \rm out}$ at 175 GeV are shown. The corresponding results for T, $T_{\rm major}$, $T_{\rm minor}$ and R_n, for $M_{\rm heavy}/E_{\rm cm}$, $M_{\rm diff}/E_{\rm cm}$, B_T and B_W, and for S, A, $|\cos\theta^*_{\rm NR}|$ and $\cos\alpha_{34}$ are shown in Figs. 9, 10, and 11, respectively. Overall, the models are seen to be in general agreement with each other. Some of the more notable exceptions to this agreement are discussed below.

1. A striking difference is observed between COJETS and the other models for the $n_{\rm ch}$ and $p_{\perp \rm in}$ distributions (Figs. 8(a) and (c)). Smaller but visible differences are observed between COJETS and the other models for a number of the other distributions as well. At the Z^0 mass, these differences between COJETS and the other models are either not present or are much smaller. This implies that the energy scaling behavior of COJETS differs from that of ARIADNE, HERWIG and PYTHIA.

2. For HERWIG, the x_p distribution is much harder using the L3 parameter set than it is using the parameter sets of the other Collaborations (Fig. 8(b)). This feature is also observed at the Z^0 energy. The primary reason for this difference between L3 and the other groups is the different treatment of the parameter CLSMR (see table 4).

3. From Fig. 9(d), it is seen that the three-jet rate from PYTHIA is significantly larger than that of the other models for $y_{\rm cut}$ values below about 0.02. Correspondingly, the two jet rate from PYTHIA is smaller. This difference is also observed at $E_{\rm cm} = 91$ GeV. From this same figure, COJETS is seen to predict a three-jet rate which is smaller than that of the other models: this last difference is not observed at LEP 1 energies.

4. COJETS exhibits a clear deviation with respect to the predictions of the other models for
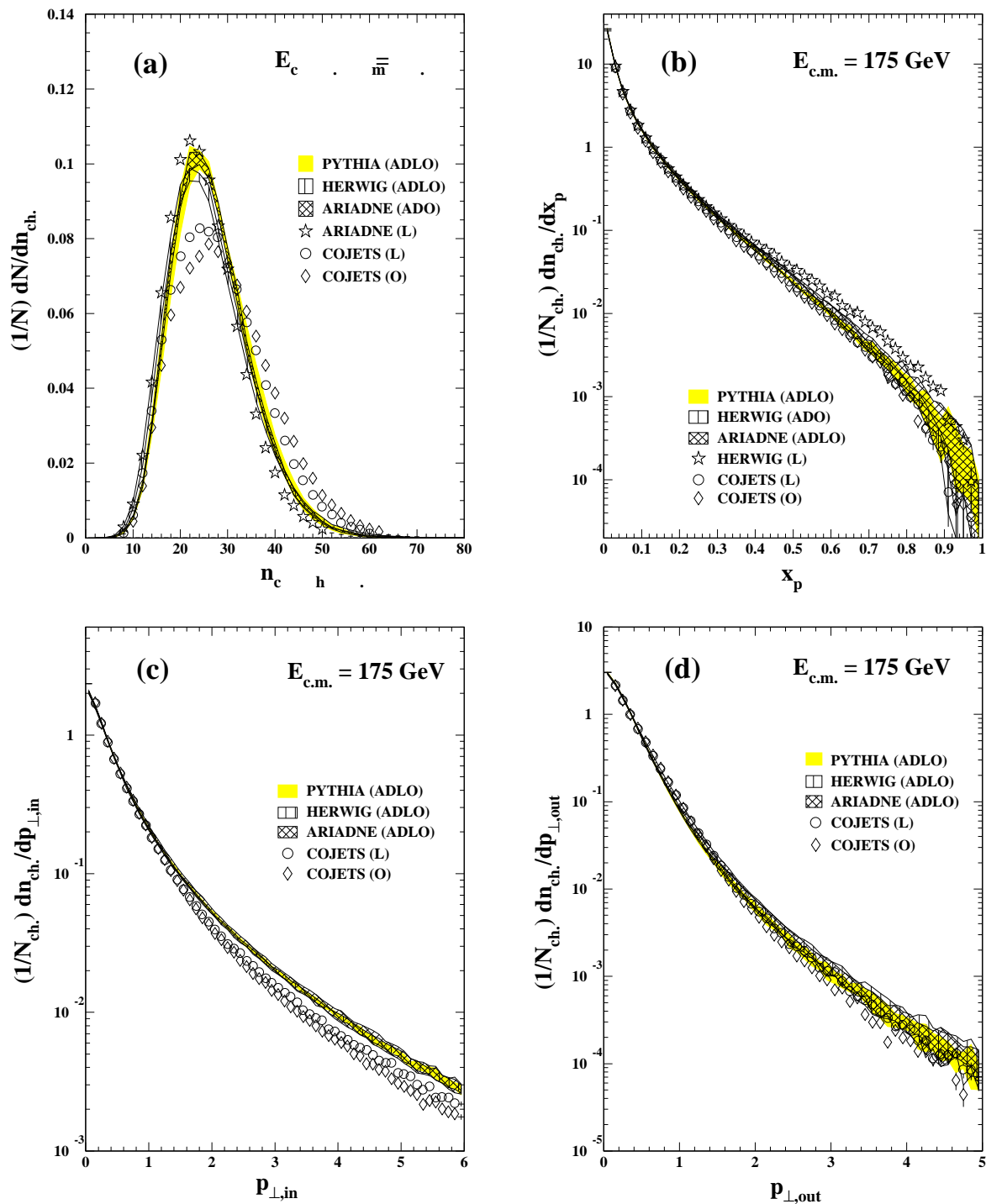
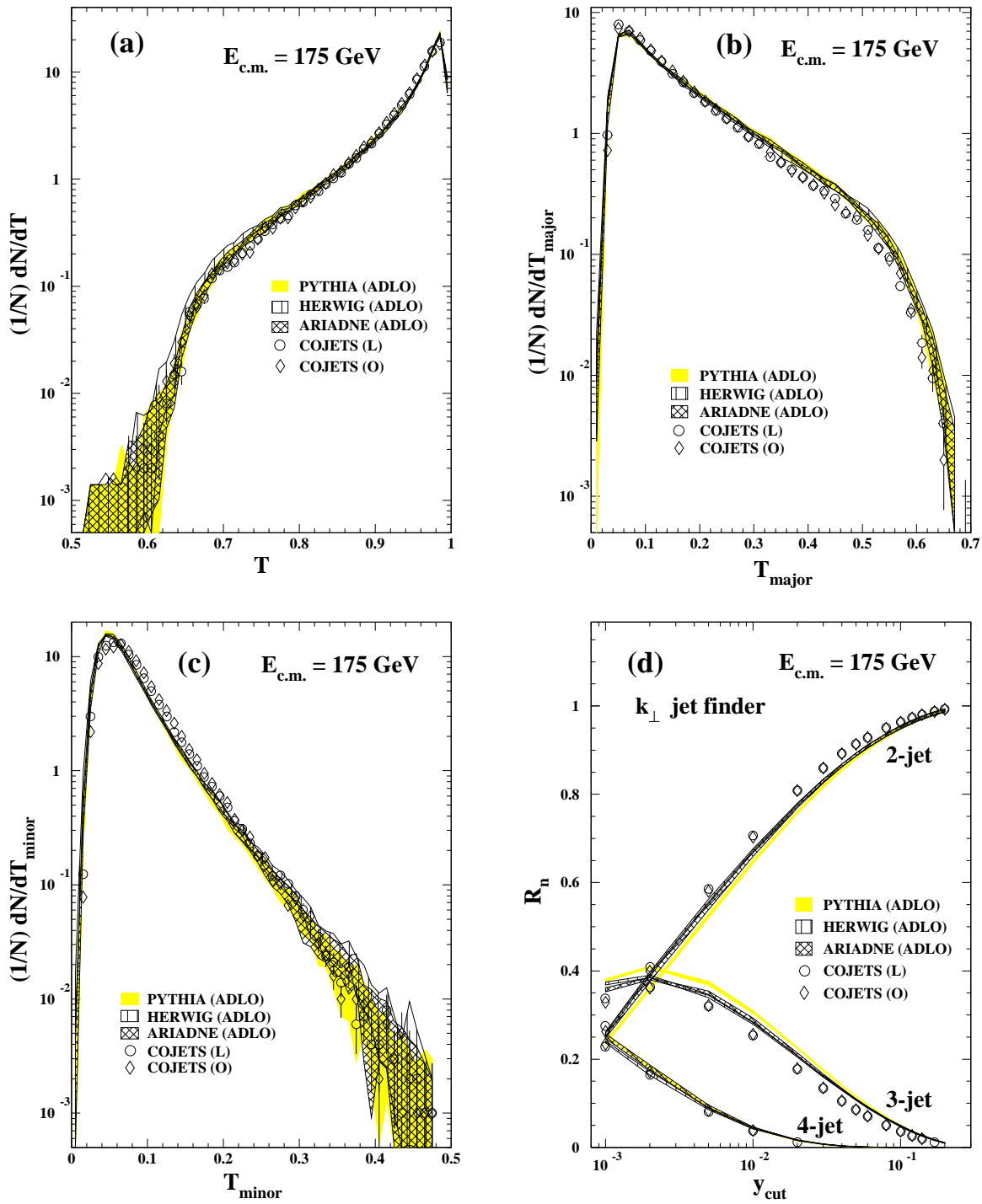Figure 8: Comparison of the predictions of QCD event generators at E_{cm}= 175 GeV.

Figure 9: Comparison of the predictions of QCD event generators at $E_{cm} = 175$ GeV.

the jet mass distributions, $M_{\text{heavy}}/E_{\text{cm}}$ and $M_{\text{diff}}/E_{\text{cm}}$ (Figs. 10(a) and (b)). Less of a deviation is present for the jet broadening variables, B_T and B_W (Figs. 10(c) and (d)). This suggests that these last two variables may be less subject to uncertainties related to the modelling of QCD and hadronization than the first two variables.

5. COJETS and HERWIG are seen to exhibit a somewhat flatter distribution in $|\cos\theta^*_{\text{NR}}|$ than ARIADNE and PYTHIA (Fig. 11(c)).

The general conclusion that can be drawn from this study is that there is relatively little uncertainty in the predictions of QCD generators for event characteristics at LEP 2. Such basic features of events as charged multiplicity, Thrust and Oblateness are described in an almost identical manner by ARIADNE, HERWIG and PYTHIA. Only COJETS deviates significantly from the predictions of the other models. On the other hand, there is modest disagreement between the models for variables which require use of a jet finding algorithm: R_n (Fig. 9(d)) and $|\cos\theta^*_{\text{NR}}|$ (Fig. 11(c)). This could have some implication for the W mass determination based on the reconstruction of jets.
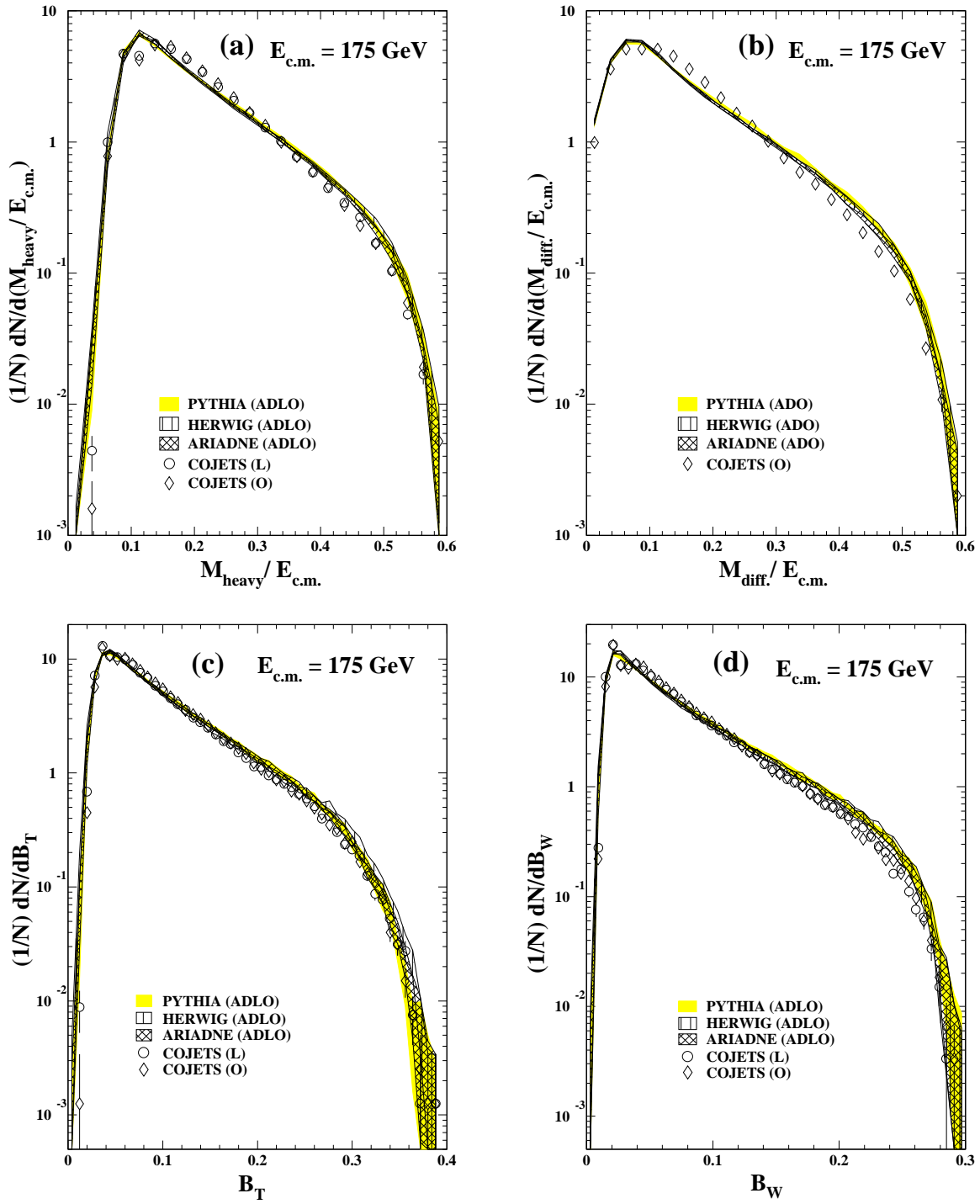
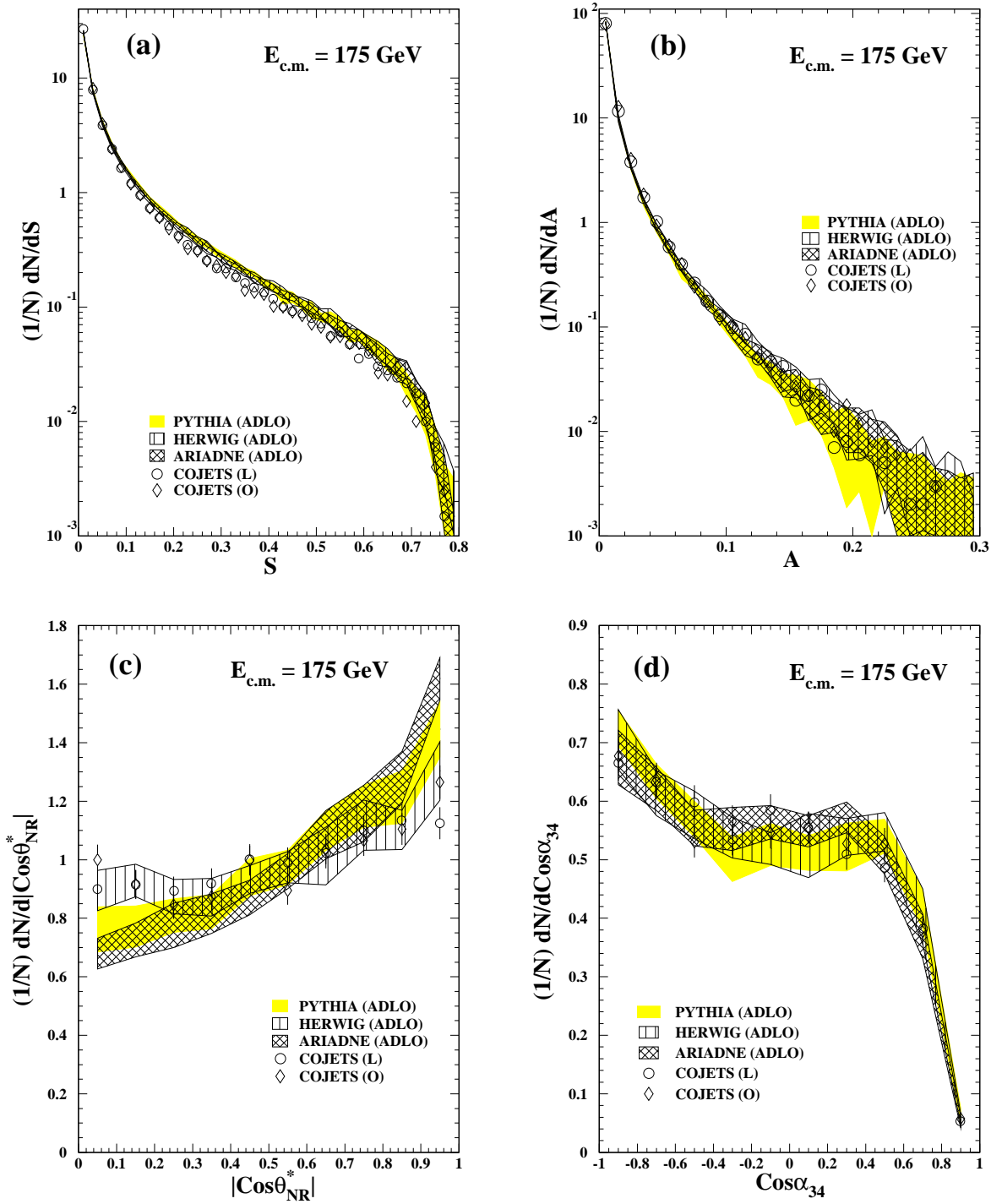Figure 10: Comparison of the predictions of QCD event generators at $E_{cm} = 175$ GeV.

Figure 11: Comparison of the predictions of QCD event generators at $E_{cm} = 175$ GeV.

4 Monte Carlo descriptions

In this section we have collected brief descriptions for the main QCD generators and other pieces of QCD code. These writeups are intended to introduce the main physics ideas and give further references to manuals and codes — a full coverage of all physics and programming aspects is excluded for space reasons. The compilation below should be rather complete for programs intended for the main QCD-related processes, such as γ^*/Z^0 and W pair production. Special emphasis is put on HERWIG and PYTHIA/JETSET, which have been used extensively at LEP 1 and are equipped with a simulation both of electroweak and QCD aspects. A few programs include QCD aspects but have still been judged to better belong elsewhere, e.g. PHOJET is a $\gamma\gamma$ physics generator and ISAJET is mainly of interest (in the e^+e^- sector) as a supersymmetry generator.

4.1 ARIADNE

Basic Facts

Program name:	ARIADNE [13]
Version:	4.08 of 30 November 1995
Author:	Leif Lönnblad
	NORDITA, Blegdamsvej 17,
	DK 2100 Copenhagen Ø, Denmark
	Phone: + 45 – 35325285
	E-mail: leif@nordita.dk
Program size:	12853 lines
Program location:	http://surya11.cern.ch/users/lonnblad/ariadne/

The ARIADNE program implements the Dipole Cascade Model (DCM) for QCD cascades [122]. In this model the emission of a gluon g_1 from a $q\bar{q}$ pair created in an e^+e^- annihilation event can be described as radiation from the colour dipole between the q and $\bar{q}$. A subsequent emission of a softer gluon g_2 can be described as radiation from two independent colour dipoles, one between the q and g_1 and one between g_1 and $\bar{q}$, neglecting the contribution from the $q\bar{q}$ dipole, which is suppressed by $1/N_C^2$. Further gluon emissions are given by three independent dipoles, *etc.* In this way, the end result is a chain of dipoles, where one dipole connects two partons, and a gluon connects two dipoles. This is in close correspondence with the Lund string picture, where gluons act as kinks on a string-like field stretched between the $q\bar{q}$ pair.

This formulation of the partonic cascade in terms of colour dipoles means that the coherence effects, handled by introducing angular ordering in conventional parton showers, is correctly taken into account. Also, the DCM has the advantage that the first gluon emission is done according to the correct first-order matrix element, so that an explicit matching procedure like the ones introduced in HERWIG and JETSET is not needed.

Although the model has been developed a lot since the last LEP workshop, much of this development has been related to the description of Deep Inelastic Scattering and hadron-hadron collisions and will be described in some detail in the report from the $\gamma\gamma$ generator working group. Here only aspects relevant to e^+e^- annihilation will be discussed.

The basic DCM only describes gluon emission, and the process of splitting a gluon into a $q\bar{q}$ pair has therefore been added according to [123]. Although this procedure reproduces fairly well the amount of secondary $c\bar{c}$ production observed at LEP [124], there has been some criticism [125] that the model may be overestimating the phase space available for this process. Therefore an extra restriction of this phase space suggested in [125] has been implemented as an option in the last versions.

The radiation of photons from quarks is handled by allowing the process of emitting a photon from the *electro-magnetic* dipole between the original $q\bar{q}$ to compete with the gluon emission from the colour dipoles [126]. This competition is governed by the ordering in transverse momenta of the emitted gluons/photons, which is different from JETSET and HERWIG, where virtuality and angle, respectively, is used for ordering.

In the latest version, a scheme for colour reconnections has been added to the program. The model is described fully in [127] and briefly in section 4.7. Unfortunately, the manual included in the code distribution has not yet been updated to describe this new feature, and users who want to try it are advised to contact the author by e-mail before doing so.

Since ARIADNE only handles the perturbative QCD cascade in an event, it has to be interfaced to the PYTHIA/JETSET programs for generation of the hard sub-process, the hadronization and the particle decays. Such an interface is included in the code, and only very minor changes to the steering program is needed to replace the parton showers in PYTHIA/JETSET with the dipole shower in ARIADNE for any type of process. In a typical steering program for running PYTHIA, the changes needed are as follows.

- Immediately before the call to PYINIT there should be inserted a call to ARTUNE('4.07') to set up default parameters in ARIADNE and PYTHIA/JETSET, followed by a call to ARINIT('PYTHIA') to initialize the PYTHIA interface. To change the default behavior of ARIADNE, changes may be made to the ARDAT1 common block *between* the calls to ARTUNE and ARINIT.
- Immediately after a call to PYEVNT, a call to AREXEC should be made to perform the actual dipole cascade. If PYTHIA is set up to handle fragmentation and decays in the PYEVNT call, this is now handled in AREXEC instead.

Sample programs for how to do this is included in the distribution. The distribution also includes a subroutine AR4FRM which is an interface to four-fermion generators according to the standard presented in section 5.3. Except for what is needed to run PYTHIA/JETSET, no additional software is required to run ARIADNE.

4.2   COJETS

Basic Facts
Program name: COJETS [128]
Version: COJETS 6.23 of 10 February 1992
Author: Roberto Odorico
Department of Physics
University of Bologna
Via Irnerio 46, I-40126 Bologna, Italy
Phone: + 39 − 51 - 24 20 18
E-mail: odorico@bo.infn.it
Program size: 19742 lines
Program location: http://www.bo.infn.it/preprint/odorico.html

COJETS simulates electron-positron annihilation into jets of hadrons. (It also simulates proton-proton and antiproton-proton interactions.) The simulation is based, at the parton level, on the standard model with perturbative QCD treated in the leading-log approximation. QED radiation off beam particles is treated according to the BKJ program. Partons from parton showers are independently fragmented into jets of hadrons according to a Field-Feynman model extended to include heavy quarks and baryons and modified in the generation of soft particles. Gluons are fragmented as a pair of light quark and antiquark jets of opposite random flavors, each one having half the energy of the gluon and its same direction and with fragmentation parameters distinct from those of quark jets. Jet non-perturbative masses are limited by bounds originated by an approximate treatment of global phase-space effects at the multi- jet level. A previous version of the program, COJETS 6.12, in which quarks and gluons share the same fragmentation model is also available. The jet fragmentation model adopted goes hand in hand with the setting of the minimum parton-mass cutoff to a value of 3 GeV, which is substantially larger than those used in string- and cluster-based fragmentation models.

The output common block, containing the generated particle stream, has the standard /HEPEVT/ format, with PDG codes used for particles.

COJETS is maintained with the PATCHY code management system. The appropriate FOR-TRAN77 codes are obtained by means of suitable pilot patches. The program file also includes the documentation.

Recently, the program has been mainly used to check the relevance of evidence for string fragmentation, parton coherence and quark/gluon differences in jet fragmentation. Its usage to study the signal/background enrichment for bottom non-leptonic decay events by means of neural networks has shown that differences in internal correlations between signal and background are fuzzier in COJETS than in JETSET [129]. Thus for LEP 2 COJETS could be useful when studying ways of disengaging events with W pairs decaying non-leptonically from background.

COJETS had its fragmentation parameters sensibly tuned to reproduce basic experimental distributions. So far the tuning has been done by the author, mimicking experimental apparatus

36

effects but without a proper GEANT simulation. That can be done by the user by means of the program TUNEMC, based on Minuit's Simplex algorithm (a more advanced version of the program is in preparation).

Programs COJETS 6.12 and TUNEMC can be found at the same WWW URL as COJETS 6.23.

4.3 HERWIG

Basic Facts

Program name:	HERWIG [14]
Version:	HERWIG 5.9 from 1 January 1996
Authors:	G. Marchesini[1], B.R. Webber[2], G. Abbiendi[3], I.G. Knowles[4],
	M.H. Seymour[5], L. Stanco[3]
	1, Dipartimento di Fiscia, Universita di Milano.
	2, Cavendish Laboratory, University of Cambridge.
	3, Dipartmento di Fisica, Universita di Padova.
	4, Department of Physics and Astronomy, University of Glasgow.
	5, Theory Division, CERN.
	E-mail: webber@hep.phy.cam.ac.uk, knowles@v6.ph.gla.ac.uk,
	seymour@surya11.cern.ch.
Program size:	15500 lines
Program location:	http://surya11.cern.ch/users/seymour/herwig/

4.3.1 Introduction

HERWIG (Hadron Emission Reactions With Interfering Gluons) is a large, multipurpose Monte Carlo event generator which has been extensively used at LEP 1. Version 3.2, as applied to e^+e^- annihilation, was described in detail for the LEP 1 workshop [130], here we concentrate principally on program developments and new aspects of relevance to LEP 2 physics.

QCD Monte Carlo event generators utilize the fact that any hard scattering processes can be factorized into separate components at leading twist. These are: the hard sub-process itself; perturbative initial and final state showers; non-perturbative hadronization; resonance decays; and beam remnant fragmentation. In HERWIG great emphasis is placed on making available a very sophisticated, partonic treatment of the calculable QCD showers. In contrast the description of the at present uncalculable hadronization and beam remnant components is in terms of very simple models. Since HERWIG contains many hard sub-processes and supports all combinations of hadron, lepton and photon beams this allows the physics of many types of particle collisions to be simulated in the same package. In view of the universality of the factorized components that build up HERWIG events this allows experience gained at HERA and the TEVATRON, for example, to be made directly available to LEP physicists.

Since version 3.2 was released the HERWIG code was reorganized to isolate the shower, cluster hadronization and unstable particle decay routines. This modularity facilitates the creation of hybrid programs in which sections of code are replaced with interfaces to other Monte Carlo programs. To identify HERWIG code the names of all options statements now begin `HW****`. The `/HEPEVT/` standard proposed in [131] is also now used throughout the program in `DOUBLE PRECISION`. The random number generator has been upgraded to a l'Ecuyer's algorithm as recommended in [132]. Discussion of physics changes are contained in the following sections.

4.3.2 Hard Sub-processes

An extensive range of hard sub-processes are available in the HERWIG program allowing the full spectrum of standard model LEP 2 physics to be simulated. These are illustrated in table 7; for a complete listing see the program release notes in the text file `HERWIGnm.DOC`.

The matrix elements used for the continuum processes `IPROC`=100–153 now allow for arbitrary polarization of the lepton beams, an additional Z' including complete γ^*/Z^0 interference and full mass effects ($IQ \neq 0$). When the `ZPRIME=.TRUE.` option is set the Z' weak couplings used are taken from the arrays `AFCH(*,2)` and `VFCH(*,2)`, see `HWIGIN` for details. The arrays `Q/V/AFCH(*,1)` are used consistently throughout the program for the standard model electric, weak vector and axial-vector fermion couplings. A running electromagnetic coupling $\alpha_{\rm em}(Q^2)$ is used for internal photons [133] with the hadronic part taken from [134]. It is normalized to the Thomson limit ($Q^2 = 0$) value `ALPHEM`. Process 107 is included to facilitate q/g studies; in analogy with quarks the gluons are given a $1 + \cos^2\theta$ distribution. The difference between processes 100–106 and the original 120–126 lies in the treatment of hard gluon emission. The massless matrix element matching scheme used by HERWIG is discussed under parton showers.

Specialist Matrix Element programs for W^+W^-/Z^0Z^0 production, more properly four fermion generators, employ the full set of gauge invariant diagrams. In comparison HERWIG only includes the subset of diagrams containing W^+W^- ("CC03") or Z^0Z^0 ("NC02") pairs but does provide realistic hadronic final states. These matrix elements are taken from the program of Kunszt [135] and correctly include spin correlations in the gauge boson decays. Additionally a model for colour re-arrangement within the context of HERWIG is available, see 4.7 for details. The decays of the vector bosons are controlled via the array `MODBOS`, as detailed in `HWIGIN`, and include spin correlations. Please also see the detailed prescription, discussed in section 5.3, for interfacing HERWIG to specialist four fermion Monte Carlos.

At LEP 2 the principal Higgs production mechanism is the Bjorken process, `IPROC`=300+ID, where one or both Z^0's may be off-shell, $Z^{0(*)} \to Z^{0(*)}h^0$; also available is vector boson fusion, `IPROC`=400+ID. In both cases the exact leading order matrix element is used in the improved s-channel approximation [136]. At LEP 2 a discoverable Higgs would be narrow; in the program the actual mass used is taken from within the range $[M_{\rm h} - \texttt{GAMMAX}\star\Gamma_{\rm h}, M_{\rm h} + \texttt{GAMMAX}\star\Gamma_{\rm h}]$ (default `GAMMAX=10`) using a 'Breit-Wigner' distribution corrected for an energy dependent width. The event weight is the product of the cross-section (in nb) multiplied by the branching ratio to the

channel specified by `ID`. The Higgs' partial widths are calculated in `HWDHIG`: the quark decay channels include next–to–leading logarithmic corrections and the vector boson decay modes allow for off-shell WW/ZZ pairs.

The cross-sections for $\gamma\gamma$ interactions rise with c.m. energy to become the commonest physics processes at LEP 2. When considering hadronic final states each photon may be viewed as interacting either as a point-like particle or as being resolved into constituent (anti-)quarks and gluons. This leads to three basic sets of hard sub-processes (zero, singly or doubly resolved), a division adopted in the wide selection of sub-processes made available in HERWIG. Note that this separation is in fact artificial and all three components must be combined to obtain the full cross-section. Discussion of these processes can be found in the HERWIG description provided in the gamma-gamma section of this report.

4.3.3 Initial State Radiation

In e^+e^- scattering real photons are radiated from the incoming lepton lines. At LEP 1 any effects were mitigated against by the penalty involved in going off the Z^0 resonance. However photon bremsstrahlung is expected to be an important feature at LEP 2 energies where the basic cross-section typically rises as $\hat{s}$ decreases. HERWIG uses an electron structure function approach to write the total cross-section for a process as:

$$\sigma(s) = \int_0^1 \mathrm{d}x_1 \int_0^1 \mathrm{d}x_2 f_e^e(x_1) f_e^e(x_2) \hat{\sigma}(x_1 x_2 s) \tag{2}$$

Employing a natural choice of variables, $\tau = x_1 x_2 (= \hat{s}/s)$ and $x = x_1$, this can be written:

$$\sigma(s) = \int_T^1 \mathrm{d}\tau \hat{\sigma}(\tau s) \int_\tau^1 \frac{\mathrm{d}x}{x} f_e^e(x) f_e^e\left(\frac{\tau}{x}\right) \tag{3}$$

where $\tau > T$ (`TMNISR`) is a physical cut-off used to avoid the $1/s$ pole in the cross-section's photon exchange term.

The actual structure function used is the second order solution to the full Altarelli-Parisi equation with exponentiated coefficients:

$$
\begin{aligned}
f_e^e(x) &= \beta(1-x)^{\beta-1} \exp\left\{\beta\frac{x}{2}\left(1+\frac{x}{2}\right)\right\}\left(1-\beta^2\frac{\pi^2}{12}\right) \qquad\qquad \beta = \frac{\alpha_{\text{em}}}{\pi}\left[\log\left(\frac{Q^2}{m_e^2}\right)-1\right]\\
&+ \frac{\beta^2}{8}\left[(1+x)[(1+x)^2+3\log x] - \frac{4\log x}{1-x}\right] + \mathcal{O}(\alpha_{\text{em}}^3) \tag{4}
\end{aligned}
$$

This is equivalent[3] to the expression, eqs. (58,60), given on p. 34 of [1]. This means that the single photon emission allowed for in HERWIG gives equivalent energy and $p^\perp$ spectra as

---

[3]A discrepancy in the coefficient of the π^2 term, a factor 2 too large, is believed to be their typographic error.

IPROC	Process	
	$\gamma^\star/\mathrm{Z}^0/\mathrm{Z}'$ Continuum Processes	
100+IQ	$\mathrm{e^+e^-} \to \mathrm{q\bar{q}(g)}$	IQ=1-6: $\mathrm{q} = \mathrm{d},\ldots,\mathrm{t}$; IQ=0: all flavours
107	$\mathrm{e^+e^-} \to \mathrm{gg(g)}$	
110+IQ	$\mathrm{e^+e^-} \to \mathrm{q\bar{q}g}$	IQ as above, includes masses exactly
120+IQ	$\mathrm{e^+e^-} \to \mathrm{q\bar{q}}$	IQ as above $\Big\}$ no correction to hard
127	$\mathrm{e^+e^-} \to \mathrm{gg}$	gluon branching
150+IL	$\mathrm{e^+e^-} \to \ell\bar{\ell}$	IL=2,3: $\ell = \mu,\tau$
	Di-Boson Production	
200	$\mathrm{e^+e^-} \to \mathrm{W^+W^-}$	$\Big\}$ $\mathrm{W^\pm/Z^0}$ decays controlled
250	$\mathrm{e^+e^-} \to \mathrm{Z^0Z^0}$	by MODBOS
	Bjorken process: $\mathrm{e^+e^-} \to \mathrm{Z^0h^0}$	
300+IQ	$+\mathrm{h^0} \to \mathrm{q\bar{q}}$	IQ as above
300+IL	$+\mathrm{h^0} \to \ell\bar{\ell}$	IL=1,2,3: $\ell = e,\mu,\tau$
310,311	$+\mathrm{h^0} \to \mathrm{W^+W^-},\mathrm{Z^0Z^0}$	
312	$+\mathrm{h^0} \to \gamma\gamma$	
399	$+\mathrm{h^0} \to$ anything	
	Vector Boson Fusion	
400+ID	$\mathrm{e^+e^-} \to \nu\bar{\nu}\mathrm{h^0} + \mathrm{e^+e^-h^0}$	ID as IPROC=300+ID
	Zero Resolved Gamma-Gamma: $\mathrm{e^+e^-} \to (\mathrm{e^+e^-})\gamma\gamma$	
500+ID	$\gamma\gamma \to \mathrm{q\bar{q}}/\ell\ell/\mathrm{W^+W^-}$	ID=0-10 as for IPROC=300+ID
	Gamma-W Fusion: $\mathrm{e^+e^-} \to (\mathrm{e^+}\nu_e)\gamma\mathrm{W^-}$	
550+ID	$\gamma\mathrm{W^-} \to \mathrm{q\bar{q}'}/\ell\bar{\nu}_\ell$	ID=0-9 as for IPROC=300+ID
	Doubly Resolved Gamma-Gamma	
1500	$\mathrm{gg} \to \mathrm{gg}, \mathrm{qg} \to \mathrm{qg}$, *etc.*	31 $\mathcal{O}(\alpha_s^2)$ two-to-two QCD scatterings
1700+IQ	$\mathrm{gg} \to \mathrm{Q\bar{Q}}, \mathrm{gQ} \to \mathrm{gQ}$, *etc.*	16 $\mathcal{O}(\alpha_s^2)$ heavy quark production processes
1800	$\mathrm{gq} \to \gamma\mathrm{q}, \mathrm{gg} \to \gamma\mathrm{g}$, *etc.*	17 $\mathcal{O}(\alpha_s\alpha_{em}, \alpha_s^3\alpha_{em})$ direct photon processes
2200	$\mathrm{q\bar{q}} \to \gamma\gamma, \mathrm{gg} \to \gamma\gamma$	3 $\mathcal{O}(\alpha_{em}^2, \alpha_s^2\alpha_{em}^2)$ di-photon processes
	Singly Resolved Gamma-Gamma	
5000	$\gamma\mathrm{q} \to \mathrm{gq}, \gamma\mathrm{g} \to \mathrm{q\bar{q}}$, *etc.*	3 $\mathcal{O}(\alpha_s\alpha_{em})$ dijet processes
5100+IQ	$\gamma\mathrm{g} \to \mathrm{Q\bar{Q}}$	heavy flavour pair production, IQ as above
5200+IQ	$\gamma\mathrm{Q} \to \mathrm{gQ}, \mathrm{q\bar{Q}} \to \mathrm{q\bar{Q}}$	heavy flavour excitation, IQ as above
5500	$\mathrm{gg} \to V\mathrm{g}, \mathrm{gq} \to V\mathrm{q}'$, *etc.*	6 $\mathcal{O}(\alpha_s^2\alpha_{em})$ light (u,d,s) $L = 0$ meson production
5510,5520		$J(= S) = 0, 1$ mesons only
8000	Minimum bias soft collision	
	Charged lepton Deep Inelastic Scattering	
9000+IQ	$\mathrm{eq} \to \mathrm{eq}, \mathrm{e\bar{q}} \to \mathrm{e\bar{q}}$	NC DIS on flavour IQ as above
9010+IQ	$\mathrm{eq} \to \nu_e\mathrm{q}', \mathrm{e\bar{q}} \to \nu_e\mathrm{\bar{q}}'$	CC DIS on flavour IQ as above
10000+IP		As IPROC=IP but with suppressed SUE

Table 7: The principal HERWIG hard sub-process of importance for LEP 2 physics. In QCD scatterings `IHPRO` labels the actual sub-process, allowing for colour decomposition, generated.

multiple photon emission. In the soft photon limit $f_e^e(x)$ simplifies significantly to the following form, used to efficiently generate the $\{x_i\}$ via importance sampling:

$$f_e^e(x, Q^2) \approx \beta(1-x)^{\beta-1} \tag{5}$$

In practical situations one has: $\alpha_{em}/\pi \ll \beta \ll 1$, so that $f_e^e(x)$ has an integrable singularity in the soft photon limit, $x \to 1$; $1-x$ is the energy fraction carried by the photon. To regularize this divergence HERWIG employs a resolution parameter, $x < X$, called ZMXISR (default $1 - 10^{-6}$), and includes a fraction of events with no emission, so that:

$$f_e^e(x) \mapsto \bar{f}(x) = \Theta(X - x)f(x) + \delta(1-x)(1-X)^\beta \tag{6}$$

Here X is only an internal parameter and unphysical in the sense that cross-sections should not depend on it. Observe that even for $1 - X = \mathcal{O}(10^{-6})$ the non-emission probability is $\approx 45\%$ at LEP 2. Note also setting ZMXISR=0 has the effect of switching off the initial state photon radiation.

After the emission of a photon the electron entering the hard sub-process is off-shell. In HERWIG its negative virtuality is selected from a logarithmic distribution, $\mathrm{d}q^2/q^2$, bounded in magnitude by eq.(8).

Allowing for the virtualities of the electron lines and treating x as a lightcone momentum fraction $\hat{s}$ is reconstructed as:

$$\hat{s} = \tau s - q_1^2 - q_2^2 + \frac{q_1^2 q_2^2}{s} - 2\underline{p}_1^\perp \underline{p}_2^\perp \tag{7}$$

Since $\hat{\sigma}$ is a rapidly varying function of $\hat{s}$ near the Z^0 HERWIG slightly shifts the $\{x_i\}$ fractions to preserve $\hat{s} = \tau s$. Specifically the highest $p^\perp$ photon is taken to be emitted first and its $x \mapsto x' = x + q^2/s$ (x' is the energy fraction) so that $\hat{s}$ would be preserved in the absence of emission from the other lepton. The x of the lower $p^\perp$ photon is then shifted so as to give exactly $\hat{s}$. For simplicity the program requires photon emission to be in the forward hemisphere which imposes the condition:

$$q^2 < \frac{x'}{1 + x'}(1 - x)s \tag{8}$$

This inequality is applied to both leptons. Note that this still allows the possibility for on resonance γZ^0 states to be produced but only to the accuracy of the leading logarithm approximation.

The use of the Equivalent Photon Approximation for the case of virtual photon emission in which it is the photon which enters the hard sub-process is again discussed in the report of the gamma-gamma working group.

4.3.4 Parton Showers

HERWIG employs highly developed parton shower algorithms to provide an accurate description of the perturbative QCD jet evolution. Coherence, due to leading infrared singularities [70], is

automatically included through the choice of evolution variables, ordering in which naturally restricts the branching phase space to an angular ordered region. Further angular screening due to heavy quark masses, the *dead cone*, is also fully included [137]. At each branching the azimuthal angles are distributed according to the eikonal dipole distribution for soft gluons [138], including mass effects, and to the full collinear leading logarithm accuracy for hard emission [139]. At large momentum fractions the coherent algorithm used also correctly describes next-to-leading contributions [140]. By using a two-loop expression for α_s this allows the Monte Carlo Λ to be related to $\Lambda_{\overline{\text{MS}}}$ as $x \to 1$

$$\Lambda_{\text{MC}} = \exp\left\{\frac{C_A(67 - 3\pi^2) - 10n_f}{6(11C_A - 2n_f)}\right\} \Lambda_{\overline{\text{MS}}} \approx |_{n_f=5} 1.569 \Lambda_{\overline{\text{MS}}}^{(5)} \tag{9}$$

Since the time of the LEP 1 workshop significant progress has been made in the study of final states involving photons [103], leading to the implementation of final state photon radiation in HERWIG [141]. The momentum sharing in $q \to q\gamma$ branchings and relative rate compared to $q \to qg$ branchings are controlled by the following splitting function and Sudakov form factor:

$$\begin{aligned}
P_{q\to q\gamma}(z) &= e_q^2 \frac{\alpha_{\text{em}}}{2\pi} \frac{1 + z^2}{1 - z} \\
\log \Delta_s(Q^2, Q_0^2) &= -e_e^2 \frac{\alpha_{\text{em}}}{\pi}[(\log(Q/Q_\gamma) - 3/4)^2 - (\log(Q_0/Q_\gamma) - 3/4)^2]
\end{aligned} \tag{10}$$

where, since the photon is in the final state, a fixed α_{em} is used (allowing analytic integration of the Sudakov form factor) and $Q_0 = Q_q + Q_\gamma$ with Q_q and Q_γ the cut-offs on the quark and photon scales respectively. The branching $\gamma \to q\overline{q}$ is expected to be small and is not included. Competition between the two types of quark branching is handled in the standard way. That is the Q^2 scales at which the two types of branching attain a preselected probability of occurring are found, the larger is taken to occur first and if its Q^2 is above $(Q_q + Q_\gamma)^2$ it is accepted. The scale Q^2 of any branching is bounded above by that of the last emission, irrespective of type. However the opening angle is bounded from above by the opening angle of the last emission of the same type; this is exact in the case when azimuthal photon-gluon correlations are integrated out.

Due to the choice of evolution variables in HERWIG, configurations in which a very hard gluon or photon recoils against the $q\overline{q}$ pair are not generated by the showering algorithm, that is a 'dead zone' exists [141]. This is particularly important in the photon case due to the relative ease with which they can be identified in the final state. The HERWIG solution is to find what fraction of events are missing by integrating the three parton matrix element over the dead zone and then add back this fraction starting the evolution from a correctly distributed $q\overline{q}g/\gamma$ configuration. The algorithm of [142] is used to exactly include initial/final state correlations starting from a massless $q\overline{q}$ configuration.

The matching of a hard gluon or photon to the exact matrix element is controlled by the logical HARDME (default .TRUE.). Additionally there is a 'soft' matrix element correction, where soft here means inside the phase space region accessible to the branching algorithm; SOFTME

(default .TRUE.) controls the matching of the hardest emission, not necessarily the first, to the exact matrix element [143].

4.3.5 Hadronization

The basic preconfinement inspired [73] cluster hadronization model used in HERWIG remains little changed from its original formulation [144]. The principle criterion for selecting the flavours and spins of the primary hadrons in the cluster two body decays is the phase space available; though weights PWT(1-6), VECWT, TENWT and DECWT can be used to alter the flavour/spin compositions. The cluster decays are isotropic, in their own rest frame, except when a perturbative quark is involved, that is one from the hard sub-process or a g → q$\overline{\text{q}}$ splitting. If (CLDIR=1), the default, then the hadron containing this quark is aligned with the quark direction in the cluster rest frame. The main effect is to stiffen the spectrum of heavy charm and bottom hadrons. It is possible to partially decorrelate this direction retention using the parameter CLSMR (default 0), the width of an exponential distribution in $1 - \cos\theta_{\text{qh}}$; thus increasing CLSMR increases the smearing.

New parameters have been introduced to control the treatment of clusters with anomalous masses. CLPOW (default 2) influences the decision on whether a heavy cluster $q_1\overline{q}_2$ should first be split in two prior to hadronization according to if its mass satisfies the inequality:

$$M_{cl}^{CLPOW} > CLMAX^{CLPOW} + (m_{q_1} + m_{\overline{q}_2})^{CLPOW} \tag{11}$$

Using smaller values of CLPOW leads to an increased yield of heavy clusters containing heavy quarks and thence to more heavy baryons; light quark clusters are affected less. The parameter B1LIM (default 0) can be used to increase the number of relatively light bottom clusters that undergo a one-body decay. If M_{thr} is the threshold for two-body decay then the probability of a one-body decay becomes:

$$\mathcal{P} = \begin{cases} 1 & M_{cl} < M_{thr} \\ 1 - \frac{M_{thr} - M_{cl}}{B1LIM \star M_{thr}} & M_{thr} < M_{cl} < (1 + B1LIM)M_{thr} \\ 0 & (1 + B1LIM)M_{thr} < M_{cl} \end{cases} \tag{12}$$

For light quark clusters the one-body decay criterion remains equivalent to the above with B1LIM=0. In practice CLPOW proves more effective in controlling the spectrum of both bottom and charm hadrons. When one-body decays do occur a Lorentz covariant treatment is now used to effect the necessary momentum rearrangement.

In the default version of HERWIG the quark–antiquark pairs which form the colour singlet clusters are taken to be nearest neighbour pairs, in a sense defined by the shower. However a colour reconnection model is now available. It is based upon minimizing the spatial sizes of pairs of clusters as determined from the semi-classical positions of the partons at the end of the showers. This model is discussed more fully in 4.7.

More recently the number of hadrons supported has been enlarged to incorporate all $L = 0, 1$ mesons (including the $0^{+(+)}$ and $1^{+(+)}$ states) composed of d,u,s,c,b quarks and all $J = 1/2$

('octet') and $J = 3/2$ ('decuplet') baryons composed of the form $q_1q_2q_3$ or Qq_1q_2, (Q = c,b). Should the user wish to add any new particles it is sufficient to simply specify their properties: name, PDG code number, mass, spin and flavour compositions in the arrays RNAME, IDPDG, RMASS, RSPIN and IFLAV and they will be included automatically in cluster decays. Using the array VTOCDK it is also possible to veto a particular hadron's production in cluster decays.

4.3.6   Decay Tables

The HERWIG decay routines have been largely re-written to make them more user friendly and to adopt the proposals made in section 5.2. Up to five body decays are supported with a number of standard matrix elements made available. Specific hadronic decay channels for B hadrons can now be included. This is in addition to the original partonic model based on spectator decays [137]; note this may involve some double counting. The production of a selected particle via unstable particle decays can be vetoed by specifying it in the array VTORDK; any branching ratio sums affected because of excluded channels are automatically reset to unity. The subroutine HWIODK has been added to allow the HERWIG decay tables to be inputted and outputted in the proposed standard format. When read in the program checks that the decay is kinematically allowed and does not violate electric charge conservation; if necessary the sum of branching ratios is reset to one. The use of this subroutine makes it simple for the users to adapt the provided tables for their own use. The subroutine HWMODK allows individual channels in the decay tables to be added or modified between events. The actual default decay tables themselves have also been updated to include modes at the one *per mille* level.

Interfaces to the EURODEC [145] and CLEO [146] B hadron decay packages are also built into HERWIG. The selection is made by setting BDECAY='EURO','CLEO' or 'HERW' (the default is of course 'HERW').

The production vertices of hadrons are now calculated by HERWIG and stored using the VHEP array of /HEPEVT/. This is based on the particle lifetimes in the RLTIM array. A particle is set unstable if its lifetime is less than PLTCUT however when MAXDKL=.TRUE. all decays are tested in the routine HWDXLM and required to occur within a volume specified by IOPDKL else left undecayed. If BOMIX=.TRUE. then neutral $B^0_{d,s}$ mesons are allowed to mix before decaying.

4.3.7   Source Code

In addition to the WWW site quoted above copies of the HERWIG source code and supporting files are maintained in the following VAX directories:

```
CBHEP::DISK$THEORY:[THEORY.HERWIG]HERWIGnm.*
FNALV::USR$ROOT2:[BWEBBER.HERWIG]HERWIGnm.*
VXCERN::DISK$CR:[WEBBER.HERWIG]HERWIGnm.*
```

The files supplied are HERWIGnm.COM, *.DOC, *.FOR, *.INC, *.MSG, *.SUD and *.TST. The command file HERWIGnm.COM runs a test job *.TST containing the main program. This uses the source code subroutines found in *.FOR with the declarations and common blocks in *.INC and default Sudakov form factors in *.SUD. Release notes are found in *.MSG and more complete documentation in *.DOC.

4.4   NLLjet

Basic Facts

Program names:	NLLJET [147]
Versions:	NLLJET 3.0 of September 1992
Author:	Kiyoshi Kato
	Kogakuin University
	Nishi-Shinjuku 1-24, Shinjuku, Tokyo 160, Japan
	Phone: + 81 − 3 - 3342 - 1211
	E-mail: kato@sin.cc.kogakuin.ac.jp
	Tomo Munehisa
	Yamanashi University
	Takeda 4-3, Kofu 400, Japan
	Phone: + 81 − 552 - 20 - 8584
	E-mail: munehisa@top.esb.yamanashi.ac.jp
Program size:	7742 lines
Program location:	ftp.kek.jp : kek/minami/nlljet

NLLJET is a Monte Carlo code for the generation of jet events in e^+e^- annihilation based on the parton shower method. The events are parton final states in the form of a list with particle codes and four-momenta. Connection to the hadronization is open for the user, and a standard interface to Lund hadronization is provided.

Generation of QCD jets by the parton-shower method was born of Konishi, Ukawa and Veneziano in 1979 as the "jet calculus" in which the method to make systematic summation of the collinear singularity in QCD was given. Here, the factorization of the mass singularity works well and the choice of physical gauge leads to a suppression of interference terms, so that a stochastic treatment for jets becomes possible.

Soon after that, models of the QCD parton shower in the leading-logarithmic (LL) approximation were developed. These models are good for the description of jets in high energy. However, they have no chance to determine the fundamental parameter of QCD, $\alpha_s(\mu^2)$ (or QCD Λ), because starting from *any* renormalization scheme in QCD, you obtain the *same* formula for physical quantities in LL approximation. This limits the analysis for the determination of the strong coupling constant in jet phenomena only to the calculation based on the

QCD matrix elements. However, the Monte-Carlo simulation of jets by matrix elements is not appropriate for the global description of jets since it has an avoidable defect, the discontinuity between n- and $(n+1)$-parton states.

The idea of NLLJET was spawned from observation above. In this parton-shower model, the collinear singularity of QCD is summed up to the next-to-leading logarithmic(NLL) order. All components in NLL order are computed in the $\overline{\text{MS}}$ scheme, and they are implemented in the model. Thus NLLJET has the potential to determine the QCD $\Lambda_{\overline{\text{MS}}}$ through a comparison of generated events with experiments [148]. The basic ingredients of NLLJET are as follows:

- Sudakov factor which is defined by the integral of the P function up to $O(\alpha_s^2)$.
- Two-body branching by the two-body vertex function up to $O(\alpha_s^2)$.
- Three-body branching by the three-body vertex function in $O(\alpha_s^2)$.
- Hard cross section of the primary $q\bar{q}g$ process up to $O(\alpha_s^2)$.
- Kinematical conditions and correction terms.

The effect of soft-gluon contribution is an important issue in perturbative QCD. In NLLJET, the strong coupling constant in the Sudakov factor is defined to be $\alpha_s(x(1-x)Q^2)$, and it corresponds to the inclusion of soft gluon resummation. The angular ordering is not introduced to all branchings but only to those in which the angular ordering is really required.

The important point of the formulation beyond LL order is that each kinematical modification is always controlled properly through the introduction of a correction term in the NLL order functions. The three-body vertex functions become positive with the correction for the angular ordering in $q \rightarrow q + g + g$ and $g \rightarrow g + g + g$ and that for the momentum conservation. The double cascade scheme, which is necessary to recover the symmetry between q and $\bar{q}$, also gives another correction term.

The parton shower method still has a few ambiguous points which are hard to determine from the theoretical view point in perturbative QCD. For example, the virtuality of partons in final states should be less than a cutoff value, Q_0^2. Normally, one sets it equal to Q_0^2. However, sometimes better agreement with experiments is found by taking it to be 0. In this version, this modification is included by setting `KINEM -1` parameter.

The effect of a quark mass is only counted kinematically by replacing Q^2 by $Q^2 + m_q^2$. Neither azimuthal correlations nor the parton polarization are considered.

Essential input parameters of NLLJET are W, Λ, Q_0^2, δ, and C. Here W stands for the center-of-mass energy. Physics should not depend strongly on the cutoff Q_0^2 and its dependence is to be counted as a systematic error of the theory. Parameter δ is specific to NLL parton shower and it is absent in LL order. The distribution is expected to be independent of δ. However, detailed study shows that there is small bend at the region connected by δ. If one sets δ large (~ 0.5), the events are free from the bend at the expense of the exclusion of $q\bar{q}g$ primary vertex. The scheme parameter C is available in order to replace μ^2 in $\alpha_s(\mu^2)$ from $\mu^2 = Q^2$ to $\mu^2 = CQ^2$. However, it is not possible to change C in large. In the matrix element, QCD is studied at $Q^2 = W^2$ while in parton shower, it is done for $Q^2 = W^2 \sim Q_0^2$.

4.5 PYTHIA/JETSET

Basic Facts

Program names:	PYTHIA and JETSET [15]
Versions:	PYTHIA 5.720 of 29 November 1995
	JETSET 7.408 of 23 August 1995
Author:	Torbjörn Sjöstrand
	Department of Theoretical Physics
	University of Lund
	Sölvegatan 14A, S-223 62 Lund, Sweden
	Phone: + 46 – 46 - 222 48 16
	E-mail: torbjorn@thep.lu.se
Program size:	19936 + 11541 lines
Program location:	http://thep.lu.se/tf2/staff/torbjorn/

4.5.1 Introduction

The JETSET program has been used frequently for QCD physics studies at LEP 1. For applications at LEP 2, JETSET should be complemented with the PYTHIA program. While JETSET only gives access to one hard process, $e^+e^- \rightarrow \gamma^*/Z^0 \rightarrow q\overline{q}$, PYTHIA contains a wealth of different processes. The two programs are fully integrated, in that a call to PYTHIA will not only generate a hard process but also automatically call JETSET routines to perform (timelike) parton showers and fragmentation. Output is in the normal LUJETS commonblock (with easy translation to the HEPEVT standard) and can be studied with the JETSET analysis routines. The emphasis of the PYTHIA/JETSET package is to provide a realistic description of varying hadronic final states, but also non-hadronic processes may be generated.

In addition to the briefer published description of the programs, there is a complete manual and physics description of over 300 pages [15]. The programs, the manual, update notes and sample main programs can be picked up from the web address given above; additionally the CERN program library provides the programs and hardcopies of the manual. The description given here therefore only contains some highlights, with special emphasis on the aspects of relevance for LEP 2 applications.

For the description of a typical high-energy event, a generator should contain a simulation of several physics aspects. If we try to follow the evolution of an event in some semblance of a time order, one may arrange these aspects as follows:

1. Initially the e^+ and e^- are coming in towards each other. An electron contains virtual fluctuations into photons, quarks, gluons, and so on. It is useful to employ the same parton-distribution and parton-shower language as for hadrons. Thus also electrons and photons are included in the parton concept. An initial-state parton shower develops by branchings such as $e \rightarrow e\gamma$, $\gamma \rightarrow q\overline{q}$ and $q \rightarrow qg$.

2. One parton from each of the e^+- and e^--initiated showers enters the hard process, where then a number of outgoing partons/particles are produced. It is the nature of this process that determines the main characteristics of the event. (Also some soft processes are included in the program; since much of the same framework can be used we do not here belabour the differences.)

3. If the hard process produces massive electroweak particles, such as the Z^0, the $W^\pm$ or a Higgs, the decay into lighter objects must be considered.

4. The outgoing partons may branch, to build up final-state showers.

5. Further semihard interactions may occur between the other partons in the case of two incoming resolved photons.

6. When a shower initiator is taken out of a beam particle, a beam remnant is left behind.

7. The QCD confinement mechanism ensures that the outgoing quarks and gluons are not observable, but instead fragment to colour-neutral hadrons.

8. Many of the produced hadrons are unstable and decay further.

The time-order above does not have to coincide with the generation sequence. Typically the hard process is selected first.

4.5.2   Hard processes

Close to a hundred subprocess cross sections have been encoded in PYTHIA. Lepton, hadron and photon beams are allowed; thus the program can be used for $p\overline{p}$/pp physics at the Tevatron or LHC or for ep physics at HERA. Here we concentrate on processes of relevance for LEP 2. Some of the more interesting ones are listed in table 8 and discussed below. Further comments may be found in other sections of this report.

It it important to note that PYTHIA is not intended to be a precision program for electroweak physics. The philosophy is to provide sensible first approximations to a wide selection of hard processes, as a starting point for a detailed simulation of the subsequent QCD steps, i.e. parton showers, fragmentation and decay. It is therefore orthogonal in philosophy to many dedicated electroweak generators, that attempt to provide the hard-scattering cross section with very high precision but do not go beyond a parton-level description.

Subprocess 1 is the familiar γ^*/Z^0 process that dominates LEP 1 physics. The full interference structure between the γ and Z^0 propagators is included. It supersedes the LUEEVT generator of JETSET. The main differences are:

- LUEEVT uses a matrix-element approach to generate at most one initial-state photon, while PYTHIA allows for multiple photon emission in a parton-shower approach;
- LUEEVT allows only hadronic final states, while PYTHIA also includes leptonic ones;
- LUEEVT contains a simple Breit-Wigner with the width Γ_Z as input, while PYTHIA contains an s-dependent Breit-Wigner that is dynamically calculated from electroweak parameters; and
- the option to simulate first- or second-order MEs currently only exists with LUEEVT.

Table 8: Main LEP 2 physics processes available in PYTHIA.

ISUB	Process
Gauge boson production	
1	$e^+e^- \to \gamma^*/Z^0$
18	$e^+e^- \to \gamma\gamma$
19	$e^+e^- \to \gamma(\gamma^*/Z^0)$
22	$e^+e^- \to (\gamma^*/Z^0)(\gamma^*/Z^0)$
25	$e^+e^- \to W^+W^-$
35	$e\gamma \to e(\gamma^*/Z^0)$
36	$e\gamma \to \nu W$
69	$\gamma\gamma \to W^+W^-$
70	$\gamma W \to Z^0 W$
Higgs production	
24	$e^+e^- \to Z^0 h^0$
103	$\gamma\gamma \to h^0$
110	$e^+e^- \to \gamma h^0$
123	$e^+e^- \to e^+e^- h^0$
124	$e^+e^- \to \nu_e\overline{\nu}_e h^0$
141	$e^+e^- \to \gamma^*/Z^0/Z'^0 \to H^+H^-, h^0A^0, H^0A^0$
171	$e^+e^- \to Z^0 H^0$
173	$e^+e^- \to e^+e^- H^0$
174	$e^+e^- \to \nu_e\overline{\nu}_e H^0$
Other processes	
10	$e^+e^- \to e^+e^-, \nu_e\overline{\nu}_e$
141	$e^+e^- \to \gamma^*/Z^0/Z'^0$

ISUB	Process
$\gamma\gamma$ physics	
58	$\gamma\gamma \to q\overline{q}, \ell^+\ell^-$
33	$\gamma q \to qg$
54	$\gamma g \to q\overline{q}$
11	$qq' \to qq'$
12	$q\overline{q} \to q'\overline{q}'$
13	$q\overline{q} \to gg$
14	$q\overline{q} \to g\gamma$
18	$q\overline{q} \to \gamma\gamma$
28	$qg \to qg$
29	$qg \to q\gamma$
53	$gg \to q\overline{q}$
68	$gg \to gg$
91	$\gamma\gamma \to VV'$
92	$\gamma\gamma \to XV$
93	$\gamma\gamma \to VX$
94	$\gamma\gamma \to X_1X_2$
95	$\gamma\gamma \to$ low-$p_\perp$
85	$\gamma\gamma \to Q\overline{Q}, \ell^+\ell^-$
84	$\gamma g \to Q\overline{Q}$
81	$q\overline{q} \to Q\overline{Q}$
82	$gg \to Q\overline{Q}$
DIS	
10	$eq \to eq$

Subprocess 19 contains a photon in addition to the γ^*/Z^0. This means double counting, since already process 1 can contain initial-state-radiation photons, so results from the two processes should not be added. The usage of process 19 should be restricted to events that contain a high-$p_\perp$ photon, where generation then is more efficient (and accurate) than what is offered by process 1.

Subprocess 25 describes W pair production, including subsequent decay into four fermions with full angular correlations. The formalism includes s-dependent widths in the Breit-Wigners and options to pick the set of independent electroweak parameters. However, it is restricted to the basic graphs of W pair production ("CC03").

Subprocess 22 describes γ^*/Z^0 pair production in a similar approximation ("NC02"). Note that interference terms between process 22 and 25 are not found anywhere. This is in accor-

dance with the basic philosophy of a reasonable but not exhaustive description of electroweak processes.

Subprocesses 35 and 36 describe the production of a single γ^*/Z^0 or W in the approximation of an effective photon flux. A process such as $e^+\gamma \to \overline{\nu}_e W^+$ thus is convoluted with the parton-shower approximation of the $e^- \to e^-\gamma$ branching to give an effective process $e^+e^- \to \overline{\nu}_e e^- W^+$. Process 35 has a singularity when the scattered electron has vanishing $p_\perp$ (in principle this is regularized by the electron mass, but in practice the m_e has been neglected). Therefore it is necessary to run with some minimum $p_\perp$ cut-off; for numerical reasons at least 0.01 GeV. An alternative description can be obtained by using an electron-inside-photon-inside-electron parton distribution (MSTP(12)=1) in process 1. For process 36 the decay of the W is assumed isotropic since the appropriate matrix elements have not been coded. Also subprocesses 69 and 70 assume isotropic W/Z decay. Furthermore, process 70 does not include contributions from γ^* but only from Z^0. The process implementations in this paragraph thus are less sophisticated than the single γ^*/Z^0, W pair and γ^*/Z^0 pair processes above.

PYTHIA is equipped with an extensive selection of production processes for the standard model Higgs, here denoted "h^0". (It is called "H^0" in the program, which confuses matters when two Higgs doublets are introduced, but for this report we stay with the conventional terminology.) Not all available processes have been listed, but only those of some interest. The most important by far (at LEP 2) is process 24, $e^+e^- \to Z^0 \to Z^0 h^0$. Both Z^0's in the graph have been included with a Breit-Wigner shape, so there is no formal restriction that either of them need be on or close to the mass shell. For a Higgs with $m_h + m_Z > E_{cm}$ process 124 takes over, $e^+e^- \to \nu_e\overline{\nu}_e W^+W^- \to \nu_e\overline{\nu}_e h^0$, but at a much smaller rate. Processes 110, 123 ($Z^0 Z^0$ fusion) and 103 are even further suppressed.

All major h^0 decay modes are included: $h^0 \to q\overline{q}$, $h^0 \to \ell^+\ell^-$, $h^0 \to W^+W^-$, $h^0 \to Z^0Z^0$, $h^0 \to gg$, $h^0 \to \gamma\gamma$ and $h^0 \to \gamma Z^0$. The branching ratios are automatically recalculated based on the Higgs mass. One point that should be noted is that the parton-shower algorithm matches to the same three-jet matrix element that is used for γ^*/Z^0 decays. This gives a somewhat incorrect rate for three-jet production in Higgs decay.

In the minimal supersymmetric extension to the standard model the number of production processes is further increased. The full set of Higgs particles is included in the program: h^0, H^0, A^0 and $H^\pm$. Masses and couplings can be set by the user; this is a somewhat lengthy process, however, since currently the one-loop mass relations are not built into the program. The H^0 have the same production processes as the h^0; the list in table 8 only shows the more interesting. Higgs pair production, H^+H^-, h^0A^0 and H^0A^0, proceeds only through s-channel graphs and has been included as part of $\gamma^*/Z^0/Z'^0$ decays, process 141. The Z'^0 part can easily be switched off (MSTP(44)=4), so that processes 1 and 141 become identical except for the larger selection of decay modes in the latter. (Technically, this way the program can distinguish the Z' decaying to Higgses from a Z produced in Higgs decay, and accommodate different decay modes for the two.)

Subprocess 141 is also useful for the study of virtual corrections caused by the existence of

a Z'^0 somewhere above the LEP 2 energy range. Vector and axial couplings may be set freely to simulate various scenarios, and interference with γ^*/Z^0 is automatically included.

$\gamma\gamma$ physics is a large area, in that a wealth of different subprocesses is involved. A photon may act as a pointlike particle or as a resolved, hadronlike state. A simple subdivision of processes is therefore into direct (58, 85), once-resolved (33, 54, 84) and twice-resolved (the rest, that is all processes allowed e.g. in pp collisions). The resolved part of the photon may be further subdivided into a VMD (vector meson dominance) and anomalous part. In total therefore six classes of events can be separated [149]. An automatic mix to provide a "minimum bias" sample of events is obtainable as an option (MSTP(14)=10). Processes 81–85 include masses in the matrix elements, and thus are convenient to study e.g. heavy-flavour production. It should be noted that several aspects remain to be solved, for instance that of (slightly) off-shell incoming photons. Furthermore, on a technical note, PYTHIA is originally designed for fixed energies of the incoming particles, and so the process of having $\gamma\gamma$ "hadronic" collisions at varying energies is not yet fully automated.

Finally, note that process 10 can be used both as a Bhabha and a deep-inelastic-scattering generator. In neither respect is it competitive with dedicated programs, but it may be useful for first estimates.

4.5.3   Hard process generation

The cross section for a process $ij \to k$ is given by

$$\sigma_{ij \to k} = \int \mathrm{d}x_1 \int \mathrm{d}x_2 \, f_i^{\mathrm{e}^+}(x_1, Q^2) \, f_j^{\mathrm{e}^-}(x_2, Q^2) \, \hat{\sigma}_{ij \to k}(\hat{s}) \ . \tag{13}$$

Here $\hat{\sigma}$ is the cross section for the hard partonic process, as codified in the matrix elements for each specific process. For processes with several particles in the final state it would be replaced by an integral over the allowed final-state phase space. The $f_i(x, Q^2)$ are the parton distribution functions, which describe the probability to find a parton i inside an $\mathrm{e}^{\pm}$ beam particle, with parton i carrying a fraction x of the total $\mathrm{e}^{\pm}$ momentum, when the $\mathrm{e}^{\pm}$ is probed at some squared momentum scale Q^2 that characterizes the hard process. The hard scattering therefore only involves a squared invariant mass $\hat{s} = x_1 x_2 s = x_1 x_2 E_{\mathrm{cm}}^2$, where E_{cm} is the c.m. energy of the event.

The electron-inside-electron parton distributions are based on a next-to-leading order exponentiated description, see [2]. The approximate behaviour is

$$f_{\mathrm{e}}^{\mathrm{e}}(x, Q^2) \approx \frac{\beta}{2}(1-x)^{\frac{\beta}{2}-1}; \qquad \beta = \frac{2\alpha_{\mathrm{em}}}{\pi}\left(\ln\frac{Q^2}{m_{\mathrm{e}}^2} - 1\right). \tag{14}$$

The form is divergent but integrable for $x \to 1$, i.e. the electron likes to keep most of the energy. To handle the numerical precision problems for x very close to unity, the parton distribution is set, by hand, to zero for $x > 0.999999$, and is rescaled upwards in the range $0.9999 < x < 0.999999$, in such a way that the total area under the distribution is preserved.

51

In the γe or $\gamma\gamma$ processes, an equivalent flow of photons is assumed, based on first-order formulae. There is some ambiguity in the choice of Q^2 range over which emissions should be included. In the probably most appropriate alternative (MSTP(13)=2) the form is

$$f_\gamma^e(x, Q^2) = \frac{\alpha_{em}}{2\pi} \frac{1 + (1 - x)^2}{x} \ln\left(\frac{Q_{max}^2 (1 - x)}{m_e^2 \, x^2}\right) . \qquad (15)$$

Here Q_{max}^2 (PARP(13)) is a user-defined cut for the range of scattered electron kinematics that is counted as photoproduction. Note that we now deal with two different Q^2 scales, one related to the hard subprocess itself, which appears as the argument of the parton distribution, and the other related to the scattering of the electron, which is reflected in Q_{max}^2. In the default alternative (MSTP(13)=1) only one scale is assumed, i.e. $Q_{max}^2 (1 - x)/x^2$ is replaced by Q^2 above.

Resolved photoproduction also involves the distributions of quarks and gluons inside the photon inside the electron. By default the SaS 1D set [150] is used for the parton distributions of the photon, but several alternatives are available.

4.5.4 Parton showers

In every process that contains coloured and/or charged objects in the initial or final state, gluon and/or photon radiation may give large corrections to the overall topology of events. The philosophy of PYTHIA is to stay with the lowest-order cross sections (modulo trivial loop corrections such as the running of coupling constants) and then generate higher-order corrections in the parton-shower approach. This is less exact than the explicit calculation of higher-order matrix elements, but has the advantage that it can be applied also to processes where higher orders have not yet been calculated; additionally it includes multiple emissions.

Showers may be subdivided into initial- and final-state ones, depending on whether they precede or follow the hard scattering. Of course, the subdivision often contains an element of arbitrariness, since interference terms may exist. In both initial- and final-state showers, the structure is given in terms of branchings $a \to bc$, specifically e $\to$ eγ, q $\to$ qg, q $\to$ qγ, g $\to$ gg, and g $\to$ q$\overline{q}$. The kernel $P_{a \to bc}(z)$ of a branching gives the probability distribution of the energy sharing, with daughter b taking a fraction z and daughter c the remaining $1 - z$ of the a energy. Once formed, the daughters b and c may branch in their turn, and so on.

Each parton is characterized by some virtuality scale Q^2, which gives an approximate sense of time ordering to the cascade. In the initial-state shower, spacelike Q^2 values are gradually increasing as the hard scattering is approached, while timelike Q^2 values are decreasing in the final-state showers. Shower evolution is cut off at some lower scale Q_0, typically around 1 GeV for QCD branchings and around m_e for initial-state QED ones. From above, a maximum scale Q_{max} is introduced, where the showers are matched to the hard interaction itself. Unfortunately the selection of Q_{max} for a given hard scattering is not unique, but gives rise to some slop.

52

Despite a number of common traits, the initial- and final-state radiation machineries are in fact quite different. The JETSET final-state algorithm has been used extensively for Z^0 hadronic decays at LEP 1, and is not significantly altered since the LEP 1 writeup [3].

Initial-state radiation is handled within the backwards evolution scheme [151]. In this approach, the choice of the hard scattering is based on the use of evolved parton distributions, which means that the inclusive effects of initial-state radiation are already included. What remains is therefore to construct the exclusive showers. This is done starting from the two incoming partons at the hard interaction, tracing the showers "backwards in time", back to the two shower initiators. In other words, given a parton b, one tries to find the parton a that branched into b. The evolution in the Monte Carlo is therefore in terms of a sequence of decreasing space-like virtualities Q^2 and increasing momentum fractions x. Branchings on the two sides are interleaved in a common sequence of decreasing Q^2 values. The definition of the x and z variables for off-mass-shell partons is not unique; in PYTHIA the $z = x_b/x_a$ of a branching tells how much the scattering subsystem invariant mass-squared is reduced by the branching. If originally parton b was assumed to have vanishing $p_\perp$, the reconstruction of the branching $a \rightarrow bc$ introduces a $p_\perp$ for b, which is compensated by c.

4.5.5 Beam remnants and multiple interactions

The initial-state radiation algorithm reconstructs one shower initiator in each beam. Together the two initiators delineate an interaction subsystem, which contains all the partons that partic- ipate in the initial-state showers, the hard interaction, and the final-state showers. Left behind are two beam remnants. In some cases a remnant is a single object, as when a γ is taken out of an e beam, leaving behind an e. When taking an e out of an e, a soft γ is left behind, which is then more related to the cutoff of $f_e^e(x, Q^2)$ at $x = 0.999999$ than to the ordinary beam- remnant concept, but is handled with the same machinery. In other cases a remnant consists of two objects, as when a q is taken out of an e, leaving behind e + $\overline{\mathrm{q}}$. The latter example has a coloured remnant, meaning that the fragmentation of the hard-process partons is connected with that of the beam remnants.

A resolved photon contains many partons. In a twice-resolved $\gamma\gamma$ event there is thus the possibility of multiple interactions, i.e. of multiple semi-hard parton–parton processes in the same event. A model for this phenomenon is included in PYTHIA [149], and will be further developed to better represent differences between the VMD and anomalous states.

4.5.6 Fragmentation and decay

The Lund string fragmentation description [28] and the decay routines in JETSET have not changed significantly since the LEP 1 writeup [3], and so are not described here. The string fragmentation approach has been generally successful in comparisons with LEP data, although some shortcomings have shown up. See section 2 for further details.

The issue of Bose-Einstein effects has received increased attention in recent years, e.g. in connection with possible consequences for the W mass determinations [152]. The existing algorithm [3] works well in many respects, but is by no means to be considered as a definite solution to the problem. A somewhat different approach has been implemented to allow some cross-checks, and further alternatives may appear in the future. In the current standard algorithm, identical particles are pulled closer together in such a way as to enhance the two-particle correlation at small relative momentum separation. This makes jets slightly narrower, so that fragmentation parameters have to be retuned for reasonable agreement with data. In the alternative, the shift of identical particles is somewhat reduced, while non-identical particles are pushed apart a bit, so that the average properties of jets remain unchanged. This alternative does not yet come with JETSET, but is available as a plug-in replacement for the LUBOEI routine, at http://thep.lu.se/tf2/staff/torbjorn/test/main10.f.

Also colour rearrangement has been extensively discussed in recent years. Code that allows this has not yet been integrated in the standard PYTHIA/JETSET libraries, but is obtainable separately, see section 4.7.

4.5.7 Final comments

PYTHIA/JETSET are likely to be among the major event generators at LEP 2: access to a broad selection of hard scattering subprocesses is combined with a well-tested description of parton showers and fragmentation. Limitations exist, however. PYTHIA is not a program for precision extraction of electroweak parameters; for instance, no (non-trivial) loop corrections are included in the matrix elements. One may well imagine hybrid arrangements, where dedicated generators are used to provide an improved description of some especially interesting hard scattering processes, such as four-fermion final states, while the rest of the PYTHIA/JETSET machinery is used to turn a simple parton configuration into a complex hadronic final state. An example of such an interface is discussed in section 5.3. Furthermore, the ARIADNE program for colour dipole radiation offers an alternative to the parton-shower description of JETSET, and can be used for all the hard processes in PYTHIA.

While there are no major additions planned for PYTHIA/JETSET, the intention is to continue a steady development and support activity. The $\gamma\gamma$ sector maybe is the area where most further studies are required to complete the picture, but also other aspects deserve attention.

4.6 UCLA ansatz

Basic Facts

Program names:	UCLA [44, 153]
Versions:	UCLA 7.41 of 1 October 1995
Author:	Sebong Chun and C.D. Buchanan
	Department of Physics

UCLA

405 Hilgard Ave, Los Angeles, CA 90024

USA

Phone: (310) 815-1992, 7466

E-mail: chun@physics.ucla.edu,

buchanan@physics.ucla.edu

Program size: 1922 lines

Program location: http://www.physics.ucla.edu/∼chuns

The goal of the UCLA hadronization modeling is to study and develop the underlying principles of e$^+$e$^-$ annihilation into hadrons, constructing a simple phenomenology which can be used both as a "target" for non-perturbative QCD calculations and also to accurately predict data.

The UCLA7.41 program, a spin-off of the Lund relativistic string Monte Carlo program JETSET, is the manifestation of this modelling to be used in comparing predictions with e$^+$e$^-$ data. As JETSET has upgraded to new versions, the UCLA program has likewise been adapted with a parallel nomenclature.

The modern UCLA modeling [44] presumes that, by making a few assumptions which can be rationalized within a QCD context (for example, a strong coupling expansion in lattice QCD), one can construct a Weight Function for any specified e$^+$e$^-$ → hadrons event. That is, given the center-of-mass energy of the e$^+$e$^-$ system and the flavor and momenta of the primary hadrons produced, the UCLA modeling attaches a weight to the entire event, to be used in comparison with other possible events at that E_{cm}.

The general structure of the Weight Function (in addition to kinematics of energy/momentum conservation and phase space with limited transverse momentum) depends on (a) an area law in space–time, (b) possible suppression factors at the vertices where a virtual q$\overline{q}$ pair is created from the colorfield, (c) "knitting factors" to knit a quark and antiquark together into the spatial wave function of a meson (or quark and diquark into a baryon), and (d) Clebsch–Gordon coefficients to knit the quark and antiquark (diquark) together into the flavor and spin state of the meson (baryon).

a) The area law is $\exp(-b'A)$ where b' is a constant and A is the area enclosed by the quark and antiquark trajectories in a space-time plot of the event. Almost any strong-coupling interaction will, in fact, give this sort of dependence.

b) The UCLA modeling assumes that there is no significant vertex suppression for q$\overline{q}$ pairs if the quark mass is less than the hadronic scale of ≃ 1 GeV; that is, u$\overline{u}$, d$\overline{d}$ *and* s$\overline{s}$ all have probability ≃ 1.0 of virtual creation from the colorfield.

c) The UCLA modeling assumes that all knitting factors are comparable, whether the hadron to be constructed is a spin 0 or 1 meson or a spin 1/2 or 3/2 baryon. (Probability

normalization on the fragmentation function derived below yields a value of the knitting factor of $\simeq (40 \text{ Mev})^{-2}$.)

d) The Clebsch-Gordon coefficients are simply the relevant flavor/spin coupling of a quark and antiquark (diquark) into a meson (baryon). Note that (c) and (d) taken together describe the coupling of a quark and antiquark or diquark into the complete state function of a hadron.

Although, in principle, knowing the Weight Function for the final state is enough to select an event, it is practically impossible to implement in this form. In order to implement this simple event Weight Function approach into a working Monte Carlo program, it is necessary to derive a fragmentation function for an "outside-in iterative one-particle-at-a-time" implementation such as JETSET uses.

By somewhat lengthy but straightforward algebra, this can be accomplished. The result so derived turns out to be the Lund Symmetric Fragmentation Function (LSFF) [153], with normalizing parameters of the vertex suppression, the spatial knitting factor, and the Clebsch-Gordon coefficient (see [44]). That is, the UCLA modeling simply amounts to using the LSFF as a hadronic production density weighted by Clebsch-Gordon coefficients, where the suppression of heavy mass particle production arises entirely from the $\exp(-bm^2/z)$ factor in the LSFF. (Note: the general structure of the Weight Function and the subsequent derivation of the fragmentation function can also be used to describe the Lund JETSET treatment. The difference is that JETSET presumes an $s\bar{s}$ vertex suppression of about 0.3 and a knitting factor for vector mesons of about 30% of that for pseudoscalar mesons, does not in general use Clebsch-Gordon coefficients, and adopts a normalization scheme that does not incorporate the $\exp(-bm^2/z)$ factor.)

The UCLA7.41 program uses the parton shower and decay table parts of JETSET, but replaces the flavor and momentum selection part with the UCLA modeling ansatz described above. Default values for the parton shower are $\Lambda = 0.2$ GeV and $Q_0 = 1.0$ GeV. Meson production is controlled by the two natural parameters of the LSFF with default values of $a = 2.1$ and $b = 1.1$ GeV^{-2}. Local transverse momentum compensation is approximated by a factor of $\exp(-\frac{n}{n-1}bp_\perp^2/z)$, where n is a parameter of default value 2.0. For baryon production, with "popcorn" mesons produced between baryon and antibaryon, an additional popcorn suppression factor of $\exp(-\eta m_{\text{pop}})$ is introduced with the default value of $\eta = 10$ GeV^{-1}. For more details, please refer to refs. [44].

This structure and values gives a rather good description of multiplicities, inclusive distributions, and correlations for hadron production from E_{cm} of 10 to 91 GeV, with the possible exception of the spin 3/2 baryons at 91 GeV. The description of heavy flavor (c, b) production distributions also seems reasonably good, with no additional parameterization or parameters.

For a detailed instruction on how to set up parameters and use the program, please refer to the manual at WWW location http://www.physics.ucla.edu/~chuns. A short set of instructions is available in the header to the actual program.

4.7 Colour reconnection codes

One of the QCD questions that has attracted attention in recent years is that of colour reconnection (or colour rearrangement) [127, 154, 155, 156]. This issue has implications for W mass studies, but is also of interest for our general understanding of QCD.

The concept may be illustrated by the process $e^+e^- \rightarrow W^+W^- \rightarrow q_1\bar{q}_2\,q_3\bar{q}_4$. To first approximation, the hadronic final state can be viewed as coming from the incoherent superposition of two sources of particle production: the $q_1\bar{q}_2$ and the $q_3\bar{q}_4$ ones. If colours are reconnected, the sources would instead be $q_1\bar{q}_4$ and $q_3\bar{q}_2$. The picture is complicated by the possibility of gluon emission. Gluons with an energy above the W width can be viewed as independently emitted from the respective W source, to a good first approximation: propagator effects ensure that interference terms are suppressed. No similar suppression exist for soft gluons or in the nonperturbative régime. Therefore standard calculational techniques are of limited interest, and the phenomenon mainly has to be studied within the context of specific models. By now, several independent codes exist, some part of existing QCD generators, others available as add-ons. Below we list the known ones and give some specific details.

4.7.1 A PYTHIA-based implementation
(code by T. Sjöstrand)

The code used for the studies in [155] has not (yet) been incorporated in the PYTHIA/JETSET programs. A sample main program and the colour rearrangement subroutines can be obtained at web address http://thep.lu.se/tf2/staff/torbjorn/test/main01.f. Several different options are available, among others:
- scenario I, where strings are considered as extended colour flux tubes and the reconnection probability is proportional (up to saturation corrections) to the space–time overlap of the W^+ and W^- strings;
- scenario II, where strings are considered as thin vortex lines and reconnection may occur when strings cross;
- scenario II′, a variant of scenario II where only those reconnections are allowed that reduce the total string length; and
- the instantaneous scenario, where reconnections are allowed before the parton-shower evolution [154]; unphysical but handy for comparisons.

At most one reconnection is performed per event, in scenario II the one that occurs first in time, in scenario I selected according to relative probabilities given by the overlaps. Reconnections within a W system are not considered.

4.7.2 Another PYTHIA-based implementation
(code by Š. Todorova)

The code follows the physical approach of [155]. The reconnection phenomenon is simulated

with the help of the string model, where strings are considered to be either flux tubes or vortex lines with arbitrary diameter of the core. In order to get a more realistic estimation of the effect of colour reconnection, the following features (not found in the preceding code) were incorporated in the simulation:

- space-time evolution of parton shower;
- multiple reconnections; and
- self-interaction of a string (production of glueballs).

It should be noticed that the space-time evolution of a shower together with the self-interaction of a string allow the study of string reconnection effects in a single parton shower (decay of a single Z^0).

The search for candidates for reconnection is processed in parallel with the shower development (reconnection can take place before the emission of the last partons). Overlaps of the colour fields of flux tubes are calculated numerically (using multichannel MC integration with importance sampling). The method is slow but this is the price to be paid for (relative) accuracy and individual treatment of each event. The minimal distance between "vortex lines" is found by a minimization procedure based on parabolic fit.

The code is available in the directory crnvax:[nova.colour_ reconnection].

4.7.3   An ARIADNE-based implementation
(code by J. Häkkinen)

The aim of the simulation program presented in [156] is not so much to study the effect of recoupling on the average events, but to study if rare recoupled events can be identified. Perturbative QCD favours states which correspond to "short strings", i.e. parton states which produce few hadrons. This string "length" can here be specified by the λ measure, defined in [157], which correspond to an effective rapidity range. If recoupling occurs it is conceivable that it is favoured when the recoupling produces a state with lower λ measure, and such states may also be more easy to identify. For this reason the program produces recoupling such that the λ measure for the reconnected final state is minimized. Gluons with $E \gtrsim \Gamma_W$ are emitted independently within the original $q\bar{q}$ systems [158, 155]. This emission is simulated using the Dipole Cascade Model [122] implemented in ARIADNE [13]. For gluons with c.m. energy below $\Gamma_W \approx 2$ GeV there may be unknown interference effects due to emission from the two W systems. These low-energy gluons give very little effect on the hadronic final state, however, if the hadronization phase is described by the Lund string model [28] implemented in JETSET [15]. They are therefore disregarded in the parton states, which implies that a small fraction of the energy ($\approx 4\%$) will be lost in the simulations. During minimization of λ all possible final state configurations, obtained by cutting the original gluon chains in one place only before reconnecting to two new systems, are compared with each other. In this program reconnection between the two strings occur once in every event while reconnections within the strings are not considered. Thus, the program is not expected to reproduce average events, but possibly a small admixture of recoupled events.

The C code used in [156] is available at http://thep.lu.se/tf2/hep/hep.html or through anonymous ftp at thep.lu.se:/pub/LundPrograms/Misc/wwpair.tar.Z. The code contains two more models; the instantaneous scenario of [154], and random reconnection of the strings. These models are only used for comparison with the "main" model.

4.7.4 Another ARIADNE-based implementation
(code by L. Lönnblad)

The model in [127] for colour reconnections, implemented in the ARIADNE program [13], is similar to the one in [156] in that it reconnects colour dipoles within the framework of the Dipole Cascade Model (DCM) [122] with a probability $1/N_C^2$ only if the total string length becomes reduced. The main differences are that reconnections within each W system (and also among the partons from a Z decay) is allowed, that several such reconnections are allowed in each event, and that reconnections are allowed during the perturbative cascade.

To achieve this, colour indices are assigned to each dipole, and after each emission, dipoles with identical indices are allowed to reconnect. The indices are chosen randomly, but restrictions are made to ensure physical colour flows, e.g. two gluons created by a gluon splitting should not be allowed to form a colour singlet. In the DCM, however, a gluon is radiated coherently by the dipole between two partons, and a procedure has to be introduced, where the emitted gluon is said to have been radiated off one of the two emitting partons with some probability depending on which is closer in phase space.

In the case of $e^+e^- \rightarrow W^+W^-$ reconnections are initially only allowed within each W system separately. After all gluons with $E_g > \Gamma_W$ have been emitted, reconnections between the W systems is switched on and gluon emission with $E_g < \Gamma_W$ is performed in the possibly reconnected systems before hadronization.

4.7.5 A HERWIG-based implementation
(code by B.R. Webber)

A model for colour reconnection has been implemented in a package of subroutines that can be used with HERWIG (version 5.8). The new integer parameter IRECO=0,1,2 determines the reconnection option used. IRECO=0 means no reconnection and IRECO=2 gives "immediate" reconnection of the quark–antiquark pairs in hadronic WW events, before parton shower generation, with probability PRECO (default value = 1/9). In HERWIG this changes the evolution of the showers, as well as the colour connections, because the initial opening angles are different.

The most serious option is IRECO=1, which invokes a model based on the assumption that reconnection occurs locally in space–time. First, a space–time structure is computed for each parton shower in the event. This is done using a package written by Mike Seymour to store the internal lines of showers, which is turned on by setting INTLIN=.TRUE.. The algorithm is semi-classical, but qualitative features and orders of magnitude should be correct. In the case

of W hadronic decays, each W decay point is generated with the appropriate exponential decay distribution. Then the locations of all the vertices in the showers are computed by assigning a space-time separation $\Delta x_i = q_i/(q_i^2 - m_i^2)$ to vertices joined by an internal line i of 4-momentum q_i and on-shell mass m_i.

The HERWIG cluster hadronization model, normally called immediately after showering has terminated, involves splitting each final-state gluon into a quark–antiquark pair. For each quark i there is a colour partner antiquark j, with which the quark would normally be paired to form a colour singlet cluster (ij). The `IRECO=1` option introduces a reconnection phase before cluster formation. In this phase the program looks for another colour-connected quark-antiquark pair (kl) such that (il) and (kj) could be colour singlets and

$$|\Delta x_{il}|^2 + |\Delta x_{kj}|^2 < |\Delta x_{ij}|^2 + |\Delta x_{kl}|^2 \ , \tag{16}$$

where Δx_{ij} is the (ij) cluster size, defined as the separation of the *production* vertices of i and j (note that this can be zero, e.g. if i and j come from a W decay that did not radiate any gluons). If such a pair exists, the reconnection $(ij)(kl) \rightarrow (il)(kj)$ would reduce the cluster sizes, and so it is performed with probability `PRECO`. Note that reconnection can happen inside a single shower and not just between different showers. Thus some retuning of parameters to fit data on $\mathrm{e^+e^-} \rightarrow \mathrm{Z^0} \rightarrow$ hadrons will be necessary when using `IRECO=1`.

The code can be obtained by anonymous ftp from
> `hep.phy.cam.ac.uk` $\equiv$ 131.111.66.27

The following files should be copied from directory `disk$alpha1:[public.herwig]`:
- `hwwmas58.for` – sample main program and analysis routines;
- `hwreco58.for` – modified HERWIG routines `HWBFIN`, `HWBJCO`, `HWCFOR` which *replace* those in HERWIG version 5.8, plus *new* routines `HWGCLU`, `HWGCMO`, `HWUPIP`, `HWVHEP`.

There is a new common block containing relevant parameters and counters:
> `COMMON/HWRECO/PRECO,EXAG,IRECO,MEVTS,MCLUS,MRECO,MSWCH,INTLIN`

`PRECO` is the reconnection probability (default 1/9); `EXAG` is an 'exaggeration factor' for the W lifetime, to study effects of the WW separation (default 1.0); `IRECO` is the reconnection option (see above, default 1); `MEVTS` *etc.* are integer counters for number of events, clusters, reconnections, and WW reconnections; `INTLIN` is set to `.TRUE.` when `IRECO=1` (see above).

The code is still under development; please notify `webber@hep.phy.cam.ac.uk` of any problems, bugs and/or peculiarities.

4.8 Monte Carlo Implementations of Exact Next-to-Leading Order Calculations

Basic Facts

Program name:	EVENT	EERAD	EVENT2
Authors:	Zoltan Kunszt	Walter Giele	Stefano Catani
	Paolo Nason	Nigel Glover	Mike Seymour
email:	nason@surya11.cern.ch	E.W.N.Glover@dur.ac.uk	seymour@surya11.cern.ch

There are now three publicly-available programs for calculating next-to-leading order corrections to arbitrary infrared-safe two- and three-jet quantities in e^+e^- annihilation. Although these use Monte Carlo integration techniques, they should be contrasted with Monte Carlo Event Generators in several ways. Firstly, they calculate the *exact* result in perturbation theory for the $\mathcal{O}(\alpha_s)$ corrections to a given quantity — no more nor less. Secondly, the phase-space configurations generated do not have positive-definite weights, so a probabilistic interpretation is not possible. Finally, for both these reasons, the programs only ever consider the partonic final state, and no treatment of hadronization is attempted.

There are many advantages of implementing higher-order QCD calculations as matrix-element Monte Carlo programs. For all but the simplest observables, the required phase-space integrals are not analytically tractable, and some form of numerical integration becomes mandatory. Since each phase-space point sampled by the program has a direct correspondence to a set of final-state momenta, any infrared-safe jet or event-shape definition may be used, and can be implemented exactly as in an experimental analysis. Many event properties can be analyzed simultaneously, simply by adding code to the analysis routine of the program to histogram the quantity of interest.

However as is well-known, the real and virtual corrections are separately divergent but with finite sum, so naïve numerical integration of each matrix element would fail. Thus a regularization scheme must be used to render the integrals finite. It is principally in the definitions of regularization scheme that the three programs differ, although there are other important differences.

The difference between the regularization schemes can be illustrated using a simple one-dimensional example. In dimensional regularization using $(4 - 2\epsilon)$ dimensions, the integrals we encounter are typically of the form

$$\langle O \rangle = \int_0^1 \frac{\mathrm{d}x}{x^{1+\epsilon}} O(x) + \frac{1}{\epsilon} O(0), \tag{17}$$

where the first part represents the real cross-section, the second the virtual, and x would typically be a gluon energy or parton-parton invariant mass. The function $O(x)$ represents a final-state observable that is infrared safe, i.e. with the requirement that $O(x)$ tends smoothly to $O(0)$ as x tends to 0. If the integral were analytically tractable, it would yield an ϵ-pole

that canceled the virtual term, leaving a finite result. However, in general it is not, and we must manipulate it into a form in which the physical limit $\epsilon \to 0$ can be taken *before* numerical integration, without making any assumption about $O(x)$.

The phase-space *slicing method* does this by introducing an unphysical parameter x_0,

$$\langle O \rangle = \int_0^{x_0} \frac{\mathrm{d}x}{x^{1+\epsilon}} O(x) + \int_{x_0}^1 \frac{\mathrm{d}x}{x^{1+\epsilon}} O(x) + \frac{1}{\epsilon} O(0) \approx \int_{x_0}^1 \frac{\mathrm{d}x}{x} O(x) + \log(x_0) O(0) + \mathcal{O}\left(x_0 O'(0)\right). \quad (18)$$

The result becomes exact in the limit $x_0 \to 0$, which practically means $x_0 \ll x_{\mathrm{physical}}$, where x_{physical} is the smallest physical scale in the problem.

The *subtraction method* works by subtracting and adding a term derived by projecting each point in four-parton phase-space onto some point in three-parton phase-space, and calculating the observable at this phase-space point together with an approximate matrix element. This must be such that it matches all the divergent terms of the full matrix element. In our simple example this corresponds to

$$\langle O \rangle = \int_0^1 \frac{\mathrm{d}x}{x^{1+\epsilon}} O(x) - \int_0^1 \frac{\mathrm{d}x}{x^{1+\epsilon}} O(0) + \int_0^1 \frac{\mathrm{d}x}{x^{1+\epsilon}} O(0) + \frac{1}{\epsilon} O(0) = \int_0^1 \frac{\mathrm{d}x}{x} \left(O(x) - O(0) \right). \quad (19)$$

Note that this is exact and does not depend on any unphysical parameters.

The matrix elements for $\gamma^* \to q\bar{q}g$ have been known to next-to-leading order for many years[159]. These were later checked by other groups, and used for specific calculations of a variety of event shapes. For the 'QCD at LEP' report [160], Kunszt and Nason wrote a general-purpose Monte Carlo program using the subtraction method that could calculate the next-to-leading correction to any event shape or jet definition, EVENT[161]. This has been considered the standard calculation for many years, but has two significant shortcomings owing to the matrix elements used: they have been summed over permutations of the outgoing partons, which means that quarks and gluons cannot be distinguished in the final state; and they consider the decay of a virtual photon, so can only predict quantities averaged over orientations of hadronic events, losing all information on their lab-frame directions and lepton-hadron correlations. Furthermore they neglect specific axial-axial contributions that as a point of principle are essential for describing Z^0 decays, although in practice these are never numerically significant.

More recently two groups have proposed general algorithms for calculating next-to-leading order corrections in arbitrary processes, and both have used three-jet production in e^+e^- annihilation as a simple first proving ground for their methods. These have resulted in the EERAD program by Giele and Glover[162], which uses the slicing method, and the imaginatively-titled EVENT2 program by Catani and Seymour[163], which uses the subtraction method. Both of these use the full next-to-leading order matrix elements for $e^+e^- \to q\bar{q}g$, avoiding the shortcomings of EVENT. Although EVENT2 uses the matrix elements of the Leiden group[164] by default, it has options to use the same matrix elements as EVENT or EERAD as a cross-check. Numerical results of the three algorithms are discussed in [165] and shown to be in good agreement. Since they are supposed to be exact calculations of the same quantity, rather than models, any differences between them should be treated as bugs.

5   Standardization

5.1   Particle codes and /HEPEVT/ update

The /HEPEVT/ standard [166] has been widely adopted by Monte Carlo authors for storing information on generated events. In practice the real variables are commonly declared to be DOUBLE PRECISION and often the size is expanded to NMXHEP=4000. We propose that these are now added to the standard.

In /HEPEVT/ it was intended for particles to be identified using the PDG numbering scheme [167]. However the conventional numbers assigned have deficiencies, particularly concerning the neglect of particles expected according to the quark model but not yet identified in experiment, for example the h_b. This proves troublesome for those program authors who include such states and has lead to *ad hoc* solutions. Further the higher, orbitally excited $L = 2, 3, \ldots$ and radially excited $n = 2, 3, \ldots$ mesons are labelled in a somewhat unsystematic way. In order to preserve the concept of uniqueness, allow for the missing quark model states, systematize the numbering and remain true to the spirit of the PDG scheme we suggest the following revised numbering.

Table 9 lists the $n = 1$, $L = 0, 1$ mesons and indicates their numbering, for these states this is largely in accord with the PDG scheme and with the STDHEP (JETSET) implementation [168]. In the pairs of $I = 0$, (u, d, s) mesons: (η, η'), (ω, ϕ), $(h_1(1170), h_1(1380))$, *etc.* the lighter state is labelled 22 and the heavier 33, reflecting the naive, dominant quark contents. Bound states involving top quarks are not expected, due to the quark's high mass, and therefore are not considered. The mixed K_S^0 and K_L^0 states are still labelled 310 and 130 respectively. The table should be extended to include $n = 1$, $L = 2, 3, \ldots$ states; this leads to up to four mesons of the same total spin. It is proposed to reserve the fifth digit to differentiate these states by continuing the sequence established for the $L = 1$ mesons. That is, for a given $J > 0$ the numbers would be: $(L, S) = (J - 1, 1)$: $\star \star m$, $(J, 0)$: $10 \star \star m$, $(J, 1)$: $20 \star \star m$ and $(J + 1, 1)$: $30 \star \star m$, where as usual $m = 2J + 1$. The $J = 0$ states represent an exceptional case, here we propose $(L, S) = (0, 0)$: $\star \star 1$ and $(1, 1)$: $10 \star \star 1$, as done in table 9; this may be thought of as $L0 \star \star 1$. Radially excited mesons, $n = 2, 3 \ldots$, are effectively copies of the the above states, it is proposed to introduce a sixth digit to differentiate them as follows: $n = 1 : \star \star \star \star \star$, $n = 2 : 1 \star \star \star \star \star$, $n = 3 : 2 \star \star \star \star \star$, *etc.* Thus for example the $K^{*+}(1680)$, a 1^3D_1 state would be numbered 30323 and the $\rho^0(1450)$, a 2^3S_1 state 100113. The numbering of excited mesons suggested here differs significantly from the original PDG scheme.

Table 10 lists the lowest lying $J = 1/2$, $3/2$ baryons, including the anticipated charm and bottom states. Two $J = 1/2$ states exist for baryons containing three different flavours of quarks. When the two lighter flavours are in a symmetrical $(J = 1)$ state the baryon is called a Σ, Ξ' or Ω' and a Λ, Ξ, or Ω if they are in an antisymmetric $(J = 0)$ state. To distinguish the lighter, antisymmetric states the light quark numbers are reversed; for example[4] $\Xi_b'^-$ has

---

[4] Actually the PDG naming rules do not make it clear which state to put the prime on, we have provisionally chosen to place it on the heavier state.

q_1	$\overline{q}_2$	$L=0$		$L=1$				
		$S=0$	$S=1$	$S=0$	$S=1$			
		$J=0$	$J=1$	$J=1$	$J=0$	$J=1$	$J=2$	
		$\star\star1$	$\star\star3$	$10\star\star3$	$10\star\star1$	$20\star\star3$	$\star\star5$	
d	$\overline{d}$	π^0	ρ^0	b_1^0	a_0^0	a_1^0	a_2^0	11
	$\overline{u}$	π^-	ρ^-	b_1^-	a_0^-	a_1^-	a_2^-	-21
	$\overline{s}$	K^0	$K^{\star0}$	$K_1^0(1270)$	$K_0^{\star0}$	$K_1^0(1400)$	$K_2^{\star0}$	31
	$\overline{c}$	D^-	$D^{\star-}$	$D_1^-(2420)$	$D_0^{\star-}$	$D_1^-(H)$	$D_2^{\star-}$	-41
	$\overline{b}$	B^0	$B^{\star0}$	$B_1^0(L)$	$B_0^{\star0}$	$B_1^0(H)$	$B_2^{\star0}$	51
u	$\overline{u}$	η	ω	$h_1(1170)$	$f_0(980)$	$f_1(1285)$	$f_2(1270)$	22
	$\overline{s}$	K^+	$K^{\star+}$	$K_1^+(1270)$	$K_0^{\star+}$	$K_1^+(1400)$	$K_2^{\star+}$	32
	$\overline{c}$	$\overline{D}^0$	$\overline{D}^{\star0}$	$\overline{D}_1^0(2420)$	$\overline{D}_0^{\star0}$	$\overline{D}_1^0(H)$	$\overline{D}_2^{\star0}$	-42
	$\overline{b}$	B^+	$B^{\star+}$	$B_1^+(L)$	$B_0^{\star+}$	$B_1^+(H)$	$B_2^{\star+}$	52
s	$\overline{s}$	η'	ϕ	$h_1(1380)$	$f_0(1300)$	$f_1(1510)$	$f_2'(1525)$	33
	$\overline{c}$	D_s^-	$D_s^{\star-}$	$D_{s1}^-(2536)$	$D_{s0}^{\star-}$	$D_{s1}^-(H)$	D_{s2}^-	-43
	$\overline{b}$	B_s^0	$B_s^{\star0}$	$B_{s1}^0(L)$	$B_{s0}^{\star0}$	$B_{s1}^0(H)$	$B_{s2}^{\star0}$	53
c	$\overline{c}$	η_c	J/ψ	h_c	χ_{c0}	χ_{c1}	χ_{c2}	44
	$\overline{b}$	B_c^+	$B_c^{\star+}$	$B_{c1}^+(L)$	$B_{c0}^{\star+}$	$B_{c1}^+(H)$	$B_{c2}^{\star+}$	54
b	$\overline{b}$	η_b	$\Upsilon(1S)$	h_b	χ_{b0}	χ_{b1}	χ_{b2}	55

Table 9: Proposed numbering scheme for the lowest lying mesons: for example the a_1^- has the number -20213. The names of the pseudovector particles are distinguished by their masses, if these are not currently established L and H are used to indicate light and heavy. The pseudo-vector states $K_1(1270)$ and $K_1(1400)$ are believed to be admixtures of the K_{1B} 1^1P_1 and K_{1A} 1^3P_1; in such situations the lighter state is given the lower number.

number 5312 and the Ξ_b^- number 5132. This extends the convention that heavier states are given larger numbers. Excited states are not yet incorporated into event generators and thus are not covered here.

Increasingly supersymmetric particles are found in event generators, we therefore take his opportunity to put forward the following numbering scheme for them. A seventh digit is added being: either 1 $(1\star\star\star\star\star\star)$ for the partner of a boson or left-handed fermion; or 2 $(1\star\star\star\star\star\star)$ for the partner of a right-handed fermion. When left-right mixing occurs the ordering should be by mass. Examples include:

1000011	$\tilde{e}_L^-$	-2000006	$\overline{\tilde{t}}_R$	1000022	$\tilde{\gamma}/\tilde{\chi}_1^0$
2000011	$\tilde{e}_R^-$	1000021	$\tilde{g}$	1000023	$\tilde{Z}^0/\tilde{\chi}_2^0$
1000012	$\tilde{\nu}_e$	1000024	$\tilde{W}^+/\tilde{\chi}_1^+$	1000025	$\tilde{H}_1^0/\tilde{\chi}_3^0$
2000006	$\tilde{t}_R$	1000037	$\tilde{H}^+/\tilde{\chi}_2^+$	1000035	$\tilde{H}_2^0/\tilde{\chi}_4^0$

$q_1q_2q_3$	$J=1/2$		$J=3/2$	
	$\star n_3 n_2 2$	$\star n_2 n_3 2$	$\star\star\star 4$	
ddd			Δ^-	111
udd		n	Δ^0	211
uud		p	Δ^+	221
uuu			Δ^{++}	222
sdd		Σ^-	$\Sigma^{\star-}$	311
sud	Λ	Σ^0	$\Sigma^{\star 0}$	321
suu		Σ^+	$\Sigma^{\star+}$	322
ssd		Ξ^-	$\Xi^{\star-}$	331
ssu		Ξ^0	$\Xi^{\star 0}$	332
sss			Ω^-	333
cdd		Σ_c^0	$\Sigma_c^{\star 0}$	411
cud	Λ_c^+	Σ_c^+	$\Sigma_c^{\star+}$	421
cuu		Σ_c^{++}	$\Sigma_c^{\star++}$	422
csd	Ξ_c^0	$\Xi_c^{\prime 0}$	$\Xi_c^{\star 0}$	431
csu	Ξ_c^+	$\Xi_c^{\prime+}$	$\Xi_c^{\star+}$	432
css		Ω_c^0	$\Omega_c^{\star 0}$	433

$q_1q_2q_3$	$J=1/2$		$J=3/2$	
	$\star n_3 n_2 2$	$\star n_2 n_3 2$	$\star\star\star 4$	
ccd		Ξ_{cc}^+	$\Xi_{cc}^{\star+}$	441
ccu		Ξ_{cc}^{++}	$\Xi_{cc}^{\star++}$	442
ccs		Ω_{cc}^+	$\Omega_{cc}^{\star+}$	443
ccc			$\Omega_{ccc}^{\star++}$	444
bdd		Σ_b^-	$\Sigma_b^{\star-}$	511
bud	Λ_b^0	Σ_b^0	$\Sigma_b^{\star 0}$	521
buu		Σ_b^+	$\Sigma_b^{\star+}$	522
bsd	Ξ_b^-	$\Xi_b^{\prime-}$	$\Xi_b^{\star-}$	531
bsu	Ξ_b^0	$\Xi_b^{\prime 0}$	$\Xi_b^{\star 0}$	532
bss		Ω_b^-	$\Omega_b^{\star-}$	533
bcd	Ξ_{bc}^0	$\Xi_{bc}^{\prime 0}$	$\Xi_{bc}^{\star 0}$	541
bcu	Ξ_{bc}^+	$\Xi_{bc}^{\prime+}$	$\Xi_{bc}^{\star+}$	542
bcs	Ω_{bc}^0	$\Omega_{bc}^{\prime 0}$	$\Omega_{bc}^{\star 0}$	543
bcc		Ω_{bcc}^+	$\Omega_{bcc}^{\star+}$	544
bbd		Ξ_{bb}^-	$\Xi_{bb}^{\star-}$	551
bbu		Ξ_{bb}^0	$\Xi_{bb}^{\star 0}$	552
bbs		Ω_{bb}^-	$\Omega_{bb}^{\star-}$	553
bbc		Ω_{bbc}^0	$\Omega_{bbc}^{\star 0}$	554
bbb			$\Omega_{bbb}^{\star-}$	555

Table 10: The proposed numbering scheme for the baryons. In the first $J = 1/2$ column the order of the light quark numbers is reversed; for example Λ has number 3122 whilst Σ^0 is 3212.

The possibility of numbering potential SUSY mesons and baryons in the same spirit is left open at present.

5.2 Decay Tables

The study of identified particle production and the physics underlying the hadronization mechanism continues to be an active area of research at LEP 1. In hadronic Monte Carlo event generators final state particles are produced in two stages. Primary hadrons come directly from the clusters/strings/*etc.* that model the non-perturbative parton to hadron transition. Subsequently chains of secondary particles arise from the decays of the unstable primary hadrons. Note this separation is well defined in the context of MC programs but in reality for the short lived, strongly decaying resonances it may be only semantics.

Thus a major common component of hadronic MCs are routines to do the decay of unstable particles. These are based on the use of tabulated branching ratios and basic matrix elements, though in the case of τ's and b-hadrons specialized packages are also available. The construction of these decay tables is not a simple task and requires much per-in-spiration to fill in gaps in

present measurements [169] and deal with problematic cases. It would save much duplication of effort if one basic table could be used by all programs. This implies the ability to swap decay tables and thereby would allow some control over a (spurious) source of apparent variation in the rates of primary hadron production in the different hadronization models. A common, user friendly, interface would also enable easy maintenance and modification of the tables by users.

To achieve such a goal requires a unique way of identifying the particles, and any associated matrix elements, together with a standard format for outputting and inputting the tables. The revised PDG codes above provide a unique and logical means of identifying the particles. To identify the matrix elements we propose developing a set of standard three-digit integer codes, following the convention of table 11.

Code	Matrix Element
0	Isotropic decay
1-99	Standard codes to be agreed
≥ 100	Program specific options

Table 11: Proposed convention for matrix element codes

It is reasonable to restrict both the number of decay products to five, using zeros to complete an entry, and also numerical branching ratios to five decimal places. A more than five body decay can be stored, realistically, as a sequence of decays involving intermediate resonances. In studies involving very rare decays it is sensible to use a higher branching ratio and then apply a compensating normalization factor. It is then proposed to write out the following information,

> Number of decays listed
> Decaying particle, branching ratio, matrix element code, 1–5 decay products

using the following FORMAT statements,

```
100 FORMAT(1X,I4)
200 FORMAT(1X,I8,1X,F7.5,1X,I3,5(1X,I8))
```

An example is provided by the π^0 decays:

2							
111	0.98800	0	22	22	0	0	0	$(\pi^0 \to \gamma\gamma)$
111	0.01200	101	22	11	-11	0	0	$(\pi^0 \to \gamma e^- e^+)$

It must be recognised that b-hadrons represent a special case. In the absence of detailed knowledge about a significant fraction of their decays MC programs resort to models based

on partonic decays and fragmentation. Partonic decay modes may also be stored in the above format. Suppose in a $b\overline{q}$ hadron (here $\overline{q}$ may represent a diquark) the decay is $b \rightarrow cW^- \rightarrow cq_1\overline{q}_2$, this can be coded in one of two sequences either '$q_1,\overline{q}_2,c$' or '$c,\overline{q}_2,q_1$'. These two options can be exploited to refer to the two possible colour connections separately: $(c\overline{q})(q_1\overline{q}_2)$ and $(c\overline{q}_2)(q_1\overline{q})$ respectively, at the discretion of program authors[5].

It is now simply a matter of providing a .DAT file containing the decay table listed in the above format. To standardize the interface to the individual MC programs the following two subroutines are proposed:

$$\star\star\texttt{IODK(IUNIT,IFORMAT,IOPT)} \qquad \text{and}$$
$$\star\star\texttt{MODK(IDK,BR,ME,IPRD1,IPRD2,IPRD3,IPRD4,IPRD5)}$$

were $\star\star$ identifies the MC program. The first is used to read IUNIT<0 or write IUNIT>0 the decay table to the given unit number with IFORMAT specifying how the particles are identified. The standard is IFORMAT=1, that is use the revised PDG codes; nonportable program specific options may include: $=2$ use the internal numbering or $=3$ use the internal character string names. Authors and users may prefer the later options as more transparent than the PDG numbers. If IOPT=1 then matrix element codes ≥ 100 (program specific) are accepted, if IOPT=0 then such codes are treated as not recognised and set to zero, isotropic decay. The subroutine $\star\star$MODK is intended to allow individual lines of the table to be modified or added, before or during event generation; the arguments follow the standard format. Note that when a new mode is added or an existing branching ratio modified the sum of the remaining branching ratios should be rescaled to preserve unit sum. This means that when two modes of the same particle are altered the order of the calls is important for their resultant branching ratios.

The provision of such an interface rests with the actual program authors who need to convert between the standard format and their own internal structures. These interfaces may be expected to be robust against unrecognized or blank particle names and provide basic checks of the allowed kinematics, electric charge conservation and unit sum of branching ratios. Such an interface has been established for HERWIG and successfully used to import the JETSET decay table. However if program users do modify the provided decay tables then they must accept responsibility for them making sense.

5.3   Interfaces to electroweak generators

A number of dedicated four-fermion generators are being written for LEP 2 applications. The good ones will do the electroweak theory much better than standard general-purpose QCD generators. On the other hand, they do not contain any QCD physics aspects, i.e. neither perturbative parton showers nor nonperturbative hadronization. This makes the electroweak

---

[5]Observe that if the $V - A$ matrix element was constructed as $(p_0.p_2)(p_1.p_3)$ these would both give $(b.\overline{q}_2)(q_1.c)$.

(EW) generators well suited for some applications, such as total cross sections and leptonic final states, but generally unsuited for the study of hadronic or mixed hadronic–leptonic final states. It is therefore logical to interface them with parton-shower and hadronization programs. To some extent, this is already happening. However, in writing these interfaces there are certain dangers involved. There may also be a lot of work involved.

It would therefore be advantageous if the event generator authors involved could agree on a common approach: EW authors provide the four-fermion configuration in a standard format and QCD authors provide a standard interface that converts this to a set of final hadrons. Then only one interface needs to be written for each program, instead of one for each combination of EW and QCD programs. In this section we propose such a standard and report on progress in implementing it.

5.3.1 The basic problem

In the electroweak sector, fermions can be viewed as asymptotically free final state particles. This means that the production of a specific final state is fully calculable perturbatively. Many different intermediate states can contribute to the same final state, without any ambiguities being introduced by this. The total probability for a final state is given by squaring the sum of amplitudes

$$|A|^2 = |A_1 + A_2 + \ldots + A_n|^2 \tag{20}$$

(suppressing the issue of helicity sums, *etc.* — these aspects are not important for the general discussion). Interference effects therefore are included automatically.

QCD is different. Quarks are *not* asymptotic states. The final state consists of colour singlet hadrons, not coloured partons. The transition from perturbative to non-perturbative physics is not understood from first principles, but is at present modelled. The model used describe well what happens to a simple quark-antiquark pair, e.g. $Z^0 \to q\overline{q}$ at LEP 1. At LEP 2, four-quark states $q_1\overline{q}_2q_3\overline{q}_4$ have to be mastered. If we want to make use of our hard-won phenomenological experience, it is therefore essential that the $q_1\overline{q}_2q_3\overline{q}_4$ system can be subdivided into two colour singlet subsystems, either $q_1\overline{q}_2 + q_3\overline{q}_4$ or $q_1\overline{q}_4 + q_3\overline{q}_2$. Each subsystem can then be described in the same way as a LEP 1 event. On the contrary, if we are not allowed to use such a subdivision into singlets, a completely new hadronization formalism would have to be invented (with brand new parameters to be tuned to the LEP 2 data).

Unfortunately, there are complications. As a simple illustration, consider a system $u\overline{d}d\overline{u}$. The production obtains contributions from several possible intermediate states. One is a W^+W^- pair, with $W^+ \to u\overline{d}$ and $W^- \to d\overline{u}$. Another is a Z^0Z^0 pair, with the first $Z^0 \to u\overline{u}$ and the second $Z^0 \to d\overline{d}$. These two alternative intermediate states correspond to different colour singlets, and therefore would differ with respect to the treatment of subsequent parton showers and hadronization. That is, the final state contains a "memory" of the intermediate state. Furthermore, $|A|^2$ contains an interference term between the two alternatives, where the colour flow is not well-defined in perturbation theory. This is reflected in a relative colour factor

$1/(N_C^2 - 1)$ for the interference term, meaning e.g. that both $u\bar{u}$ and $u\bar{d}$ are in relative colour singlet states. Kinematical factors are not likely to compensate for the colour suppression, so numerically the interference terms may not be large. However, when the aim is to make a precision measurement of the W mass (to better than one *per mille*), one cannot rashly neglect their possible contribution. Since we know of no "correct" procedure to calculate it the reasonable approach is to adopt a "good bet" default with a method to define a "band of uncertainty".

5.3.2 Flavour and kinematics specification

It is natural to use the HEPEVT common block specification [166] to transfer flavour and kinematics information from the electroweak generator to the QCD one. After all, the HEPEVT standard was devised specifically with this kind of tasks in mind. The original standard has been changed so that real variables are given in DOUBLE PRECISION.

For the current interface, only NHEP, IDHEP and PHEP are actually mandatory. EW generator authors are invited to fill also the other information, such as mother–daughter pointers, but that is optional. Furthermore, any number of entries may be used in the event record to indicate the incoming e^+e^- pair and intermediate states, but the only objects allowed to have status code ISTHEP= 1 are the two final fermion–antifermion pairs and an arbitrary number of photons. The fermions may be interspersed with photons in the listing, but the relative order of fermions is strict:

    1 one outgoing fermion, i.e. $q/\ell^-/\nu_\ell$;

    2 one outgoing antifermion, i.e. $\bar{q}/\ell^+/\bar{\nu}_\ell$;

    3 another outgoing fermion; and

    4 another outgoing antifermion.

The pairing of the outgoing fermions and antifermions should be done so that, when W^+W^- intermediate states can contribute, the pair 1 and 2 corresponds to a possible decay of the W^+, and the pair 3 and 4 to a possible decay of the W^-. An example of an allowed order is $u\bar{d}d\bar{u}$, while $u\bar{u}d\bar{d}$ is not correct. When a W^+W^- pair cannot contribute, the ordering should be instead made consistent with the decay of of one Z^0 to the pair 1 and 2, and another Z^0 to the pair 3 and 4, e.g. $u\bar{u}c\bar{c}$. This way, coloured and uncoloured fermions can not be mixed in a pair, i.e. $ue^-\bar{\nu}_e\bar{d}$ is not an allowed ordering.

Of course, adopting the fixed order above is not crucial, but it avoids the need for QCD generators to do a lot of rearrangements, and establishes a standard for the colour flow weights in the next section.

5.3.3 Colour flow specification

As was already mentioned above, the colour flow is not uniquely specified when both outgoing fermion pairs are of quark-antiquark type. A QCD event generator is therefore required to

69

make a choice. We propose the following procedure.

The acceptance of a kinematical configuration by the electroweak generator (including specific helicities for some generators) is based on the total squared amplitude, $|A|^2$, so this number is available "for free". Internally, a generator has access to the subamplitudes, $A = A_1 + A_2 + \ldots + A_n$. Each subamplitude does correspond to a well-defined colour flow, so split the amplitudes into two classes, I and II, with I corresponding to colour singlets $1+2$ and $3+4$, and II to singlets $1+4$ and $3+2$. The total squared amplitude can then be written as

$$|A|^2 = |A_{\mathrm{I}} + A_{\mathrm{II}}|^2 = |A_{\mathrm{I}}|^2 + |A_{\mathrm{II}}|^2 + 2\mathrm{Re}(A_{\mathrm{I}} A_{\mathrm{II}}^*) = |A_{\mathrm{I}}|^2 + |A_{\mathrm{II}}|^2 + \Delta \ . \qquad (21)$$

This subdivision should be gauge invariant.

Each electroweak event generator should return the three (positive) numbers $|A|^2$, $|A_{\mathrm{I}}|^2$ and $|A_{\mathrm{II}}|^2$. Then the colour-suppressed interference term Δ is easily found as $\Delta = |A|^2 - |A_{\mathrm{I}}|^2 - |A_{\mathrm{II}}|^2$.

A "good bet" approach to the colour assignment problem is for the QCD generator to neglect the interference term, and use the relative magnitude of $|A_{\mathrm{I}}|^2$ and $|A_{\mathrm{II}}|^2$ to make a choice at random between the two possible colour flows.

More sophisticated recipes are used for QCD processes like qg $\rightarrow$ qg in HERWIG and PYTHIA, where the interference terms are split between the non-interference ones in accordance with the pole structure. However, such an approach presupposes a detailed study for each specific combination of allowed graphs, and so cannot be part of a generic interface. Should a generator provide such a subdivision, maybe as an option, it would be easy to represent by modified numbers $|A_i|^2 \rightarrow |A_i|^2 + \Delta_i$ so that $\Delta \rightarrow \Delta - \Delta_{\mathrm{I}} - \Delta_{\mathrm{II}} = 0$.

When Δ is nonvanishing, the uncertainty can be estimated by assigning the interference terms so that either class I or class II is maximized. Specifically, class I is maximized when the choice of colour flow is based on the relative magnitude of R_{I} and R_{II}, where

$$
\begin{aligned}
R_{\mathrm{I}} \ &= |A_{\mathrm{I}}|^2 + \Delta \quad & R_{\mathrm{II}} \ &= |A_{\mathrm{II}}|^2 & &\text{if } \Delta > 0 \\
&= |A_{\mathrm{I}}|^2 & &= \max(0, |A_{\mathrm{II}}|^2 + \Delta) \quad & &\text{else}
\end{aligned}
\qquad (22)
$$

and correspondingly with I$\leftrightarrow$II for class II maximized. If the difference between these two extremes is small, then presumably the default procedure can be trusted.

5.3.4   Further problems

A number of potential problems exist, where the current approach may not be enough. These are discussed in the following.

It has implicitly been assumed that the scale of perturbative QCD parton-shower evolution is set by the mass of the respective colour singlet. An example of a process where this need not be the case is $e^+e^- \rightarrow \gamma^*/Z^0 \rightarrow u\bar{u} \rightarrow u\bar{u}Z^0 \rightarrow u\bar{u}d\bar{d}$. The $u\bar{u}$ pair here has a large original mass,

70

which is reduced by the emission of a Z^0. It is not clear whether the QCD radiation can be well approximated by that of the final $u\bar{u}$ mass, or whether the original mass is somehow felt e.g. by a larger rate of hard-gluon emission. A study of the matrix element for $e^+e^- \to q\bar{q} \to q\bar{q}Z^0g$ would here be necessary. However, these graphs are not expected to give a major contribution, so presumably the uncertainty from this source is not significant.

When QCD processes are introduced, interference terms need not be colour-suppressed. Specifically, the graph $e^+e^- \to \gamma^*/Z^0 \to u\bar{u} \to u\bar{u}g \to u\bar{u}d\bar{d}$ gives two colour singlets $u\bar{d}$ and $d\bar{u}$, just like a W^+W^- intermediate state would. Therefore a suppression of interference contributions has to be based entirely on kinematical considerations.

Since separation of quark and gluon jets is very difficult on an individual basis, also $q\bar{q}gg$ gives a background to four-fermion final states. Here, of course, there can be no interference with the other processes.

The addition of parton showers to a QCD four-jet event, either $q\bar{q}gg$ or $(q\bar{q}g \to)q\bar{q}q'\bar{q}'$, has to follow quite different rules from that of other four-fermion events, e.g. with respect to angular-ordering constraints in the parton shower. These rules have not yet been worked out for any of the QCD generators. The input that electroweak generators can give here is therefore not so meaningful. The main thrust in this area should be an improved matching between the matrix-element and the parton-shower strategies already present in QCD generators. Electroweak generators (if they contain QCD graphs) should therefore have the option of switching off all QCD contributions, i.e. (the amplitudes for) the graphs above.

Some further input parameter may be required to specify whether QCD showers should be allowed also to involve the emission of photons. At LEP 1 we have learned that the "competition" between photon and gluon emission is a not unimportant aspect, that tends to reduce the total amount of photon radiation compared to the no-QCD-radiation scenario. Something similar is likely to hold at LEP 2. However, the situation is far worse here, since the number of charged particles is much larger, and the presence of intermediate charged states (W^+W^-) makes a subdivision of the full emission rate much more complicated. One could therefore consider two extremes:

- If an EW generator attempts to do the full job of photon radiation from all charged legs, then the QCD generator should not add further photon radiation. In fact, if anything, one may question whether the EW generator overestimated the amount of photon radiation off the quarks.
- If an EW generator only claims to have initial-state photon radiation, then the QCD generator could add final-state radiation inside each fermion-antifermion pair (also leptons, if implemented). This would still not be the full answer, but likely to be better than having no final-state radiation at all. (Since there is no unique, gauge-independent definition of final-state γ radiation in four-fermion processes, the usefulness of such an approach should be checked from case to case.)

Traditionally, QCD generators are not good at handling the polarization of τ's in the decay treatment. This is better done by dedicated τ decay packages. Therefore EW generators that

do provide the spin of outgoing τ's should give this information for the τ entries in

    COMMON/HEPSPN/SHEP(4,NMXHEP)

using the standard conventions [166]. A flag could be set by the EW generator, and used by the QCD generator to inhibit it from decaying the τ's.

We remind the reader that the production vertices at the femtometer level may be of interest for physics such as colour reconnection and Bose-Einstein effects. If any generator should provide such output, the VHEP part of HEPEVT can be used to define vertices. The original objective was for vertices at the scale of mm, but also numbers of order 10^{-12} mm could be stored with maintained precision so long as the primary event vertex is designed to be at the origin.

5.3.5   Existing codes:

Several interfaces now exist that are based on the philosophy outlined above.
- Output from EXCALIBUR, with amplitude information for the different colour singlets. Can be obtained at
  http://wwwcn.cern.ch/$\sim$charlton/excalibur/excalibur.html.
- Input into HERWIG. Can be obtained at
  http://surya11.cern.ch/users/seymour/herwig/.
- Input into JETSET. Can be obtained at
  http://thep.lu.se/tf2/staff/torbjorn/test/main07.f.
- Input into ARIADNE. Is part of the standard ARIADNE distribution.

Further information is available in the respective files.

5.4   Systematic errors

At LEP 2, several physics issues will involve hadronized quarks, both for QCD studies and for Electroweak measurements or searches. The following can be envisaged as case studies:
- Establish the running of α_s from the Z pole to LEP 2 energies.
- Measurement of hadronic cross-sections, e.g. $e^+e^- \to Z/\gamma \to q\overline{q}$ or $e^+e^- \to W^+W^- \to q_1\overline{q}_2q_3\overline{q}_4$, and discrimination between the two.
- Reconstruction of jet-jet invariant masses in the above two processes, or even in $e^+e^- \to ZH \to q\overline{q}b\overline{b}$.

The first item seems the easiest case. α_s has been measured using a great variety of observables at the Z peak, with nearly infinite statistics. The *variation* with $\sqrt{s}$ of well defined quantities such as energy-energy correlations or their asymmetry, or jet rates for a given y_{cut} should be much less prone to systematic errors than their relationship to α_s itself.

Two difficulties can be expected here. First, the flavour composition of the sample will be different at LEP 2. In particular, the rate of $b\bar{b}$ production will decrease from 22% down to less than 10%. The fact that the specific fragmentation parameters for b quarks [170] have been measured at LEP 1 should be of great help. In order to extrapolate to higher energies, these results have to be incorporated in the simulation in one way or another. The three-jet rate has been used at the Z peak to test the universality of the strong coupling [171] with an accuracy of about 0.005. The argument can be turned around as, the sensitivity of a determination of α_s to flavour composition, leading to a rough uncertainty estimate of about 0.0005 on the difference in α_s from the Z peak to LEP 2.

The second difficulty will arise when one tries to go from establishing the running to more quantitative estimates of it. The running will be compared to the expectation from the QCD fragmentation models. Given that the most popular generators are presently based on $\mathcal{O}(\alpha_s)$ exponentiated showers, one can rightfully challenge their capability to predict the $\sqrt{s}$ evolution, because of missing higher orders. The solution to this issue will probably have to come from a better mapping of the shower models to second order matrix elements.

The impact on acceptance corrections was limited at the Z peak by two positive factors: large statistics and limited initial state radiation. A simple event rotation technique [172] was sufficient to reduce the uncertainty on event selection down to 10^{-3} or better. The precision required at LEP 2 for such studies is less stringent, statistical errors being at the level of 1%, so that the same method applied to high energy annihilation events should be adequate. One difficulty will arise from initial state radiation (ISR): the optimum sensitivity for electroweak effects is obtained by removing the radiative return to the Z peak using an s' cut. Most of the ISR photons being emitted at small angles, the invariant mass of the hadronic system has to be used to implement this cut. The issue here is to understand how accurately one can reconstruct an invariant mass from a system of boosted jets. An important experimental constraint can presumably be placed by using $e^+e^- \rightarrow Z + \gamma \rightarrow q\bar{q} + \gamma$ events. However the issue of flavour dependence will come up again here, as the mass of the b quark and missing energy from neutrinos are expected to have sizeable effects on the jet angles and energies after a boost. A similar problem will be encountered when reconstructing $W \rightarrow q\bar{q}$ invariant mass, where the difference in flavour composition is even more drastic.

Finally one last but important issue is the discrimination between $e^+e^- \rightarrow Z/\gamma \rightarrow q\bar{q}$ and $e^+e^- \rightarrow W^+W^- \rightarrow q_1\bar{q}_2 q_3\bar{q}_4$ events for the determination of the W^+W^- cross-section at threshold [173]. There is a finite probability that a four-jet event from the first process with two hard QCD-radiated partons will mimic the second process. In the present state of QCD generators with only $\mathcal{O}(\alpha_s)$ exponentiated showers, it is not obvious that the Monte Carlo gives the right answer. One way to obtain direct experimental information is to see how often a hadronic Z decay can be reconstructed as two heavy systems of 45 GeV mass and compare with the predictions of the fragmentation model. The extrapolation to the appropriate center-of-momentum energies and invariant mass requires a fragmentation Model.

In most of these problems, an experimental constraint can be found in e.g. Z decays. However every time fragmentation event generators are needed to perform the necessary extrapolations. Evaluating the corresponding systematic errors has been performed traditionally by either i) varying some (well chosen) input parameters within "reasonable limits" or ii) comparing the results obtained when using two different models. Recently, a more complex situation has emerged for the analysis of the jet charge asymmetries in Z decays [174]. This is a clear example of an electroweak measurement performed using jets. The jet charge separations are ultimately obtained from a fragmentation model, upon which many constraints are imposed: measured production spectra for pions, kaons and baryons (p and Λ), resonances such as ρ, K^* and η, average jet charge measured from opposite hemisphere charge correlation, *etc.* Imposing these constraints immediately leads to extremely strong correlations among fragmentation parameters. In JETSET, it is possible to find enough parameters to describe very completely the production of each particle species. The weak points remain the transverse momentum distributions and the baryon spectra. In HERWIG fewer parameters are available and the χ^2 is worse. Nevertheless the value of the electroweak asymmetry can be extracted for both models, with systematic errors related to the goodness of fit. A consistency check is supplied by the agreement of the values obtained from the two models within the systematics pertaining to each model. Similar procedures can be envisaged for measurements of electroweak quantities at LEP 2.

To conclude, there is no unique prescription for evaluating systematic errors. In each problem specific sources of errors and the corresponding fragmentation model parameters have to be found. Incorporating experimental constraints generally leads to very strong correlations among parameters, but this can be solved by for example using a combined linearized fit. The most general problem in extrapolating results obtained at the Z pole to LEP 2 will be the change in flavour composition. A mapping of the parton shower models to the second order matrix elements would be most useful.

6   Summary and Recommendations

It is useful to remember the last words of the LEP 1 QCD generators report [3]: *Due to the large uncertainty present in any realistic Monte Carlo, physics studies must be based on the use of at least two complete and independent programs.* Nothing has been changed in this regard; QCD is still not solved and the need for models is as large as ever.

The QCD generators of today may be considered more mature than the pre-LEP ones, in that they have successfully survived a number of experimental tests. However, there is always the danger that "incorrect" models do not just fade away — they are only modified and retuned for agreement. The increased energy lever arm provided by LEP 2 could give additional discrimination power, or at lease necessitate further fine tuning of programs.

Furthermore, in comparing with the LEP 1 data, we see that no generator is perfect. Depending on the physics area studied, it is therefore important to beware of generators with known shortcomings in that area. These shortcomings may indicate basic problems in the models, but could also come from further effects (e.g. higher-order matrix-element corrections) that authors never claimed to include. Generator authors are encouranged to sort out known problems in the light of LEP 1 experience, and in particular those with implications for LEP 2 studies. For some areas, such as colour reconnection and Bose-Einstein effects, the modelling is only in its infancy, and further efforts obviously are required.

The World Wide Web offers new opportunities to make programs accessible, including manuals, update notes, sample main programs and so on. To the extent authors did not yet adapt their distribution practices to the new opportunities, they are encouraged to do so. A common practice of having a "home page" for each generator will allow the construction of useful generator directories.

Standardization is as important as ever, in order to avoid confusion among experimentalists required to run a multitude of different codes. We have here proposed modifications to the /HEPEVT/ standard, extensions and a few corrections to the PDG particle code, a standardized decay table and an interface between electroweak four-fermion generators and QCD generators. A continued dialogue about possible standards would be very useful.

References

[1] G. Altarelli, R. Kleiss and C. Verzegnassi, Z Physics at LEP 1, CERN yellow report 89-08.

[2] R. Kleiss *et al.*, in [1], vol.3, p.1.

[3] T. Sjöstrand *et al.*, in [1], vol.3, p.143.

[4] TPC Collaboration: H. Aihara *et al.*, Zeit. Phys. **C28** (1985) 31;
J.W. Gary, Ph. D. Thesis, U. of California, LBL-20638, 1985.

[5] TASSO Collaboration: M. Althoff *et al.*, Zeit. Phys. **C26** (1984) 157 and W. Braunschweig *et al.*, Zeit. Phys. **C41** (1988) 359.

[6] OPAL Collaboration: M.Z. Akrawy *et al.*, Zeit. Phys. **C47** (1990) 505.

[7] L3 Collaboration, B. Adeva *et al.*, Zeit. Phys. **C55** (1992) 39.

[8] ALEPH Collaboration: D. Decamp *et al.*, Zeit. Phys. **C55** (1992) 209.

[9] DELPHI Collaboration: K. Hamacher *et al.*, contribution 548 to EPS HEP95, Brussels; Wuppertal Preprint WU B 95-07 and internal note DELPHI 95-80 PHYS 515.

[10] ALEPH Collaboration, contribution 449 to EPS HEP95, Brussels.

[11] M. Weierstall, Dissertation, Bergische Univ. – G.H., WUB-DIS 95-11, Wuppertal.

[12] S. Bethke *et al.* Nucl. Phys. **B370** (1992) 310.

[13] L. Lönnblad, Comp. Phys. Comm. **71** (1992) 15.

[14] G. Marchesini *et al.*, Comp. Phys. Comm. **67** (1992) 465.

[15] T. Sjöstrand, Comp. Phys. Comm. **82** (1994) 74 and Lund University report LU TP 95–20.

[16] R. Vogl, Dissertation, Universität Innsbruck, Innsbruck 1995.

[17] ALEPH Collaboration: contribution 529 to ICHEP 94, Glasgow.

[18] G. Kramer and B. Lampe, Zeit. Phys. **C39** (1989) 101;
N. Magnussen, Dissertation, Bergische Univ. – G.H., WUB-DIS 88-4, Wuppertal;
DESY int. report F22-89-01, 1989.

[19] OPAL Collaboration: contribution 319 to EPS HEP95, Brussels.

[20] D. Michelsen, H. Müller and F. Wäckerle, IEKP-KA/94-11, Karlsruhe;
F. Wäckerle, Diplomarbeit, IEKP-KA/93-19, Karlsruhe.

[21] A. De Angelis, CERN-PPE/95-135.

[22] ALEPH Collaboration: D. Busculic. *et al.*, CERN-PPE/95-96.

[23] ALEPH Collaboration: to be published, data kindly supplied by G. Rudolph.

[24] ALEPH Collaboration: D. Decamp, *et al.*, Phys. Lett. **B284** (1992) 163;
DELPHI Collaboration: P. Abreu, *et al.*, Zeit. Phys. **C59** (1993) 21;
OPAL Collaboration: P.D. Acton, *et al.*, Zeit. Phys. **C55** (1992) 11;
SLD Collaboration: F. Abe, *et al.*, Phys. Rev. **D51** (1995) 962.

[25] ALEPH Collaboration: D. Busculic, *et al.*, CERN-PPE/95-82.

[26] DELPHI Collaboration: P. Abreu *et al.*, to be published.

[27] R.D. Field and R.P. Feynman, Nucl. Phys. **B136** (1978) 1.

[28] B. Andersson, G. Gustafson, G. Ingelman and T. Sjöstrand, Phys. Rep. **97** (1983) 31.

[29] R.J. Hemingway, OPAL technical note, TN279.

[30] ALEPH Collaboration: D. Buskulic, *et al.*, CERN-PPE/95-108;
DELPHI Collaboration: P. Abreu, *et al.*, CERN-PPE/95-53;
L3 Collaboration: M. Acciarri, *et al.*, Phys. Lett. **B345** (1995) 589.

[31] ALEPH Collaboration: D. Buskulic, *et al.*, Zeit. Phys. **C62** (94) 1;
DELPHI Collaboration: P. Abreu, *et al.*, contribution xyz to ICHEP94.

[32] G.T. Jones, *et al.*, Zeit. Phys. **C27** (1985) 43;
V. Ammosov, *et al.*, Phys. Lett. **B93** (1980) 210;
EMC Collaboration: M. Arneodo, *et al.*, Zeit. Phys. **C34** (1987) 283 and Phys. Lett. **B145** (1984) 156;
N.J. Barker, *et al.*, Phys. Rev. **D34** (1986) 1251.

[33] ZEUS Collaboration: M. Derrick, *et al.*, DESY 95-084.

[34] H1 Collaboration: S. Aid, *et al.*, contribution 479 to EPS HEP95, Brussels.

[35] Y.J. Pei, "Studies of meson production in Z decays", CERN Seminar, September 6 1994 (unpublished).

[36] OPAL Collaboration: R. Akers, *et al.*, Zeit. Phys. **C63** (1994) 181.

[37] ALEPH Collaboration: D. Buskulic, *et al.*, Zeit. Phys. **C66** (1995) 355.

[38] OPAL Collaboration: G. Alexander, *et al.*, Phys. Lett. **B264** (1991) 467.

[39] DELPHI Collaboration: P. Abreu, *et al.*, Phys. Lett. **B275** (1992) 231.

[40] ALEPH Collaboration: D. Buskulic, *et al.*, CERN-PPE/95-92;
DELPHI Collaboration: P. Abreu, *et al.*, Zeit. Phys. **C59** (1993) 533;
OPAL Collaboration: G. Alexander, *et al.*, contribution 284 to EPS HEP95, Brussels.

[41] ALEPH Collaboration: D. Buskulic, *et al.*, CERN-PPE/95-94.

[42] DELPHI Collaboration: M. Feindt, *et al.*, contribution 563 to EPS HEP95, Brussels.

[43] L3 Collaboration: B. Adeva, *et al.*, Phys. Lett. **B288** (1992) 395.

[44] C.D. Buchanan and S.B. Chun, UCLA-HEP-95-02;
C.D. Buchanan and S.B. Chun, Phys. Lett. **B308** (1993) 153.

[45] P.V. Chliaponikov and V.A. Uvarov, Phys. Lett. **B345** (1995) 313.

[46] M. Szczerkowski, Phys. Lett. **B359** (1995) 387.

[47] F. Becattini, Firenzi preprints: DFF 234/10/1995 and F. Becattini *et al.*, DFF 233/10/1995.

[48] ALEPH Collaboration: D. Buskulic, *et al.*, Zeit. Phys. **C64** (1994) 361;
DELPHI Collaboration: P. Abreu, *et al.*, Phys. Lett. **B318** (1993) 249;
OPAL Collaboration: P.D. Acton, *et al.*, Phys. Lett. **B305** (1993) 415.

[49] SLD Collaboration: K. Abe, *et al.*, SLAC-PUB-95-6920.

[50] L3 Collaboration: M. Acciarri, *et al.*, contribution 92 to EPS HEP95, Brussels.

[51] DELPHI Collaboration: P. Abreu, *et al.*, CERN-PPE/95-28.

[52] DELPHI Collaboration: P. Abreu, *et al.*, CERN-PPE/95-39;
L3 Collaboration: M. Acciarri, *et al.*, Phys. Lett. **B328** (1994) 223;
OPAL Collaboration: P.D. Acton, *et al.*, Phys. Lett. **B291** (1992) 503.

[53] ALEPH Collaboration: D. Buskulic, *et al.*, Zeit. Phys. **C62** (1994) 1;
DELPHI Collaboration, P. Abreu, *et al.*, contribution 557 to EPS HEP95, Brussels;
OPAL Collaboration: P.D. Acton, *et al.*, CERN-PPE/94-217 and G. Alexander, *et al.*,
contribution 284 to EPS HEP95, Brussels.

[54] ALEPH Collaboration: D. Buskulic, *et al.*, Zeit. Phys. **C62** (1994) 179;
DELPHI Collaboration: P. Abreu, *et al.*, CERN-PPE/95-08;
L3 Collaboration: O. Adeva, *et al.*, Phys. Lett. **B261** (1991) 177;
OPAL Collaboration: R. Akers, *et al.*, Zeit. Phys. **C60** (1993) 199.

[55] ALEPH Collaboration: D. Buskulic, *et al.*, CERN-PPE/95-113;
OPAL Collaboration: contribution 666 to EPS HEP95, Brussels.

[56] ALEPH Collaboration: contribution 403 to EPS HEP95, Brussels.

[57] DELPHI Collaboration: O. Podobrin, *et al.*, contribution 560 to EPS HEP95, Brussels.

[58] C. Peterson, D. Schlatter, I. Schmitt and P. Zerwas Phys. Rev. **D27** (1983) 105.

[59] S.J. Brodsky and J. Gunion, Phys. Rev. Lett. **37** (1976) 402;
K. Konishi, A. Ukawa and G. Veneziano, Phys. Lett. **B78** (1978) 243.

[60] M.B. Einhorn and B.G. Weeks, Nucl. Phys. **B146** (1978) 445.

[61] J.W. Gary, Phys. Rev. **D49** (1994) 4503.

[62] OPAL Collaboration: G. Alexander, *et al.*, Phys. Lett. **B265** (1991) 462 and P.D. Acton, *et al.*, Zeit. Phys. **C58** (1993) 387.

[63] DELPHI Collaboration: CERN-PPE/95-164.

[64] OPAL Collaboration: G. Alexander, *et al.*, CERN-PPE/95-126.

[65] OPAL Collaboration: R. Akers, *et al.*, Zeit. Phys. **C68** (1995) 179.

[66] ALEPH Collaboration: D. Buskulic, *et al.*, Phys. Lett. **B346** (1995) 389.

[67] S. Catani, Yu. Dokshitzer, F. Fiorani and B.R. Webber, Nucl. Phys. **B383** (1992) 419.

[68] ALEPH Collaboration: contribution 589 to EPS HEP95, Brussels.

[69] C. Peterson and T.F. Walsh, Phys. Lett. **B91** (1980) 455.

[70] Yu. Dokshitzer, V.A. Khoze, S.I. Troyan and A.H. Mueller, Rev. Mod. Phys. **60** (1988) 373 and Basics of Perturbative QCD, Editions Frontières, Paris, 1991.

[71] B.I. Ermolaev and V.S. Fadin, JETP Lett. **33** (1981) 269;
A.H. Mueller, Phys. Lett. **B104** (1981) 161;
A. Bassetto, M. Ciafaloni, G. Marchesini and A.H. Mueller, Nucl. Phys. **B207** (1982) 189;
G. Marchesini and B.R. Webber, Nucl. Phys. **B238** (1984) 1.

[72] R. Odorico, Comp. Phys. Comm. **72** (1992) 235.

[73] D. Amati and G. Veneziano, Phys. Lett. **83B** (1979) 87.

[74] Ya.I. Azimov, Yu.L. Dokshitzer, V.A. Khoze and S.I. Troyan, Zeit. Phys. **C27** (1985) 65.

[75] Ya.I. Azimov, Yu.L. Dokshitzer, V.A. Khoze and S.I. Troyan, Phys. Lett. **B165** (1985) 147.

[76] B. Andersson, G. Gustafson and T. Sjöstrand, Phys. Lett. **B94** (1980) 211.

[77] JADE Collaboration: W. Bartel, *et al.*, Phys. Lett. **B101** (1981) 129.

[78] L3 Collaboration: M. Acciarri, *et al.*, Phys. Lett. **B345** (1995) 74.

[79] OPAL Collaboration: CERN-PPE/95-83.

[80] ALEPH Collaboration: contribution 518 to EPS HEP95, Brussels.

[81] CDF Collaboration: F. Abe, *et al.*, Phys. Rev. **D50** (1994) 5562.

[82] Yu.L. Dokshitzer, V.A. Khoze and S.I. Troyan, Zeit. Phys. **C** (1992) 107.

[83] OPAL Collaboration: R. Akers, *et al.*, Zeit. Phys. **C68** (1995) 1.

[84] L3 Collaboration: O. Adriani, *et al.*, Phys. Rep. **236** (1993) 1.

[85] OPAL Collaboration: R. Akers, *et al.*, Zeit. Phys. **C63** (1994) 363.

[86] B.A. Schumm, Yu.L. Dokshitzer, V.A. Khoze and D.S. Koetke, Phys. Rev. Lett. **69** (1992) 3025.

[87] V.A. Petrov and A.V. Kisselev, Zeit. Phys. **C66** (1995) 453.

[88] DELPHI Collaboration: P. Abreu, *et al.*, Phys. Lett. **B347** (1995) 447.

[89] OPAL Collaboration: R. Akers, *et al.*, Phys. Lett. **B352** (1995) 176.

[90] SLD Collaboration: SLAC-PUB-95-6924.

[91] OPAL Collaboration: P.D. Acton, *et al.*, Zeit. Phys. **C58** (1993) 207.

[92] ALEPH Collaboration: contribution 455 to EPS HEP95, Brussels.

[93] Yu.L. Dokshitzer, *et al.*, Phys. Lett. **B245** (1990) 243.

[94] Yu.L. Dokshitzer, *et al.*, Nucl. Phys. **B387** (1992) 675.

[95] M. Chmeissani, ALEPH internal note 93-097.

[96] Aly Aamer Syed, Ph.D. thesis, Univ. of Nijmegen (1994), ISBN 90-9007038-9.

[97] L3 Collaboration: M. Acciarri, *et al.*, Phys. Lett. **B353** (1995) 145.

[98] OPAL Collaboration: G. Alexander, *et al.*, Phys. Lett. **B264** (1991) 219.

[99] ALEPH Collaboration: D. Buskulic, *et al.*, Zeit. Phys. **C57** (1993) 17;
L3 Collaboration: O. Adriani, *et al.*, Phys. Lett. **B292** (1992) 472;
OPAL Collaboration: P.D. Acton, *et al.*, Zeit. Phys. **C58** (1993) 405.

[100] M.H. Seymour, Lund preprint, LU TP 94-6.

[101] DELPHI Collaboration: P. Abreu, *et al.*, CERN-PPE/95-101.

[102] ALEPH Collaboration: D. Buskulic, *et al.*, CERN-PPE/95-089.

[103] S. Cartwright, Workshop on Photon Radiation from Quarks, CERN yellow report 92-04.

[104] P. Perez, in [103] p.14;
F. Marion, *ibid.* ,p.97.

[105] D. Kirkby, in Perturbative QCD and Hadronic Interactions, ed. J. Tran Thanh Van,
Editions Frontières, 1995 and A study of Final-State Radiation in Hadronic Z Decays,
Ph.D. thesis, California Institute of Technology, September 1995.

[106] ALEPH Collaboration: D. Decamp, *et al.*, Zeit. Phys. **C54** (1992) 75;
DELPHI Collaboration: P. Abreu, *et al.*, Phys. Lett. **B286** (1992) 201 and Zeit. Phys.
C63 (1994) 17;
OPAL Collaboration: P.D. Acton, *et al.*, Phys. Lett. **B267** (1991) 143.

[107] S. Haywood, RAL-94-074.

[108] E.A. de Wolf, in Multiparticle Dynamics 1994, eds. A. Giovannini *et al.*, World Scientific,
Singapore, 1995, p. 15;
Y.F. Wang, L3 Internal Note 1621, 1994.

[109] ALEPH Collaboration: D. Buskulic, *et al.*, Zeit. Phys. **C64** (1994) 361;
DELPHI Collaboration: P. Abreu, *et al.*, contribution to ICHEP94, Glasgow;
OPAL Collaboration: R. Akers, *et al.*, CERN-PPE/95-024.

[110] DELPHI Collaboration: P.Abreu *etal.*, Phys. Lett. **B355** (1995) 415.

[111] ALEPH Collaboration: D. Buskulic, *et al.*, CERN-PPE/95-100;
DELPHI Collaboration: P. Abreu, *et al.*, Phys. Lett. **B298** (1993) 236, Zeit. Phys. **C65**
(1995) 587 and Zeit. Phys. **C63** (1994) 17;
OPAL Collaboration: P.D. Acton, *et al.*, Zeit. Phys. **C56** (1992) 521.

[112] K. Münich, Diplomarbeit, Bergische Univ. – GH, WU-D 95-5, Wuppertal.

[113] B. Andersson, Presented at the 25th International Symposium on Multiparticle Dynamics,
Stara Lesna, 1995.

[114] S. Brandt, *et al.*, Phys. Lett. **12** (1964) 57;
E. Fahri, Phys. Rev. Lett. **39** (1977) 1587.

[115] A. De Rújula, *et al.*, Nucl. Phys. **B138** (1979) 387.

[116] S. Catani, *et al.*, Phys. Lett. **B269** (1991) 432.

[117] T. Chandramohan and L. Clavelli, Nucl. Phys. **B184** (1981) 365;
L. Clavelli and D. Wyler, Phys. Lett. **B103** (1981) 383.

[118] S. Catani, G. Turnock and B.R. Webber, Phys. Lett. **B295** (1992) 269.

[119] J.D. Bjorken and S.J. Brodsky, Phys. Rev. **D1** (1970) 1416;
SLAC-LBL Collaboration: G. Hanson, *et al.*, Phys. Rev. Lett. **35** (1975) 1609.

[120] PLUTO Collaboration: C. Berger, *et al.*, Phys. Lett. **B82** (1979) 449.

[121] O. Nachtmann and A. Reiter, Zeit. Phys. **C16** (1982) 45;
M. Bengtsson, Zeit. Phys. **C42** (1989) 75.

[122] G. Gustafson, Phys. Lett. **B175** (1986) 453;
G. Gustafson and U. Pettersson, Nucl. Phys. **B306** (1988) 746.

[123] B. Andersson, G. Gustafson and L. Lönnblad, Nucl. Phys. **B339** (1990) 393.

[124] OPAL Collaboration: R. Akers, *et al.*, Phys. Lett. **B353** (1995) 595.

[125] M.H. Seymour, Nucl. Phys. **B436** (1995) 163.

[126] L. Lönnblad, in [103] p.109.

[127] L. Lönnblad, CERN-TH/95-218.

[128] R. Odorico, Comp. Phys. Comm. **72** (1992) 238.

[129] P. Mazzanti and R. Odorico, Zeit. Phys. **C59** (1993) 273.

[130] G. Marchesini and B.R. Webber in [1] vol.3, p.235.

[131] T. Sjöstrand, *et al.*, in [1] vol.3, p.325.

[132] F. James, Comp. Phys. Comm. **60** (1990) 329.

[133] R. Kleiss, *et al.*, in [1] vol.3, p.129.

[134] H. Burkhardt, *et al.*, Zeit. Phys. **C43** (1989) 497.

[135] Z. Kunszt, private communication.

[136] M.H. Seymour, Phys. Lett. **B354** (1995) 409.

[137] G. Marchesini and B.R. Webber, Nucl. Phys. **B330** (1990) 271.

[138] G. Marchesini and B.R. Webber, Nucl. Phys. **B310** (1988) 461.

[139] I.G. Knowles, Nucl. Phys. **B310** (1988) 571 and Comp. Phys. Comm. **58** (1990) 271.

[140] S. Catani, B.R. Webber and G. Marchesini, Nucl. Phys. **B349** (1991) 635.

[141] M.H. Seymour, Zeit. Phys. **C56** (1992) 161.

[142] R. Kleiss, Phys. Lett. **B180** (1986) 400.

[143] M.H. Seymour, Comp. Phys. Comm. **90** (1995) 95.

[144] B.R. Webber, Nucl. Phys. **B238** (1984) 492.

[145] A. Ali and B van Eijk, in [1] vol.3, p.226.

[146] Available by kind permision from the CLEO Collaboration.

[147] K.Kato and T.Munehisa, Comp. Phys. Comm. **64** (1991) 67.

[148] K.B.Lee, *et al.*, Phys. Lett. **B313** (1993) 469;
Y.Ohnishi, *et al.*, Phys. Lett. **B313** (1993) 475.

[149] G.A. Schuler and T. Sjöstrand, Nucl. Phys. **B407** (1993) 539 and in Two-Photon Physics from DAΦNE to LEP200 and Beyond, World Scientific, Singapore, 1994, eds. F. Kapusta and J. Parisi, p. 163.

[150] G.A. Schuler and T. Sjöstrand, Zeit. Phys. **C68** (1995) 607.

[151] T. Sjöstrand, Phys. Lett. **157B** (1985) 321.

[152] L. Lönnblad and T. Sjöstrand, Phys. Lett. **B351** (1995) 293.

[153] B. Andersson, G. Gustafson and B. Söderberg, Zeit. Phys. **C20** (1983) 317.

[154] G. Gustafson, U. Pettersson and P. Zerwas, Phys. Lett. **B209** (1988) 90.

[155] T. Sjöstrand and V.A. Khoze, Phys. Rev. Lett. **72** (1994) 28 and Zeit. Phys. **C62** (1994) 281.

[156] G. Gustafson and J. Häkkinen, Zeit. Phys. **C64** (1994) 659.

[157] B. Andersson, P. Dahlqvist and G. Gustafson, Phys. Lett. **B214** (1988) 604 and Zeit. Phys. **C44** (1989) 455.

[158] Yu.L. Dokshitzer, V.A. Khoze, L.H. Orr and W.J. Stirling, Nucl. Phys. **B403** (1993) 65.

[159] R.K. Ellis, D.A. Ross and A.E. Terrano, Nucl. Phys. **B178** (1981) 421.

[160] Z. Kunszt, P. Nason, G. Marchesini and B.R. Webber, in [1] vol.1, p.373.

[161] Z. Kunszt and P. Nason, unpublished.

[162] W.T. Giele and E.W.N. Glover, Phys. Rev. **D46** (1992) 1980.

[163] S. Catani and M.H. Seymour, in preparation.

[164] E.B. Zijlstra and W.L. van Neerven, Nucl. Phys. **B383** (1992) 525.

[165] QCD working group: P. Nason, *et al.*, these proceedings.

[166] T. Sjöstrand, *et al.*, in [1] vol.3, p.327.

[167] Particle Data Group: G.P. Yost, *et al.*, Phys. Lett. **B204** (1988) 113;
T. Sjöstrand, *et al.*, in [1] vol.3, p.326.

[168] L. Garren, URL `http://fnpspa.fnal.gov/stdhep_manual.ps`.

[169] Particle Data Group: M. Aguilar-Benitez, *et al.*, Phys. Rev. **D50** (1994) 1173.

[170] ALEPH Collaboration: D. Buskulic, *et al.*, CERN-PPE/95-113;
DELPHI Collaboration: P. Abreu, *et al.*, Phys. Lett. **B347** (1995) 447;
OPAL Collaboration: R. Akers, *etal.*, Phys. Lett. **B352** (1995) 176, Zeit. Phys. **C65** (1995) 31 and G. Alexander *et al.*, CERN-PPE/95-126.

[171] ALEPH Collaboration: D. Buskulic, *et al.*, Phys. Lett. **B355** (1995) 381;
DELPHI Collaboration: P. Abreu, *et al.*, Phys. Lett. **B307** (1993) 221;
OPAL Collaboration: R. Akers *et al.*, Zeit. Phys. **C65** (1995) 31.

[172] ALEPH Collaboration: D. Buskulic, *et al.*, Zeit. Phys. **C62** (1994) 539.

[173] W mass working group: Z. Kunszt, *et al.*, these proceedings.

[174] ALEPH Collaboration: D. Decamp, *et al.*, Phys. Lett. **B259** (1991) 377 and contribution 449 to EPS HEP95, Brussels;
DELPHI Collaboration: P. Abreu, *et al.*, Phys. Lett. **B307** (1993) 221;
OPAL Collaboration: P.D. Acton *et al.*, Phys. Lett. **B294** (1992) 436 and internal physics note PN195 (1995).